

HYD 542

UNITED STATES
DEPARTMENT OF THE INTERIOR
BUREAU OF RECLAMATION

MASTER
FILE COPY

BUREAU OF RECLAMATION
HYDRAULIC LABORATORY
NOT TO BE REMOVED FROM FILES

HYDRAULIC MODEL STUDIES OF
THE EUCUMBENE-TUMUT TUNNEL
JUNCTION SHAFT FOR THE AUSTRALIAN
SNOWY MOUNTAINS AUTHORITY

Hydraulic Laboratory Report No. 392

ENGINEERING LABORATORIES



OFFICE OF THE ASSISTANT COMMISSIONER AND CHIEF ENGINEER
DENVER, COLORADO

August 31, 1954

CONTENTS

	<u>Page</u>
Purpose of Study	1
Conclusions	1
Junction-shaft Inlet	1
Junction-shaft Inlet Control	2
Junction-shaft Cylinder Gate	2
Recommendations	3
Acknowledgement	3
Introduction	4
Investigation	5
The Junction-shaft Inlet	5
Description of model	5
Initial observations and test procedure	5
Inlet crest free flow	6
Operation of the inlet with bulkhead gate openings submerged	7
Junction-shaft Inlet Control	8
Description of model	8
Model operation	8
Flow characteristics of model	8
Test for cavitation erosion	9
The Junction-shaft Cylinder Gate--Preliminary Design	9
Description of model	9
Initial testing and observations	10
Unbalanced pressure on gate along tunnel axis-- Preliminary gate	11
Coefficient of discharge for preliminary cylinder gate	11
Pressures on preliminary gate seat shape	13
Study of seat shape using low-velocity air	13
Seat with 9-inch vertical upstream face, 1-1/4-inch seat surface and a 45° slope downstream	15
Seat, 9 inches high, with 20° slope upstream, and 60° slope downstream	15
Seat with two radii curve upstream of seat surface	15
Recommended Cylinder Gate	16
Modification of 1:18 scale model	16

CONTENTS (Continued)

	<u>Page</u>
Gate discharge coefficient	16
Pressures on gate seat shape with 2-1/8- and 6-1/2-inch radii at upstream edge	17
Unbalanced pressures on the gate along tunnel axis	17
Pressures on top and bottom of cylinder gate	18
Pressure cell measurements--Top and bottom surfaces of cylinder gate	19
Possible gate movement	20
 Cylinder-gate Top seal	 20
Seal problem	20
Description of gate seal model	21
Cavitation in flow passage of preliminary gate seal	21
Cavitation index--Preliminary gate seal--1/2-inch flow passage	21
Electric analog studies of upper gate seal-- 1/2-inch flow passage	23
Preliminary frame seal boundary--1/4-inch radius	23
Frame seal boundary 2 radii, 3/4 and 1-3/4 inches	25
Frame seal boundary of 3 radii (0.555, 1.182, and 2.39 inches)	25
Cavitation index--3 radii frame seal--1/2-inch flow passage	25
Cavitation at frame seal offset	26
Preliminary gate seal boundary--1/16-inch flow passage	27
Recommended 1/16-inch flow passage	27
Pressure change on gate seal ring for gate openings 0 to 5.5 inches	28

CONTENTS (Continued)

	<u>Figure</u>
Location Map	1
Junction-shaft Structure	2
Junction-shaft Inlet Structure Sections	3
Junction-shaft Cylinder Gate	4
Model Inlet and Construction Details	5
Construction Details of Model Inlet Overflow Section	6
Construction Details of Inlet Structure and Topography	7
Free Flow at Inlet Crest--Discharge 3,900 cfs	8
Free Flow at Inlet Crest--Discharge 5,000 cfs	9
Free Flow at Inlet Crest--Discharge 9,000 cfs	10
Head Loss for Shaft Inlet	11
Submerged Flow at Inlet Crest--Discharge 3,000 and 5,000 cfs	12
Submerged Flow at Inlet Crest--Discharge 9,000 cfs	13
Schematic Model of Shaft with Inlet Control	14
Flow in Shaft Model with Inlet Control	15
Photomicrograph of Surface of Concrete Lined Pipe Damaged by Cavitation--First Area Approximately 2 inches from top	16
Second Area Approximately 2 inches from top	17
Third Area Approximately 2 inches from bottom	18
Fourth Area Approximately 2 inches from bottom	19
 Preliminary Cylinder Gate Model Transition and Gate Sections	 20
Construction Details of Model Cylinder Gate and Gate Chamber	21
Model Operating Curves	22
Modifications to Cylinder Gate Model	23
Coefficient of Discharge Curves for Preliminary Design Gates with Maximum Openings of 10.8 and 8.5 feet	24
Pressures on Preliminary Design Gate Seat	25
1:4 Scale Low-velocity Air Model	26
Pressure Factors from Water and Air Model for Preliminary Design Gate Seat	27
Pressure Factors for Gate Seat with 2-radii Curve	28
Coefficient of Discharge Curve for Recommended Cylinder Gate	29
Model Operating Curves, Pressures on Lower Frame and on Gate Seat of Recommended Design Cylinder Gate	30
Unbalance of Pressure on Cylinder Gate Along Tunnel Axis--Recommended Design	31
Pressures on Top and Bottom of Recommended Cylinder Gate	32
Pressure Cell Installation 1:18 Scale Cylinder Gate Model and Gate Seal Model	33

CONTENTS (Continued)

	<u>Figure</u>
Cavitation in Preliminary Seal Flow Passage--	
Electric Analog	34
Cavitation Index of Frame Seal Boundary Shapes	35
Potential Drop Curves for Frame Seal Ring Shapes	36
Vapor Pockets on Frame Seal Boundary Offset--	
Recommended Frame Seal Ring	37
Cavitation in Gate Seal Flow Passage	38
Recommended Cylinder Gate Top Seal	39
Pressure Change on 30° Chamfer of Gate Seal Ring	40

UNITED STATES
DEPARTMENT OF THE INTERIOR
BUREAU OF RECLAMATION

Office of the Assistant Commissioner
and Chief Engineer
Engineering Laboratories
Denver, Colorado
August 31, 1954

Laboratory Report No. 392
Hydraulic Laboratory
Written by: J. C. Schuster
Checked and
reviewed by: J. W. Ball

Subject: Hydraulic model studies of the Eucumbene-Tumut Tunnel--
Junction shaft for the Australian Snowy Mountains Authority

PURPOSE OF STUDY

The main objective of the hydraulic model investigation covered by this report was to determine the best method of controlling the flow of water through the vertical junction shaft to the Eucumbene-Tumut Tunnel. Three methods studied were:

1. A free-discharge-type shaft inlet with the crest controlling the discharge
2. A submerged-type shaft inlet with a cylinder gate at the tunnel-shaft junction controlling the flow down the shaft and preventing air entrainment
3. A device at the shaft inlet designed to control the flow so as to exclude air from the shaft and cause the jet to fall through a vacuum equal to the vapor pressure of water

CONCLUSIONS

Junction-shaft Inlet

1. The inlet of the Eucumbene-Tumut junction shaft should be operated submerged because:

- a. Water plunging into the open shaft will entrain air which may collect in large pockets and be expelled with explosive force past the gate structures and from the tunnel exit causing a surging of the tunnel and shaft flow. These pressure surges might damage parts of the system.

- b. Objectionable vibration will occur if the water over the crest flows alternately against and away from the concrete surface of the inlet structure as shown on Figure 10B.

2. Air will be entrained by the water flowing from the reservoir to the shaft when the difference in reservoir and shaft water level

exceeds 1 foot (prototype) unless the inlet bulkhead gate openings are submerged.

3. With adequate submergence of the inlet the flow conditions will be tranquil and the head loss small for flows up to the design discharge of 9,000 cfs (cubic feet per second).

4. Water levels in the float wells that transfer the reservoir and shaft levels to the gate control mechanism will have a minimum fluctuation when the inlet operates submerged.

Junction-shaft Inlet Control

1. A control at the shaft inlet, which causes a vacuum equal to the water vapor pressure within the shaft, should not be used for the Eucumbene-Tumut junction shaft. Water vapor cavities would be entrained as the water jet plunges into the water in the shaft to cause cavitation damage to the shaft walls. A concrete test section in the model was slightly damaged by cavitation after 100 hours' operation and damage could be expected in the prototype.

2. The dispersion of a jet of water surrounded by a pressure equal to approximately the vapor pressure of the water is essentially the same as the dispersion of a jet surrounded by atmospheric pressure.

Junction-shaft Cylinder Gate

1. A cylinder gate at the base of the shaft, controlled to keep the shaft inlet and bulkhead gate openings submerged, will prevent entrainment of air in the tunnel system.

2. The gate chamber or enlargement in the tunnel at the base of the shaft (Figure 2) will satisfactorily direct the flow from the cylinder gate to the tunnel.

3. A divergence of the bottom 4 feet of the water passage of the lower gate frame from a diameter of 18 feet to a diameter of 18 feet 11 inches (Figure 4) eliminated a decrease in capacity that occurred between gate openings of 80 and 100 percent without the divergence.

4. A gate 9 feet 1 inch high with a maximum opening of 7.5 feet will have sufficient capacity for the design discharge of 9,000 cfs. The preliminary design was 12 feet high and had a maximum opening of 10.8 feet. The coefficient of discharge for the 9-feet 1-inch-high gate will have a maximum value of approximately 0.83 at a 7.5-foot gate opening (Figure 29).

5. Subatmospheric pressures will not occur on the 9-1/2 inches high by 10 inches wide recommended gate seat with a section profile from upstream to downstream of a 6-1/2-inch vertical tangent, a compound curve of 2-1/8- and 6-1/2-inch radii, a 2-3/8-inch horizontal tangent for the seating surface, and a vertical downstream face (Figure 30B).

6. The vibration characteristics of the prototype cylinder gate could be evaluated only qualitatively by the model studies, because it was infeasible to accomplish similarity for the physical properties of the field and model structures.

7. Movement of the prototype gate is possible if the frequency of the pressure fluctuations coincides with the natural period of the gate, and the gate is not restrained in its freedom of movement. The gate movement will be partially restrained if the clearance at the gate guides is held to a minimum. The unbalanced pressure across the gate when there is flow from the gate to the tunnel, will cause contact at the guides and result in resistance to vertical movement of the gate.

8. Cavitation will not occur at the lower edge of the frame seal ring with the section profile of a horizontal 0.62-inch tangent, a compound curve of radii of 0.555, 1.182, and 2.390 inches and a vertical tangent 4-1/4 inches long (Figure 39).

9. There will be no cavitation in the flow passage constriction between the frame seal ring and the gate seal ring of the recommended design (Figure 39).

10. The presence or absence of cavitation in the water passages of the top seal of the gate can be predicted from a plot of cavitation index versus discharge coefficient data obtained for the full-scale sectional model under heads up to 160 feet.

11. The pressure on the 30° sloped lower surface of the 1-1/4-inch thick gate seal ring changes from that in the shaft to essentially that in the gate recess between gate openings of 4 and 4-3/4 inches (Figure 40).

RECOMMENDATIONS

It is recommended that the cylinder gate be operated to keep the bulkhead gate openings of the inlet submerged so as to prevent air entrainment into the shaft and tunnel.

ACKNOWLEDGEMENT

The design of the hydraulic features of the Eucumbene-Tumut junction shaft was evolved through the cooperation of engineers of

the Australian Government, and engineers of the Canals, Mechanical, and Hydraulic Laboratory Branches of the Assistant Commissioner's Offices of the Bureau of Reclamation, Denver, Colorado, U.S.A.

INTRODUCTION

The Eucumbene-Tumut Project is located in the Snowy Mountains area of Southeastern Australia (Figure 1). The Snowy Mountains Hydroelectric Authority, responsible for the development of the project, has established its headquarters at Cooma, near the site of construction, approximately 250 miles southwest of Sydney. The project includes a large reservoir on the Eucumbene River near Adaminaby, a 14-mile-long 21-foot-diameter tunnel that connects this reservoir to Tumut Pond and Powerplant on the Tumut River, and a diversion dam and an 18-foot-diameter vertical shaft to the tunnel at the confluence of the Tumut and Happy Jacks Rivers. The 18-foot shaft intersects the 21-foot-diameter tunnel approximately three-quarters of the tunnel distance from Adaminaby Reservoir to Tumut Pond (Figure 2). This shaft and appurtenant structures will divert water from the Tumut and Happy Jacks Rivers to the tunnel and Adaminaby Reservoir when the combined flow of the Rivers exceeds the demand at Tumut Pond. The stored water will flow from Adaminaby Reservoir to Tumut Pond through the 21-foot tunnel when there is insufficient water in the rivers to supply power and irrigation demands.

The main problems of the model investigation concerned the 18-foot-diameter junction shaft and its pertinent parts located within a small reservoir (Junction Pond) formed at the diversion dam near the confluence of Tumut and Happy Jacks Rivers. The crest of the diversion dam is at elevation 3910 and the maximum flood level for Junction Pond is elevation 3940. The crest of the inlet structure, hexagonally-shaped in plan, is at elevation 3885 (Figures 2 and 3). The inlet water passage is tapered downward from hexagonal at the crest to the 18-foot circular shaft in a 25-foot vertical distance. Piers at the corners of the hexagon support a hexagonally-shaped enclosure of concrete extending upward to elevation 3940. This enclosure supports the trash-racks, the cylinder-gate hoist mechanism, and the bulkhead gates. The bulkhead gates are for closure of the six 9-foot-high by 15-foot-wide rectangular openings between piers through which water passes from Junction Pond to the shaft. These openings will be kept submerged to minimize air entrainment when water is flowing down the shaft. Submergence will be accomplished by pressurizing the 18-foot shaft using a 20-foot 4-inch inside-diameter cylinder gate at the shaft bottom (Figure 4). The cylinder-gate hoists are controlled by float-operated mechanisms actuated by shaft and pond-water levels. Water levels in the shaft are to be maintained at a sufficiently high elevation by the cylinder gate to prevent air entrainment.

The cylinder gate is located in a gate chamber or enlargement of the tunnel. The chamber consists of two 31.5-foot-long transitions

which are symmetrical upstream and downstream of the gate axis. The cross section at the gate axis consists of two 21-foot-diameter semicircles separated by a rectangle 21 feet high and 25 feet wide, while that at the transition ends is the same as the 21-foot-diameter circular tunnel. The transitions have a constant height of 21 feet and their semicircular sidewalls are aligned on a 23-foot-radius reverse curve from points opposite the gate axis to points where they join and are tangent to the main tunnel (Figure 2).

The shaft diameter increases abruptly from 18 to 25.5 feet at the shaft and tunnel junction to enclose the gate frame and provide a recess for the cylinder gate when it is opened. The gate is operated by means of three 4-1/2-inch-diameter stems which extend upward about 330 feet to the hoists at the shaft inlet. The gate is 9 feet 1 inch high with a maximum opening of 7.5 feet. The gate seat is fastened to a 23-foot-diameter concrete pedestal rising 10.7 feet above the tunnel floor. The gate seat surface is 8 inches above the tunnel center line. Six splitters, attached to a 30° cone on top and at the center of the concrete pedestal, keep the cylinder gate concentric with the shaft center line.

INVESTIGATION

The Junction-shaft Inlet

Description of model. --A 1:21.6-scale hydraulic model of the shaft inlet was constructed in a sheet-metal-lined head box 12 feet square and 4 feet deep (Figure 5A). The model included a portion of Junction Pond, the inlet structure, and part of the 18-foot-diameter vertical shaft. The converging section of the inlet structure from the crest to the 18-foot-diameter shaft was formed of cement-sand mortar over wire lath backed by a sheet-metal framework (Figures 5B and 6). The upper inlet enclosure, constructed of sheet metal, was attached to the lower part by means of wooden piers (Figures 7A and B). Wooden columns, representing trashrack supports, were added between the lower and upper parts of the inlet. A portion of the vertical shaft was represented by a 10-inch inside-diameter transparent plastic pipe. Topography surrounding the inlet structure was formed of a cement-sand mortar over a framework of wire lath and wood (Figure 7C). The flow approaching the crest was passed through rock baffles to represent flow from the Tumut and Happy Jacks Rivers. Point gages with vernier graduations to thousandths of a foot were used to measure model reservoir and shaft water levels.

Dimensions and quantities referred to in the following discussions are for the prototype structure unless otherwise noted.

Initial observations and test procedure. --Two methods of operating the junction-shaft inlet were considered in the initial stages of the investigation: (1) operation as a free-discharge weir with discharge controlled by the crest and the hydraulic losses in the shaft

and tunnel, and (2) operation with the inlet submerged by means of a separate control in the shaft to prevent air entrainment.

The model was first operated as a morning-glory-type spillway with the flow plunging over the crest and into the partially-filled shaft. Large quantities of air were entrained and much turbulence and surging were observed.

Operation of the model, with the inlet submerged by controlling the flow through the structure with a gate in the discharge pipe, prevented air entrainment. Flow conditions were tranquil with this method of operation which represented a control placed in the base of the shaft or in the tunnel.

As a result of the initial observations and discussions with the designers, it was decided that the investigation should be continued to determine (1) the minimum shaft water level with respect to the pond level that would prevent air entrainment with free flow at the crest, and (2) the head loss through the submerged bulkhead gate openings. This decision was reached after meager information concerning surging and the damaging effects of entrained air released under high pressures was reviewed and found to be of an adverse nature. The model tests disclosed that large quantities of entrained air could be expected in the prototype junction shaft if it were operated with free flow over the inlet crest (Figures 8, 9, and 10).

Water from the junction shaft flows through the tunnel and past gates into the Adaminaby Reservoir. A shaft approximately 200 feet deep at the Adaminaby Reservoir provides access to the tunnel control gates and would serve to vent any air entrained in the tunnel flow. However, any air collected along the top of the tunnel might be released with explosive force up the shaft to cause a surging which might damage the control facilities, or released into Adaminaby Reservoir to cause waves and possible erosion of the banks in the vicinity of the portal. Since the forces accompanying such air release could not be predicted from the small scale models and limited information of an adverse nature was available, the free-discharge inlet was abandoned and a controlled pressure shaft was selected for study. However, a limited number of observations were made for the free-flow condition and the results will be discussed in this report.

Inlet crest free flow. -- When the inlet structure was operated in free flow, the nappe of water was alternately in contact and free from the interior surface of the inlet. This unstable flow action occurred for nearly all discharges to the maximum of 9,000 cfs (Figure 10B). The changing flow conditions of one or more nappes could cause undesirable vibration of the inlet structure. This type of inlet structure was not considered suitable for free-flow operation.

A determination by model studies of the minimum water level in the shaft with respect to the pond-water level to prevent air entrainment was difficult because air quantities entrained in model flow do not represent the larger quantities that are present in prototype flow. The lower velocity and lesser degree of turbulence in the model at the interface of the air and water within the shaft are the principal reasons for the lack of similarity.

A known flow was passed through the inlet while the shaft level was controlled by the gate in the discharge pipe. The differential level was obtained with point gages when no entrained air was visible in the flow down the plastic pipe shaft. An approximate maximum difference of 1-foot prototype from pond level to shaft level without air entrainment was indicated by the 1:21.6 scale model for discharges from 1,000 to 9,000 cfs. Air entrainment is likely to occur at a relatively smaller differential in the prototype because of the more turbulent flow.

Operation of the inlet with bulkhead gate openings submerged. -- The opening of the cylinder gate for submergence of the inlet will be related to the pond level and the shaft water level by a float-operated mechanism connected to the gate hoists. The model inlet was operated submerged to obtain the difference between the pond and shaft water levels or the loss of head across the bulkhead gate openings. The loss of head was obtained for discharges representing up to a maximum of 9,000 cfs. The head loss curve was obtained by taking water surface readings with the bulkhead gate openings submerged the equivalent of 1 foot (Pond level 3895) at 3,000 cfs and 16 feet (Pond level 3910, crest of diversion dam) at 9,000 cfs. These head losses which ranged from 0.21 to 2.17 feet (Figure 11) were for use in designing the gate controls.

Flow conditions were tranquil in the inlet and pond for the submerged operation. A slight surging and surface roughness occurred within the shaft (Figures 12 and 13). Small vortexes formed within the pond outside of the inlet structure at the maximum discharge of 9,000 cfs with a pond level of 3910, but none formed within the shaft and no air was entrained in the model flow. The water level outside the inlet structure was progressively lowered for a constant discharge representing 9,000 cfs. At a level corresponding to pond elevation 3901 the vortexes that formed at the bulkhead gate openings entrained bubbles of air. When the pond level was lowered to correspond to elevation 3896, (2-feet prototype above the top of the bulkhead gate openings) the openings were not submerged and a vortex formed at the center of the shaft and entrained air. Operation at a discharge of 9,000 cfs for pond levels below elevation 3906 is not contemplated.

Flow conditions in the inlet were satisfactory when sufficient submergence was maintained. The submergence was sufficient for discharges up to 3,000 cfs when the pond was kept at elevation 3895. To maintain the proper submergence for discharges from 3,000 to 9,000 cfs, the pond elevation had to be raised from elevation 3895 to 3910 in direct proportion to the discharge.

Junction-shaft Inlet Control

Description of model. -- Another plan for regulating the flow of water from Junction Pond to the Adaminaby Tunnel was to provide a control at the shaft inlet. This control would exclude air from the shaft and the water would fall in the shaft where its ejector action would create a vacuum equal to water vapor pressure. A schematic model of the proposed control was constructed to demonstrate the characteristics of such a design (Figure 14). A 1-1/2-inch sharp-edged orifice was used to represent the control. A 6-inch inside-diameter pipe 16.5 feet long represented the vertical shaft. Two 12-inch centrifugal pumps in series supplied water to the orifice through a 6-inch Venturi meter used for measuring the flow. There was insufficient height of fall in the laboratory to overcome pipe losses and reduce the pressure downstream of the orifice to vapor pressure; therefore, an 8-inch turbine pump was attached to the lower end of the pipe to withdraw water and produce the desired vacuum. A gage glass with the upper end attached to a piezometer in the pipe approximately 1-1/2 feet downstream of the orifice and with the lower end attached to another piezometer 18 feet below the orifice gave a visible indication of the water level within the 6-inch pipe.

Model operation. -- A jet of water having a velocity of approximately 110 feet per second was discharged from the orifice down the pipe. The pipe downstream from the orifice flowed full unless the turbine pump was operated. The water level could be adjusted throughout the length of the 6-inch pipe by controlling the discharge from the 8-inch turbine pump. A pressure of 9 inches of water, absolute, surrounding the jet could be obtained by pumping the water from the 6-inch pipe.

Flow characteristics of model. -- The jet of water had the same appearance as one discharged into atmospheric pressure and had a divergence rate of about 1:50. Irregular surface eruptions were visible with high-speed photography (Figure 15). These surface eruptions were presumably caused by turbulent eddies originating in the pipe system upstream of the orifice and not by the vacuum surrounding the jet. No attempt was made to reduce the turbulence because a turbulent jet is likely to occur in any large control of this type.

The characteristic noise of cavitation was heard in the 6-inch pipe in the region where the jet penetrated the water. The maximum level occurred when the water vapor entrained by the water jet collapsed in a 4-foot length of pipe centered 14 feet below the orifice. Because of the sound transmitting quality of the brass pipe, the extent or area of maximum intensity of collapse of the cavities on the pipe wall could not be clearly defined. A section of plastic pipe, approximately 4-1/4 feet in length, was placed 14.2 feet below the orifice to facilitate observation of the flow action. The flow in this pipe appeared to be a very turbulent mixture of water and vapor cavities. High-speed movies through the plastic pipe disclosed a turbulent mixture, but separate cavities were not distinguishable. Apparently

vapor cavities were entrained in the turbulent flow and no definite concentration of collapse could be detected. The maximum noise seemed centered 2 or 3 diameters downstream of the jet and water junction. With the water level in the pipe controlled by a valve in the 8-inch turbine pump discharge line, the jet-water junction was maintained near a level 12 feet below the orifice. A 2-foot length of concrete-lined pipe was placed to begin at and extend below this elevation to test for erosion by cavitation (Figure 14).

Test for cavitation erosion. --A rapid erosion of the concrete lining by cavitation was expected because of the relatively high noise level when compared to other laboratory cavitation apparatus. For this reason it was not deemed necessary to photograph the surface of the concrete in detail and only an over-all photograph of the interior was taken before the test. After 25 hours of operation with a jet velocity of 110 feet per second and a pressure of 9 inches of water absolute, the test section was removed and inspected. No damage definitely attributable to cavitation could be detected. Before replacing the pipe for additional testing four areas chosen at random, two at each end, 90° apart, and 2 inches from the pipe ends, were photographed through a microscope at 12 times magnification. The 2-inch distance was limited by the photographic equipment. Photomicrographs were again taken after 75 hours additional testing (total of 100 hours) because no increase in damage to the surface was evident to the naked eye. The photographs disclosed a change in the surface texture near the top of the pipe where the cavitation seemed concentrated. Small holes in the concrete at 25 hours were enlarged after 75 hours more testing. Small amounts of the sand-cement mortar were removed and the texture of the surface seemed to have a spongy appearance characteristic of cavitation erosion (Figures 16 and 17). The concrete surface photographed at a 2-inch distance from the bottom of the pipe was essentially unchanged (Figures 18 and 19). Although no erosion of large magnitude occurred, the smaller forces of the model compared to those of the prototype, the characteristic noise of cavitation in the model, and the slight erosion of the concrete surface in the region of cavitation concentration led to the conclusion that this type control was not suitable for the junction shaft of the Eucumbene-Tumut Tunnel.

An enlargement of the shaft in the cavitation region might make this type of control suitable for an installation where the shaft water level is relatively constant. Such an enlargement would cause the cavity collapse to take place in the flow away from the shaft surfaces. Such an enlargement was not feasible for the junction shaft since the water level will vary almost the full length of the shaft.

The Junction-shaft Cylinder Gate--Preliminary Design

Description of model. --A cylinder gate located at the junction of the shaft and tunnel seemed the most feasible discharge control. A 1:18 scale model of the gate and gate chamber was constructed from a preliminary design. The model consisted of a 12-inch inside-

diameter pipe representing the 18-foot-diameter shaft, a cylinder gate formed and machined from brass, a gate chamber formed by two plastic transitions, and a 6-foot-long tunnel section of 14-inch inside-diameter pipe (Figure 20A). The 14-inch pipe was connected by a 3-foot-long reducer to a length of 12-inch pipe containing a valve for controlling the back pressure on the model. Water supplied to the model from a 12-inch centrifugal pump was measured by venturi meters.

The cylinder gate model was constructed to facilitate dismantling and removal from the gate chamber transitions (Figures 20B and 21A). The transitions were formed of 1/4-inch plastic to permit observation of flow from the gate (Figures 21B and C). Plastic tubing was attached to the gate-leaf piezometers and extended through the plastic transitions to allow a free gate movement (Figure 21D).

Initial testing and observations. --The model was operated at head differentials based on the computed head loss curves for the tunnel between the cylinder gate and Adaminaby Reservoir. A value of $n = 0.10$ was used to determine the back pressure in the tunnel at the base of the shaft for discharges to 9,000 cfs. Using the difference between the maximum normal head available at the shaft inlet and the computed back pressure, gate openings were determined for discharges ranging from 0 to a maximum of approximately 9,000 cfs. The gate opening for a particular discharge was obtained by adjusting the model gate until the computed differential for that discharge was attained. With an increasing discharge, the tunnel back pressure would increase and the shaft pressure decrease such that the tunnel becomes the discharge control at approximately 9,000 cfs (Figure 22). The plastic transitions of the model were not strong enough to withstand the scaled static head, approximately 13.9 feet of water (250-foot prototype) so the gate opening for a given differential and discharge was obtained by adjusting the gate to give the proper differential with reference to a constant tunnel back pressure of 3.3 feet (model) which kept the gate submerged. Flow conditions from the gate into the gate chamber were made visible by injecting small amounts of air into the water. Pressures were measured by open tube water and mercury manometers and reactance-type pressure cells.

Preliminary tests and observations of the gate model disclosed no adverse flow conditions that would require major changes to the design. Pressures measured within the gate structure were above atmospheric or positive with the exception of those on the gate seat. Negative pressures of 18 feet of water on the seat indicated a change of shape to be necessary. Pressure fluctuations were evident in the gate chamber as the jet energy was dissipated, but no movement of the model gate was discerned in the preliminary tests in which the gate was suspended on three 1/4-inch stainless steel rods 18.5 inches long.

Unbalanced pressure on gate along tunnel axis--Preliminary gate. --Water from the junction shaft passes radially between six splitters from the gate into the gate chamber and flows (downstream) toward the Adaminaby Storage Reservoir. The preliminary gate chamber transition toward Adaminaby Reservoir had been tapered in plan view to converge at a 10° angle in the direction of flow. It was designed to aid in directing the flow from the gate to the tunnel toward Adaminaby with a minimum of resistance. The forcing of the water to flow through the tunnel in one direction caused an unbalance of hydraulic pressure on the gate. A test was made to determine the magnitude of the unbalanced pressure for use in designing the gate guides. Pressures were taken by piezometers at six points on the gate, one each upstream and downstream at elevations 2 feet, 6.88 feet, and 11.38 feet above the gate lip.

A pressure unbalance, measured at the top piezometers, varied from a maximum of 1 foot of water in the upstream direction at 2,500 cfs to a maximum of 2 feet of water in the downstream direction at 9,000 cfs. The unbalanced pressure at the middle piezometers varied from a maximum upstream of 1.8 feet at 5,000 cfs to approximately 0 at 9,000 cfs. The unbalance at the bottom piezometers was a maximum of 1.5 feet upstream at 7,000 cfs and varied to 0 at 9,000 cfs. These small pressure differences were not considered objectionable since the change from a pressure upstream to a pressure downstream occurred gradually.

The need for the 10° convergent transition was investigated because, structurally, the reversed curve transition of the Tumut side of the gate chamber offered greater strength at a lower construction cost. Since there would be no flow in the tunnel upstream from the gate, it was assumed that the 10° transition would simulate the upstream portion of a gate chamber with symmetrical reversed-curve transitions without modification to the model. Therefore, the model gate chamber was tested in a reversed position (Figure 23A).

The maximum pressure unbalance on the top piezometers was 2 feet of water upstream at 3,500 cfs, 0 at 5,300 cfs, a maximum of 1.7 feet downstream at 6,000 cfs, and 0.5 foot downstream at 9,000 cfs. The unbalance at the center piezometers reached a maximum of 3 feet upstream at 6,000 cfs and decreased to 2 feet at 9,000 cfs. The unbalance at the bottom of the gate was 1 foot upstream at 3,000 cfs and 7.20 feet downstream at 9,000 cfs. The maximum unbalance recorded in either test was 7.20 feet. This value was considered satisfactory and a gate chamber of two 21-foot-high transitions with their semicircular walls aligned on 23-foot-radius reverse curves was accepted for the final design (Figure 2).

Coefficient of discharge for preliminary cylinder gate. --A calibration of the gate model indicated more than adequate capacity for the maximum design discharge. Discharge coefficients were computed from model data, which included the discharge, the pressure

head in the inlet shaft measured at a point 43.21-feet prototype above the gate seat, the gate opening, and the pressure head in the tunnel 53.1 feet downstream of the shaft center line. The equation used was:

$$C_d = \frac{Q}{A_s \sqrt{2gH}}$$

where

Q = flow rate, cubic feet per second

A_s = area of inlet shaft, square feet

H = difference in total head (pressure head plus velocity head in feet of water) between shaft and tunnel measuring stations both referred to the tunnel center line

g = gravity = 32.2

The coefficient of discharge reached a maximum of 0.90 at an 8.5-foot gate opening and decreased to approximately 0.73 at a 10.8-foot maximum opening (Curve a, Figure 24). The decrease in the coefficient over the range of opening from 8.5 to 10.8 feet indicated that for a given differential head, a loss in capacity would result by opening the gate beyond 8.5 feet. The maximum coefficient of 0.90 was higher than anticipated, and with a reduction in coefficient for gate openings greater than 8.5 feet, it was reasoned that the gate travel and thus the gate height could be reduced. The cause of the reduction in coefficient was first determined.

An abrupt enlargement of the flow passage from the inside diameter of the shaft to the inside diameter of the gate occurred at the bottom of the lower frame (Figure 24B). It was believed that the flow lines in this expanded region varied with the gate opening and influenced the contraction under the gate. A change in flow lines and thus in the contraction occurs as the gate is raised and its bottom edge approaches the offset. As the edge reaches a point where the contraction is influenced by the frame, the contraction increases and the discharge coefficient is lowered accordingly. This action was indicated by the behavior of the pressures on the bottom surface of the lower gate frame. When referred to the same datum these pressures were higher than those on the top of the gate for gate openings up to 7 feet, equal to them at the 7-foot opening, 5 feet less at an 8-1/2-foot opening, and again equal to them at a 10-foot opening.

The lower frame of the model gate was extended downward the equivalent of 2.3 feet to ascertain if the coefficient curve was a general shape for an abrupt enlargement from the frame inside diameter to the gate inside diameter. The coefficient curve obtained for this arrangement was of the same general shape as for the initial gate but with the maximum discharge coefficient of 0.83 occurring at an

opening of about 6.75 feet (Curve b, Figure 24). From the results of this test it was concluded that the sudden expansion and its position with respect to the bottom of the gate were the main factors contributing to the shape of the coefficient curve. Two solutions to the problem were possible; either a tall gate with the opening limited to that where the discharge coefficient was a maximum, or a shorter gate, with the sudden expansion reduced and the relative maximum opening increased. The smaller gate was desired because of its lower initial cost.

A gradual expansion from the inside diameter of the shaft to the inside diameter of the gate seemed most desirable since this would make the expansion effective throughout the full gate travel, prevent the inner edge of the lower frame from influencing the contraction under the gate, give maximum capacity at full gate opening, and make the gate height a minimum for a given discharge. Structural limitations prevented the use of such an expansion so a compromise was necessary. An expansion of the 4-foot-long lower gate frame from the 18-foot diameter of the shaft to 18 feet 11 inches was later represented in the model, tested, and found satisfactory. The test results are discussed in a subsequent section of this report.

Pressures on preliminary gate seat shape. -- Except for those on the gate seat, the pressures measured in areas of the model gate where subatmospheric pressures were most likely to occur were above atmospheric. Subatmospheric pressures of approximately 18 feet were recorded on the gate seat for a discharge of 5,400 cfs and a gate opening of 1.15 feet (Piezometer 38, Figure 25). As water flowed across the gate seat, the discontinuities of the seat in the form of steps caused a tendency toward flow separation and a reduction in pressure. The gate seat was not considered satisfactory because of the subatmospheric pressure of 18 feet of water.

Study of seat shape using low-velocity air. -- A low cost two-dimensional air model of wood to a 1:4 scale was utilized for the study of the seat shape (Figure 26) because the dismantling and machining of successive gate seat shapes for the hydraulic model would have been time consuming and expensive if several shapes were involved. A section representing 2 feet of the prototype seat was studied in the air model. Pressures on the gate seat were measured by piezometers and the total head by a Pitot tube.

Since the jet from the gate was submerged by water in the gate chamber, the condition was represented by the jet from the air model discharging into atmospheric pressure. There was one main difference however; the air jet was not confined by walls representing the gate chamber, and thus currents adjacent to the gate were not the same. An incomplete but satisfactory correlation was obtained by the use of pressure factors from the following equation:

$$\text{Pressure factor} = \frac{\frac{P_A}{\gamma} - \frac{P_B}{\gamma}}{H_T - \frac{P_B}{\gamma}}$$

where

$\frac{P_A}{\gamma}$ = piezometric head in the critical area of gate seat

$\frac{P_B}{\gamma}$ = pressure head into which jet discharges

and

H_T = total head in shaft, pressure plus velocity head

The minimum pressure indicated by pressure factors from the air model was approximately 2.5 times that for the water model, while the gate opening at which the pressure occurred differed by 0.5 foot (prototype) (Curves a and b, Figure 27). The greater reduction of pressure in the air model was attributed to the absence of the gate chamber walls. In the water model a portion of the jet from the gate flowed down the gate chamber walls and up the gate pedestal. This circulating flow, deflected the water jet from under the gate upward, partially relieving the subatmospheric pressure on the downstream side of the seat. This action was less pronounced on the air model because of the difference in confinement of the gate flow. A shortening of the gate seat base on the downstream side in the air model (the equivalent of decreasing the pedestal diameter) resulted in a minimum pressure factor of approximately -0.45 for the water and air models. The gate openings for the minimum pressure factors differed by approximately 1.0-foot prototype (Curve c, Figure 27). The water and air models still did not give identical results, but the air model was satisfactory for indicating feasible seat shapes.

For small gate openings, air injected into the discharge of the water model flowed downward along the vertical side of the gate pedestal. The cause of this flow condition was not understood until a similar flow action was observed on the air model. For gate openings to approximately 0.5-foot prototype in the air model, the jet could be forcibly deflected from a horizontal direction to a downward direction across the gate seat base (X to Y, Figure 27A), which might have occurred naturally if the gate chamber confinement had been represented in the model. The air in the area downstream and adjacent to the gate seat was rarified by the deflected jet and a pressure indicating cavitation occurred at the gate seat. The jet flowed in a downward direction until it was aerated to relieve the negative pressure. Cognizance was taken of this critical range of openings in subsequent tests.

Seat with 9-inch vertical upstream face, 1-1/4-inch seat surface and a 45° slope downstream. --Pressures were measured on a gate seat shape that had a vertical upstream face with a spring point 9 inches above the gate pedestal, a 1-1/4-inch flat section on which the gate seated, and a 45° downstream sloping face (Shape 2, Figure 26C). Pressure factors computed from the measurements made on the seating surface and the 45° slope disclosed the shape to be satisfactory except at the smaller gate openings, 0 to 0.5 foot. In this range of gate opening the jet could be forcibly deflected downward where it would remain and cause a subatmospheric pressure on the seat surface equal to approximately 0.9 of the total upstream head. This seat shape would be unsatisfactory because of possible cavitation at the small gate openings.

Seat, 9 inches high, with 20° slope upstream, and 60° slope downstream. --Pressures were measured on a wedge-shaped gate seat that had a height of 9 inches, at 20° upward slope on the upstream face and a 60° slope on the downstream face extended to the edge of the gate pedestal (Shape 3, Figure 26C). Pressures on this seat were above atmospheric and the jet would not flow downward without a continuous application of a deflecting force. Although acceptable from a hydraulic standpoint, the shape was undesirable because the gate must seat on a 20° sloping surface. Machining and setting of the gate and seat to provide a satisfactory sealing surface would be difficult because of the angle of the seat. A soft material such as babbitt or rubber inserted in the slope would be undesirable should it loosen and be removed by the flow of water.

It was concluded that a vertical or nearly vertical downstream face on the seat was desirable, that the downstream face of the seat should be close to the edge of the gate pedestal to prevent subatmospheric pressures on the seat and that the upstream edge of the seat should be rounded. These factors were taken into account in selecting a gate seat for further study.

Seat with two radii curve upstream of seat surface. --Radii of 2-1/8 and 6-1/2 inches were combined to form a compound curve on the upstream edge of a 9-1/2-inch-high gate seat. A 2-3/8-inch flat section tangent to the 6-1/2-inch radius provided a horizontal seating surface. The width of the gate seat was 7-1/8 inches and the downstream face was vertical. Operation was satisfactory at all openings except for the range between 0 to 0.6 foot. Severe vacuum pressures were encountered on the downstream side of the seat when the jet was forcibly deflected downward and remained in that position. (Piezometer 6, Figure 28).

The width of the gate seat was increased from 7-1/8 inches to 10 inches in an attempt to eliminate this condition. The jet could still be forcibly deflected downward and would continue to flow in that direction so the width was increased to 11 inches. For this width the jet was stable in a horizontal position throughout the range of the gate openings. When the jet was deflected downward and the

deflecting force removed, the jet would return immediately to the horizontal position where pressures were satisfactory. With a seat width of 11 inches, the fastening of the prototype gate seat to the gate pedestal would be difficult and a lesser width was desirable. Since the air model results were conservative because of the unconfined jet (comparison air and water preliminary design) a gate seat width of 10 inches (Figure 28) was selected for installation in the final hydraulic model.

Recommended Cylinder Gate

Modification of 1:18 scale model. --The hydraulic model was revised to include the several features determined from the previous tests. These included a new gate seat design, a deflector curtain around the gate recess at the top of the gate chamber, a reduction in maximum gate opening, an increased gate pedestal height, and an expansion of the lower gate frame flow passage.

The gate seat was the equivalent of 9-1/2 inches high, having a compound curve at the upstream edge with radii of 2-1/8 and 6-1/2 inches, an over-all width of 10 inches, a 2-3/8-inch-wide horizontal seating surface, and a vertical downstream face (Figure 28).

A 1-foot-high deflector curtain wall was extended down and completely around the gate recess at the top of the gate chamber to prevent direct, horizontal impingement on the top portion of the gate of water flowing along the chamber walls (Figures 4 and 29A).

The gate pedestal height was increased the equivalent of 2 feet to decrease the gate opening and represent a shorter gate, but the model gate height was not altered because the extra height was at the top and always contained within the gate recess where any dynamic influence would be similar to that of the shorter gate.

The expansion of the flow passage in the lower gate frame section of the model represented a change in diameter from 18 feet to 18 feet 11 inches in 4 feet (Figures 4 and 23B). This expansion was the maximum which could be included and still provide a stiffener ring of sufficient size to support the frame and seal ring.

Gate discharge coefficient. --A maximum coefficient of discharge of approximately 0.83 was obtained at the maximum design gate opening of 7.5 feet (Figure 29). At an 8.0-foot opening, which was the maximum obtainable on the model, the coefficient increased to approximately 0.84. A further expansion of the lower gate frame passage would probably have increased the coefficient of discharge between the 6- and 7.5-foot gate openings, but the expansion was not practicable; moreover, the gate capacity was adequate and a maximum at full opening.

Pressures at the lower frame and gate junction were positive and slightly lower than the shaft pressure with both pressures referred to a common datum. This indicated a reduction in pressure as the flow expanded to the passage inside the gate. The expansion of flow and the reduction in pressure was gradual and did not cause a decrease in the gate capacity at the larger openings. Apparently the inner edge of the bottom surface of the lower frame did not influence the contraction under the gate. Operating curves for the recommended design model and the pressures at the lower frame and gate junction are shown on Figure 30A. The expansion of the lower frame from 18 feet to 18 feet 11 inches in diameter was satisfactory.

Pressures on gate seat shape with 2-1/8- and 6-1/2-inch radii at upstream edge. --No subatmospheric pressures were measured in the water model on the gate seat with the upstream edge rounded on a compound curve of 2-1/8- and 6-1/2-inch radii (Figure 30B). Pressures at Piezometer 29 on the downstream side of the seat at the splitter center line were slightly lower than at Piezometer 32 located in the same respective seat position but between splitters. Pressures at both points were equal to the tunnel pressure at gate openings less than 0.5 foot and increased in a positive direction as the discharge and gate opening increased. With the 10-inch seat width, water did not flow down the face of the pedestal as observed for the preliminary gate seat design.

Pressures measured at Piezometer 28 on the seating surface downstream of a splitter first decreased and then increased between discharges of 0 and 6,000 cfs, and then decreased to a discharge of 9,000 cfs (Figure 30B). Pressures at Piezometer 31, located radially the same as Piezometer 28 but in the flow between the splitters, decreased gradually as the discharge increased. Pressures at Piezometer 28 were lower than at Piezometer 31 to a discharge of 5,000 cfs because of the reduced pressure in the eddy on the downstream side of the splitter. The pressure at Piezometer 28 exceeded that at Piezometer 31 by approximately 20 feet at 7,000 cfs. The pressures at the two piezometers were nearly equal at the 9,000 cfs and 20 feet greater than the tunnel pressure. The pressures on the seat at Piezometers 28 and 31 were satisfactory because they changed gradually and were positive for all discharges.

Piezometer 30 on the upstream edge of the gate seat measured the shaft pressure with the gate closed. As the gate was opened the pressure decreased to a value of approximately 60 feet (20 feet above the tunnel pressure) at 9,000 cfs. There was no indication of subatmospheric pressure on the gate seat so the seat shape was satisfactory.

Unbalanced pressures on the gate along tunnel axis. --The unbalanced pressures for water flowing from the shaft to Adaminaby Reservoir were obtained for the recommended cylinder gate design. The piezometers used to measure the unbalanced pressure at the top of the preliminary gate were now 2.3 feet higher than the top of the

recommended gate because the gate height was not changed from that of the preliminary design. The pressures measured by these piezometers were considered applicable because in both the preliminary and recommended design, the top of the gate is within the gate recess above the crown of the gate chamber. The maximum average pressure unbalance, measured 11.38 feet above the lip of the gate, was 0.7 foot for a gate opening of 5.38 feet and a discharge of 9,000 cfs (Figure 31A). Pressures upstream and downstream of the gate on the crowns of the gate chamber transitions were plotted along with the pressures on the gate at these elevations (Piezometers A, B, 33, and 34, Figure 31A).

Unbalanced pressures on the gate 6.88 feet above the lip reached a maximum of approximately 6 feet in a downstream direction at a discharge of 7,000 cfs (Figure 31B). The pressure unbalance decreased to approximately 5 feet at 9,000 cfs. The pressure unbalance at piezometers located 2.00 feet above the lip gradually increased from 0 to approximately 10 feet in a downstream direction as the discharge increased to 9,000 cfs (Figure 31C). A maximum unbalanced pressure of 10 feet of water applied uniformly to the projected gate area would not overstress the guides and thus the gate chamber reverse-curve transition design was acceptable.

Pressures on top and bottom of cylinder gate. --The suspension of the gate on lift stems approximately 330 feet long introduced the problem of vertical movement of the gate caused by an unbalanced pressure on its top and bottom surfaces. A vertical movement of the gate would not result from pressure fluctuations on the top and bottom if they were in phase and equal in magnitude and occurred simultaneously around the gate. Movement could result if the fluctuations occurred simultaneously around the gate in phase but unequal in magnitude, or out of phase and equal in magnitude. These combinations were unlikely because of the random nature of turbulent flow in the gate chamber as the energy in the gate discharge was dissipated.

To determine the probable downpull forces and tendency toward vertical oscillation of the gate, the pressure fluctuation and unbalance on the top and bottom of the gate were investigated. Water manometers were used to obtain the average pressure differences. Reactance-type pressure cells were used for obtaining magnitude, frequency, and phase relationship of fluctuations. Pressures were measured in only one section of the gate between adjacent splitters at three positions in the section. Position 1 was at the center line of the upstream splitter; Position 2, 22-1/2° to the left; and Position 3, 45° to the left (Figure 32D).

Pressure curves for Piezometers 13, 15, 16, 17, and 18 indicated a uniform pressure distribution on the gate top in the flow section (Figures 32A, B, and C). It was thus assumed that a uniform distribution would occur in the other sections of the gate, but the values would be progressively lower toward the downstream side because of the decrease in pressure in the direction of flow in the transition.

Pressures on the gate bottom at the center line of the splitter were approximately 3.5 feet lower than at the top for a discharge of 2,000 cfs; were approximately equal at 6,000 cfs; and were approximately 5 feet higher at 9,000 cfs (Figure 32A). Pressures on the gate bottom 22-1/2° from the center line of the splitter were in general lower than at the top for discharges to 7,500 cfs and higher than at the top for discharges greater than 7,500 cfs. Pressures on the gate bottom 45° from the splitter center line were lower than the top for all discharges. The maximum difference of approximately 4 feet occurred at a discharge of 6,500 cfs (Figure 32C).

From this investigation, it was apparent that a change of loading would occur on the gate lift stems and hoists. Unless the loading change occurred suddenly, no movement of the gate would be expected because the pressure differentials would be small. The inertia of water manometers tended to dampen pressure surges. To better define the pressure fluctuations on the gate, reactance-type pressure cells were attached to Piezometers 1, 13, 18, and 9 (Figure 32D).

Pressure cell measurements--Top and bottom surfaces of cylinder gate.--Oscillograms of the pressure fluctuations for 1,000 cfs increments of discharge were obtained with the model attached directly to the laboratory supply system (Figure 23A). The instruments and pressure cells used are shown on Figure 33A. Pressure fluctuations at the gate top and bottom were essentially in phase, but the fluctuation at Piezometer 9 slightly lagged those of Piezometers 1, 13, and 18. There was a difference in the magnitude of the fluctuation, top and bottom. The maximum difference of 11.0 feet occurred between Piezometers 13 and 1 for discharges of 7,000 and 8,000 cfs. Pressure differences were not consistently upward or downward but occurred at random at the two piezometer locations with frequencies varying between 2.5 to 5 cycles per second.

A question was raised concerning the influence of the water supply system on the pressure fluctuations in the model. Some surge was known to be present in the supply lines; and to exclude the influence of the piping system, the model was connected to an available head tank with a free water surface. Water flowed from the 6-foot-diameter head tank through a bellmouth entrance into the 12-inch pipe representing the 18-foot-diameter inlet shaft (Figure 33A).

Oscillograms of pressure fluctuations were obtained for discharges of 2,000, 4,000, and 6,000 cfs. The head differential across the gate at the model discharge representing 7,500 cfs was insufficient to prevent air entrainment into the model from the head tank and thus the test limit was 6,000 cfs. Although the peak to peak average of the pressure fluctuations was reduced by approximately 50 percent with the head tank, a maximum differential of 11.0 feet was obtained for a discharge of 6,000 cfs. The frequency of pressure fluctuations had increased slightly with those at Piezometers 1, 13, and 18 essentially in phase at from 4 to 5 cycles per second. Fluctuations at Piezometer 9 had increased to 7 cycles per second. Because it was infeasible to

attain similarity of the physical properties of the prototype and model structures, the effect of the pressure fluctuations and their frequency of occurrence can be only qualitatively evaluated.

Possible gate movement. --The short stems of the model (Figure 21A) restrained the gate and did not provide the freedom of movement that would occur on the prototype gate with long unsupported stems. To demonstrate the possibility of a prototype gate movement, the model gate was suspended on springs. The springs for the suspension of the model gate were made to have a natural period of approximately 5 cycles per second to approximately correspond with the frequency of the pressure fluctuations. It was assumed for the purpose of testing, that if the pressure forces were large enough, the gate could move at the frequency of the pressure changes.

Operation disclosed that the model gate moved up and down under the influence of the pressure changes within the gate chamber. The movement was not regular nor at a frequency of the pressure fluctuations; but at a random and lower frequency. Nevertheless, the possibility of a prototype movement was demonstrated provided (1) the natural period of the gate was near the frequency of prototype pressure fluctuations, and (2) the gate had sufficient freedom of movement to react readily to the pressure changes. The model indicated that a slight friction applied to the gate stems would damp the movement of the gate. The friction at the guides of the prototype gate resulting from unbalanced hydraulic pressure across the gate is expected to provide ample damping. Installation of the prototype gate should be carefully checked to affirm that substantial friction will be available for damping.

Cylinder-gate Top Seal

Seal problem. --The cylinder gate at the base of the junction shaft is not readily accessible so studies were made to reduce maintenance and inspection to a minimum. One of the studies concerned the seal at the top of the gate.

This seal was designed to eliminate contact of the gate and lower frame that occurs with high-pressure rubber seals; thus, the clearance between the inner surface of the cylinder gate and the outer surface of the bottom of the lower frame formed an annular space or gap between the frame and gate (Section H-H, Figure 4). The clearance gap between the seal rings placed near the top of the gate and the bottom at the lower frame changes with gate opening. Water may be discharged through this gap from the junction shaft to the tunnel under differential heads up to 277 feet. With the gate closed or nearly closed, the water flow passage clearance gap was $1/16$ inch; and as the gate opened beyond $1-1/4$ inches the gap increased to $1/2$ inch. It was impracticable to study the flow characteristics of this flow passage on a scale of 1:18 so a separate sectional model to a larger size was constructed to investigate the possibility of cavitation in the $1/16$ - and $1/2$ -inch flow passages.

Description of gate seal model. --A full-scale, 1-foot-long section of the frame seal ring and gate seal ring was constructed and installed in facilities previously used for testing rubber gate seals. The equipment consisted of a hydraulic lift for positioning the seal, a housing with transparent plastic windows for observation and an outlet pipe with a gate for controlling the downstream pressure on the gate seal (Figure 33B). Although the gate moved with respect to the frame, it was expedient on the model to simulate the same relative motion, by moving the shape representing the frame seal ring with respect to the fixed gate seal ring (Figure 33C). Piezometers were located in both shapes to study critical pressure areas. Pressure heads to a maximum of 160 feet of water upstream of the 1/2- and 1/16-inch flow passages were supplied by two 12-inch centrifugal pumps in series.

Cavitation in flow passage of preliminary gate seal. --Preliminary tests indicated the 1/2- and 1/16-inch flow passages of the gate seal to be unsatisfactory because of cavitation. For the 1/2-inch flow passage a vapor pocket formed downstream of the 1/4-inch radius near the bottom of the frame seal ring. The vapor pocket extended downstream along the frame seal ring boundary to connect with a second pocket that formed in an offset of the frame seal ring boundary (Figure 34A). A vapor pocket formed in the 1/16-inch flow passage between the two seal ring surfaces and extended downstream of the passage along the frame seal boundary (Figure 38A).

Cavitation index--Preliminary gate seal--1/2-inch flow passage. --The laboratory pump facilities could not produce full prototype differential head (277 feet), so it was necessary to use a parameter common to both model and prototype seals to investigate the possibility of cavitation in the prototype. This parameter was a cavitation index. For flow past submerged shapes at high Reynolds numbers, the distribution of pressure is a function of the boundary geometry and the presence of cavitation. The cavitation index, a dimensionless pressure relationship, K , is a measure of the presence and intensity of cavitation. It was expedient to define K_i as a value of K at which cavitation was incipient. For all conditions giving values of K larger than K_i there would be no cavitation and the pattern of flow would be unaffected. The index may be defined in several ways.

The cavitation index used for analyzing the pressure conditions in the 1/2-inch flow passage was:

$$K = \frac{h_b - h_v}{h_o - h_b}$$

where:

h_b = model pressure representing the gate recess pressure (feet of water)

h_v = vapor pressure in feet of water (atmosphere as datum)

h_o = model pressure representing pressure in 18-foot-diameter shaft (feet of water)

The numerator of this equation represents a measure of the pressure head available to prevent cavitation in the flow passage. The denominator is a measure of the differential head producing the velocity through the flow passage.

A change in the pattern of flow with a tendency toward separation, or the formation of a vapor pocket, would result in a change of the capacity of the flow passage. As vapor cavities formed and the cavitation pocket enlarged to decrease the effective area of the flow passage, the cavitation index and discharge capacity would decrease. This characteristic was used to define K_1 .

A coefficient of discharge for the flow passage, computed from the measured discharge, the area of the 1/2- by 12-inch space, and the difference in pressure head (shaft to gate recess pressure) was used.

$$C = \frac{Q}{A \sqrt{2g(h_o - h_b)}}$$

Q = model discharge (cfs)

A = area 1/2- by 12-inch space (square feet)

h_o = model pressure head, representing shaft pressure (feet of water)

h_b = model pressure head, representing gate recess pressure (feet of water)

The transition from flow unaffected by cavitation to flow with cavitation was gradual so an exact value of K_1 was not indicated; however, by a plot of the two parameters, approximate values could be determined for a study of the design. For values of K from 0 to 0.8, a vapor pocket was formed along the boundary and across the width of the frame seal model. General cavitation did not occur for values of K greater than 0.8, thus $K_1 = 0.8$. Vapor pockets due to local roughness were observed in the model before a change in the flow pattern was indicated by the index curve. A cavitation index of 0.45 was computed for the prototype. This index was based on the maximum available shaft pressure and a minimum gate recess pressure for a discharge of approximately 3,000 cfs and a 4-1/2-inch gate opening. This value was in the cavitation range (Figure 35A) so the shape was unsatisfactory. The study was then extended to replace the 1/4-inch radius with a curved boundary that would be free from cavitation.

Electric analog studies of upper gate seal--1/2-inch flow passage. --

An electric analog was utilized to reduce the time required for obtaining a cavitation-free passage shape. The analog equipment consisted of a graphite-coated paper, a potentiometer with dial reading to 1/10 of 1 percent, a precision galvanometer, and a 22-1/2-volt battery. This equipment was mounted on plyboard for use on a drafting table or desk (Figure 34B).

The seal passage cross-section shape for the 1/2-inch gap was cut from the graphite-coated paper. Electrodes were cut from aluminum foil and clamped to the paper with sponge rubber strips backed with plyboard. The contact of the electrode with the graphite coating was checked by measuring an equipotential line near the electrode. With good contact, the distance of the line from the electrode would be uniform for potentials within 1 or 2 percent of the electrode potential. Small deviations were corrected by adjusting the electrode clamps. Although not used in this study, a silver paint applied directly to the graphite-coated paper was later found to be an improvement over the aluminum foil electrodes.

To study the pressure change along the boundary, it was not necessary to establish the flow net but only the potential drop between points along the boundary. A single probe was first used to obtain the spacing of points for equal increments of potential (Figure 34B). This method proved unsatisfactory because of the difficulty of accurately measuring the distance between points. A probe with two points, one electrically insulated from the other, provided a stepwise measurement of the boundary length and the potential drop between points. Equal lengths were thus set and the precision of the potentiometer was utilized to obtain the potential drop for each step. This method overcame the inaccuracy of measuring distance for the single probe method. The change of potential between equal increments of boundary length indicated changes in velocity and pressure. This factor was used to investigate the tendency toward cavitation pressures at the flow surfaces.

Preliminary frame seal boundary--1/4-inch radius. --The potential drop along the preliminary frame seal boundary was determined from an analog model four times actual size. This potential drop was plotted against the developed length of the boundary to indicate the rate of change of the velocity at the boundary as the water flowed through the passage. For the passage to be free of cavitation, the velocity of the water must increase in a gradual manner to a maximum in the 1/2-inch flow passage. Thus the passage shape must be such that the slope of the potential drop ($\frac{d\phi}{ds}$) versus distance (S) curve increases to the maximum at the uniform section of the analog which represented the 1/2-inch flow passage. A higher velocity on the boundary than at the uniform section would be indicated by a slope steeper than that for the uniform section. The observed vapor pocket at the 1/4-inch radius in the water model (Figure 34A) coincided with the region for the steepest slope on the analog potential drop curve (Curve a, Figure 36).

The ratio of the maximum slope ($\Delta \phi_1 / \Delta S_1$), to the slope at the uniform section ($\Delta \phi_2 / \Delta S_2$) was used with the data from the water model to predict cavitation. The velocity at the 1/4-inch radius was related to the velocity in the uniform section by

$$\frac{V_1}{V_2} \approx \frac{\Delta \phi_1 / \Delta S_1}{\Delta \phi_2 / \Delta S_2} \quad (\text{Figure 36D}) \quad (1)$$

The pressure change from S_1 to S_2 from the Bernoulli equation is

$$h_1 - h_2 = \frac{V_2^2}{2g} - \frac{V_1^2}{2g} \quad \text{losses assumed negligible}$$

and by substitution

$$h_1 - h_2 \approx \frac{V_2^2}{2g} - \left(\frac{\Delta \phi_1 / \Delta S_1}{\Delta \phi_2 / \Delta S_2} \right)^2 \frac{V_2^2}{2g} \quad (2)$$

or

$$h_1 - h_2 \approx \left[1 - \left(\frac{\Delta \phi_1 / \Delta S_1}{\Delta \phi_2 / \Delta S_2} \right)^2 \right] \frac{V_2^2}{2g} \quad (3)$$

The slope of the potential drop curve indicated the maximum velocity along the boundary would be 1.4 times the velocity in the uniform section (Curve a, Figure 36). For cavitation to occur along the boundary, h_1 (Equation 3) must equal the vapor pressure of water (minus 27 feet of water referred to atmospheric at Denver, Colorado). Then Equation 3 becomes

$$h_1 \approx h_2 + \left[1 - (1.4)^2 \right] \frac{V_2^2}{2g} \quad (4)$$

Data used for the computed values of K for Figure 35A of the water model were substituted into Equation 4. Computed values of h_1 indicated negative pressures greater than 27 feet for values of $K < K_1$ and thus indicated cavitation. For example, from model data with cavitation present,

$$h_2 = 0.5 \text{ foot of water}$$

$$\frac{V_2^2}{2g} = 45 \text{ feet of water}$$

$$h_1 \approx 0.5 + \left[1 - (1.4)^2 \right] 45$$

$$h_1 \approx -42.7 \text{ feet}$$

Cavitation was indicated because the negative value for h_1 obtained is greater than the -27 feet of water or actual vapor pressure. For $K > K_j$, the computed values of h_1 would have smaller negative or even positive values and would indicate absence of cavitation. It was concluded that the analog indications of cavitation were satisfactory, and the method could be applied to the study of additional shapes.

Frame seal boundary 2 radii, 3/4 and 1-3/4 inches. --The surface profile of a two-dimensional jet from a slot which defines a constant velocity and pressure boundary was not practicable for the frame seal ring because of machining cost. Slight variations in the profile could readily produce increases in local velocities and decreases in pressures to cause cavitation. Vapor pockets were observed in the water model at local variations in the preliminary boundary surface. A frame seal ring boundary consisting of two radii (3/4 and 1-3/4 inches) was studied as a means of obtaining an increasing velocity from the shaft to the uniform 1/2-inch section of the seal flow passage (Figure 36B). An analog study of the flow passage four times actual size gave a ratio of the maximum to the uniform section velocity of 1.2 near the point of tangency of the 1-3/4-inch radius and the wall of the 1/2-inch flow passage (Curve b, Figure 36). The pressure in this region would be reduced by 44 percent of the velocity head in the 1/2-inch flow passage or approximately -17 feet of water for a velocity head of 45 feet. This seal ring shape was an improvement over the preliminary design, but vapor pressure was indicated for a velocity head of approximately 61 feet which was much less than the 250 feet for a 4.5-inch gate opening in the prototype. The shape was unsatisfactory because of the rapid velocity change near the tangent point of the 1-3/4-inch radius and the wall of the 1/2-inch flow passage.

Frame seal boundary of 3 radii (0.555, 1.182, and 2.39 inches). --The previous test showed that a more gradual curvature was needed near the tangent point of the 1-3/4-inch radius and the wall of the 1/2-inch flow passage. A compound curve of 3 radii that approximated an ellipse was used in place of the 2-radii curve. The minor axis of the approximate ellipse was set at 0.88 inch and the major axis at 1.50 inches. This gave a frame seal boundary with radii of 0.555, 1.182, and 2.39 inches (Figure 36C).

The slope of the potential drop curve for this design progressively increased with an increase in distance along the boundary. The slope reached a maximum at the entrance to the 1/2-inch flow passage. This indicated that the maximum velocity was in the 1/2-inch flow passage (Curve c, Figure 36). No subatmospheric pressure was indicated by the analog for the 3-radii design, and the frame seal on the water model was machined to this shape.

Cavitation index--3 radii frame seal--1/2-inch flow passage. --Cavitation did not occur along the flow passage boundary with the 3-radii curve in the 1-foot-long water model for the maximum available laboratory pressure of 160 feet of water and a discharge of 3.9 cfs. The pressure of -13 feet at Piezometer B was 6 feet lower

than the pressure of -7 feet, Piezometer A (Figure 35F), in the 1/2-inch flow passage for a differential head of 112 feet. This indicated that the velocity in the flow passage at Piezometer B was higher than in the 1/2-inch flow passage. This reduction in pressure was not evident in the analog model. A further increase in the radius of curvature near the tangent point with the 1/2-inch flow passage wall would have increased the pressure in this region. The model jet was discharging into a pressure of -10 feet of water with a 112-foot differential head. With a minimum water surface in Adaminaby Reservoir approximately 70 feet of back pressure would be available for gate openings greater than 4-1/2 inches, thus the low pressure was not considered critical and the boundary shape was recommended.

Cavitation at frame seal offset. --Cavitation occurred in the 1/2-inch offset of the frame seal boundary downstream from the 1/2-inch flow passage (Figures 37A and 35B). The offset was increased to raise the pressure at the jet contraction and cause a separation of the flow from the boundary of the offset. The offset was limited to a maximum of 1 inch by the gate guides (an increase of 1/2 inch from the preliminary design) (Figure 35F). Cavitation occurred with the 1-inch offset but no decrease in the coefficient of discharge could be detected for the maximum pressure head and discharge of the laboratory pumps (Figures 35C and 37B).

Severe cavitation occurred at the 1-inch offset for a gate opening of 2-9/16 inches. The jet from the 1/2-inch flow passage was deflected across the offset by the gate seal ring (Figure 37C). This prevented a return flow and resulted in cavitation and a decrease in the discharge coefficient. A computed index for this opening on the prototype was in the cavitation region (Figure 35D). Flow conditions were improved for a gate opening of 4 inches but were still unsatisfactory for the 2-9/16-inch opening.

Cavitation could be eliminated by sufficiently increasing the amount of the offset to provide a return flow as evidenced by tests for the 4-inch opening. A discussion with the designers resulted in the elimination of the offset in the frame seal ring (Figures 37D, 35F). This change eliminated the offset in the seal ring boundary but formed an offset approximately 2 inches at the six 7-1/2-inch-wide upper gate guides. An offset of 6-1/2 inches existed between the frame seal boundary and other parts of the lower frame. The offset of 2 inches at the guides was considered sufficient because no cavitation and no decrease in coefficient could be obtained for this distance in the model (Figure 35E). The computed index for the prototype indicated satisfactory pressures would exist in the flow passage. No critical gate opening was discerned in the model between 0 and 5 inches, and none would be expected for larger openings because of increased back pressures and decreased shaft pressures. The 3-radii curve and 4-1/4-inch tangent was recommended for the lower frame seal boundary (Figure 39).

Preliminary gate seal boundary--1/16-inch flow passage.--

The gap of 1/16-inch between the gate seal ring and the final frame seal ring (gate openings less than 4-1/2 inches) was set up on the full scale sectional model to study the cavitation tendencies. The side of the 1/16-inch flow passage formed by the surface of the frame seal was parallel to the skin plate of the gate and the gate seal face. The preliminary gate seal ring was 1-1/4 inches thick with a 45° chamfer from the top surface for a 1/4-inch distance down from the top surface, a 1/4-inch flat face at the inner diameter and a 30° chamfer at the bottom (Figure 35D). The 30° slope was provided to facilitate the positioning of the gate as it neared the closed position.

A vapor cavity formed within and extended downstream of the 1/16-inch flow passage (Figure 38A). The dimensions of the flow passage between the frame and gate seal for the gate in the closed or nearly closed position formed a short tube in which water flowing through the passage first contracted at the upstream end of the passage and then expanded to fill the downstream end. The contraction and expansion of flow was sufficient to produce vapor pressure within the passage. The coefficient of discharge for the flow passage could not be used to define K_1 because of the difficulty of accurately measuring the model discharge. A pressure factor was substituted for the coefficient in this study. This pressure factor was the shaft pressure (h_0) minus the pressure in the contraction (h_p) divided by the shaft pressure minus the gate recess pressure (h_b). The pressure factors were constant with decreasing values of K until K equaled approximately 0.30. The pressure factor values then increased at a rate of approximately 2:1 with decreasing values of K . Cavitation was present for all values of K below about 0.30. The computed index of 0.34 for the prototype was considered to be in a critical region.

The gate seal shape was modified in an attempt to eliminate the conditions causing the short tube flow. The 1/4-inch face of the gate seal was reduced to 1/16 inch. A flow contraction formed at the upstream end of the passage and expanded along the 45° chamfer to cause cavitation (Figure 38B). The short tube action was not eliminated from the design because of the 45° surface and the gate seal was unsatisfactory.

Recommended 1/16-inch flow passage.--A modification of the gate seal ring to eliminate the vapor cavity in the 1/16-inch constriction was based on the results of the tests on the frame seal ring. An increase of pressure at the jet contraction caused by a separation of the flow from the boundary was required to prevent cavitation. A discussion of this problem with the designers resulted in the elimination of the 45° chamfer on the inner diameter of the gate seal ring. The gate seal ring was 1-1/4-inches thick and had a 1/8-inch vertical face down from the top surface at the inner diameter and a 30° chamfer at the bottom (Figure 39).

The length of flow passage was 1/8 inch or equal to the minimum length of a short tube when based on the 1/16-inch gap between the frame and gate seal rings. The exit of the minimum flow section was now at the top surface of the gate seal ring. Although cavitation at the downstream end of the 1/8-inch-long flow passage was possible, the seal was considered acceptable. No damage to the frame or gate seal rings should occur because any vapor cavities that form will collapse within the water in the gate recess.

Pressure change on gate seal ring for gate openings 0 to 5.5 inches. --Pressures were measured on the 30° chamfered surface of the gate seal ring to study any condition that might induce a vertical movement of the gate as the gate is raised and the clearance between the frame and gate seal rings increases from 1/16 to 1/2 inch.

Because of the lower heads used in the model study a pressure factor was employed to determine the change of pressure on the seal at the higher prototype heads. The pressure factor used was:

$$\text{Pressure factor} = \frac{h_o - h}{h_o - h_b}$$

where

h = pressure on 30° chamfered surface, feet of water

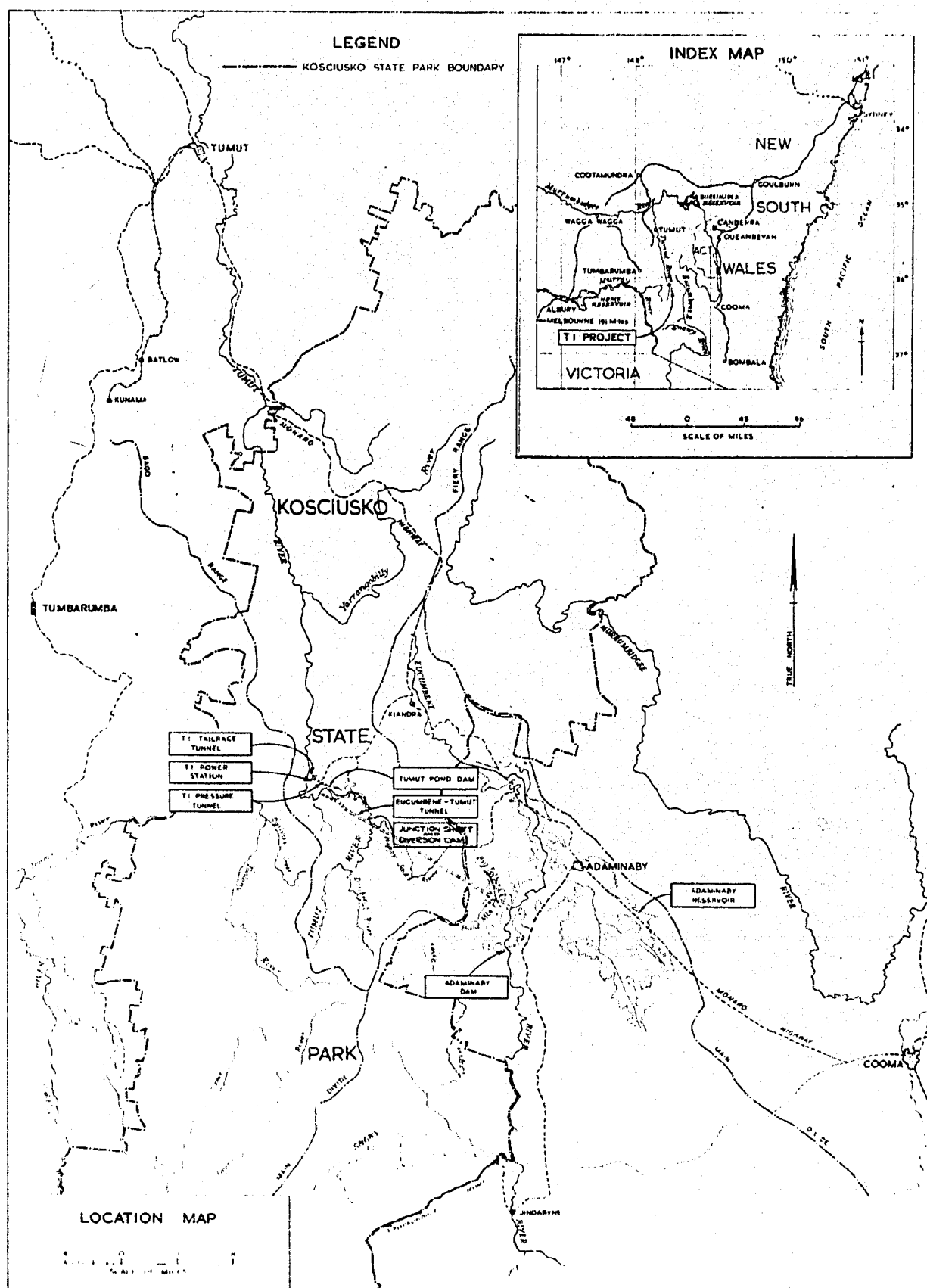
h_o = shaft pressure, feet of water

h_b = gate recess pressure, feet of water

The pressure factor varied on approximately a straight line relationship from 0.11 to 0.85 between gate openings of 4 and 4-3/4 inches (Figure 40).

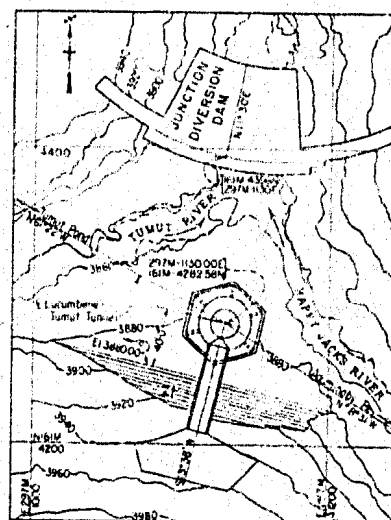
This study showed that the pressure on the 30° chamfer surface would change at a rapid rate from the shaft pressure to the gate recess pressure in less than 1 inch of gate movement. Pressures for the prototype gate can be evaluated by using the pressure factor and computed values of the prototype shaft and gate recess pressures.

Any tendency for movement of the gate by pressure fluctuations in the shaft or gate chamber may be accentuated at gate openings between 4 and 4-3/4 inches because of the rapid rate at which the seal pressure changes with opening in this range of gate travel. No movement was noted in the gate seal model but the tendency for movement with the rigidly supported model would be less than for the prototype gate supported by three 330-foot-long stems.



CIVIL DESIGN DIVISION		SNOWY MOUNTAINS HYDRO ELECTRIC AUTHORITY	
DRAWN	SUBMITTED	T1 PROJECT	
6 M 2	1/1/1963	POWER STATION, PRESSURE SHAFTS AND	
TRACED	RECOMMENDED	TAILRACE TUNNEL	
11 M 2	2/5/1963	LOCATION AND VICINITY MAPS	
PRINTED	1/1/1963	1:50,000 N.T.M.	
		20th April 1963	

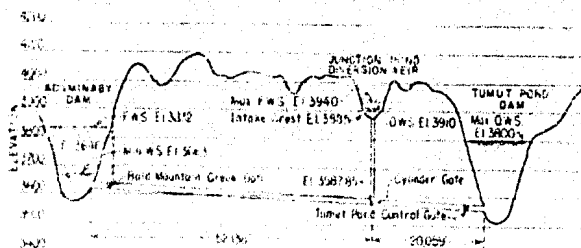
726 149 MAY 1981



SCALE OF FEET



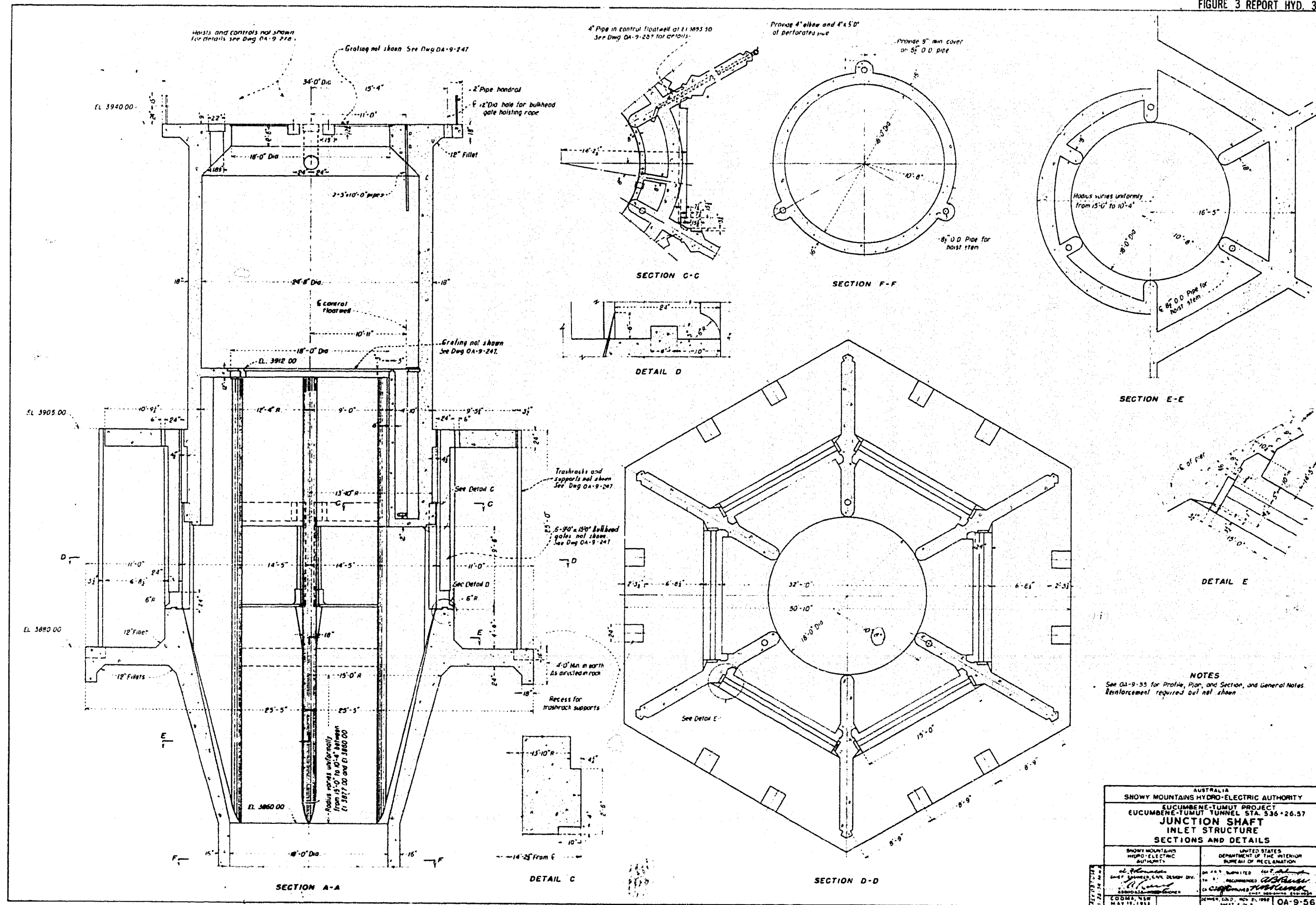
SCALE OF 100

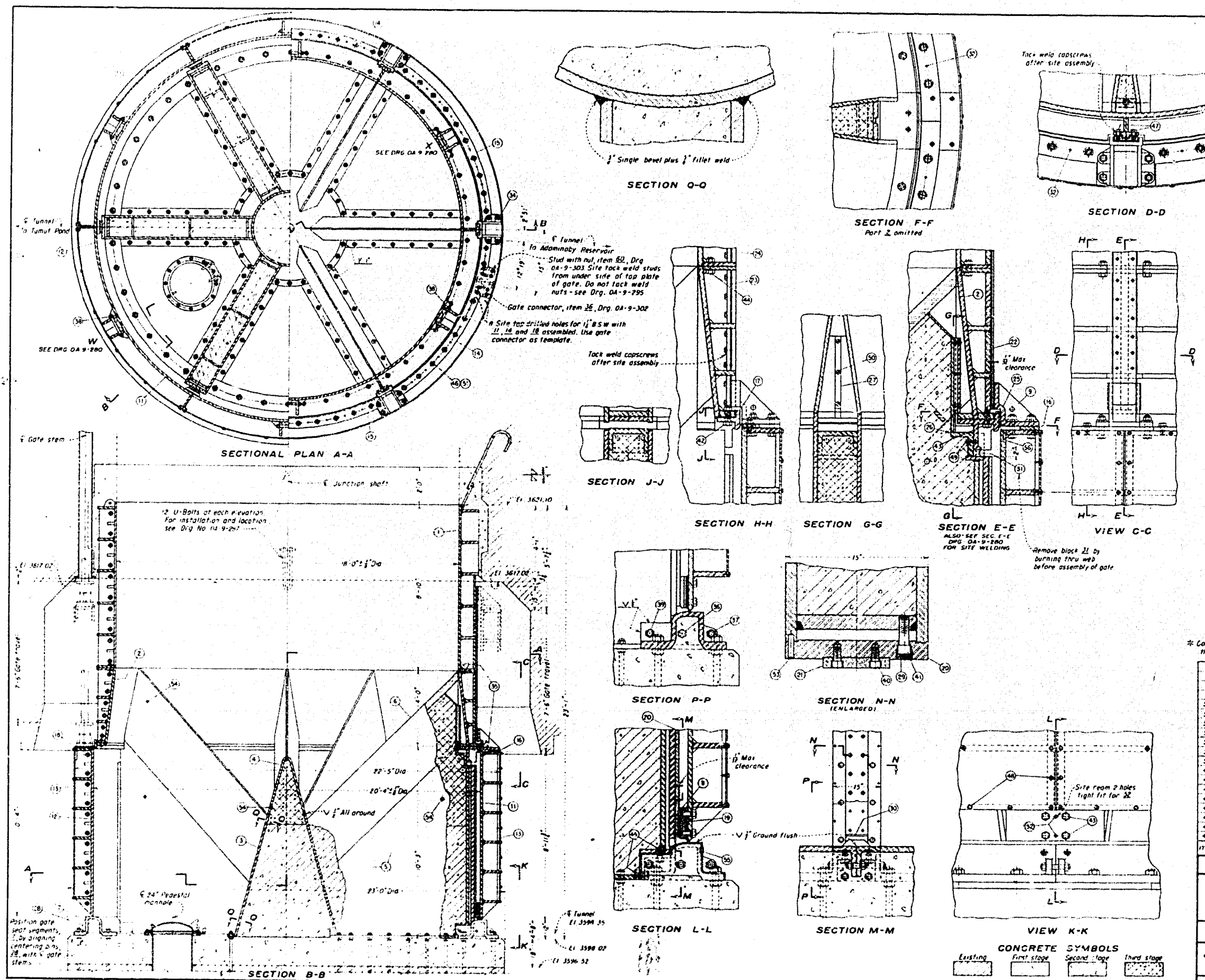


TUNNEL PROFILE FROM ADAMINARY TO TUMUT POND

EUCUMBENE - TUMUT TUNNEL JUNCTION SHAFT

JUNCTION SHAFT STRUCTURE





LIST OF DRAWINGS

ASSEMBLY AND SITE WELDING DETAILS (ITEMS 42 TO 56) OA-9-279
 SITE WELDING DETAILS (ITEMS 1 AND 2) OA-9-280
 UPPER AND LOWER FRAMES (ITEMS 3 TO 6) OA-9-281
 CONE CONE CAP-SPLITTER-SPLITTER CAP (ITEMS 7 TO 9) OA-9-282
 GATE SEAT SEGMENT - BRACKET (ITEMS 10 TO 12) OA-9-283
 GATE SEAT SEGMENT - BRACKET (ITEMS 13 TO 15) OA-9-284
 GATE SKIN PLATE - SEAL SEGMENTS (ITEMS 16 TO 19) OA-9-285
 GUIDES - STUDS - DETAILS (ITEMS 20 TO 41) OA-9-286

REFERENCE DRAWING

20.33' DIA. CYLINDER GATE AND HOIST
 GENERAL INSTALLATION OA-9-278

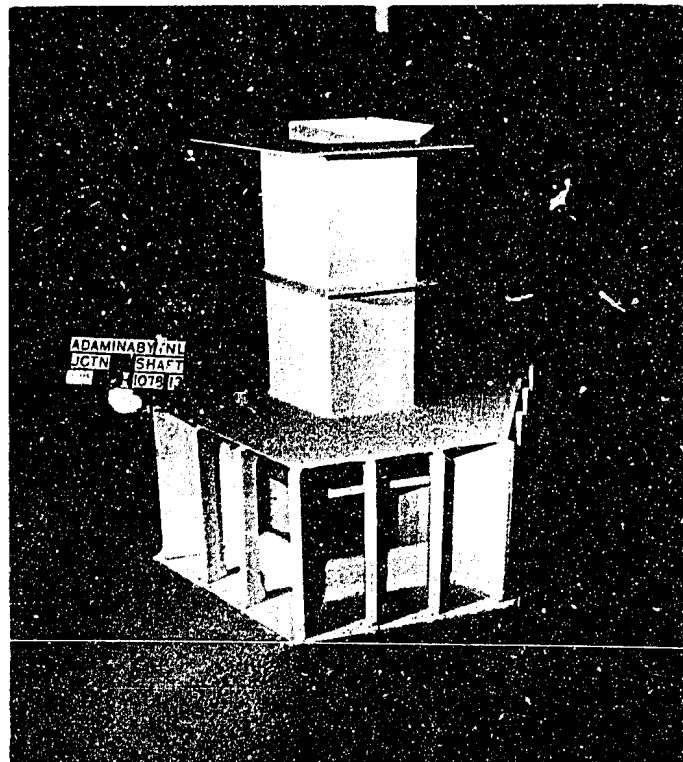
NOTES

Welding S.A.A. Boiler code J.S. No. C.B.1 Part 1-1951
 Welding symbols S.A.A. A.S. No. C.2.1-1951
 All welding symbols shown to be site welded
 Tack weld all bolts and nuts after site assembly, except as noted

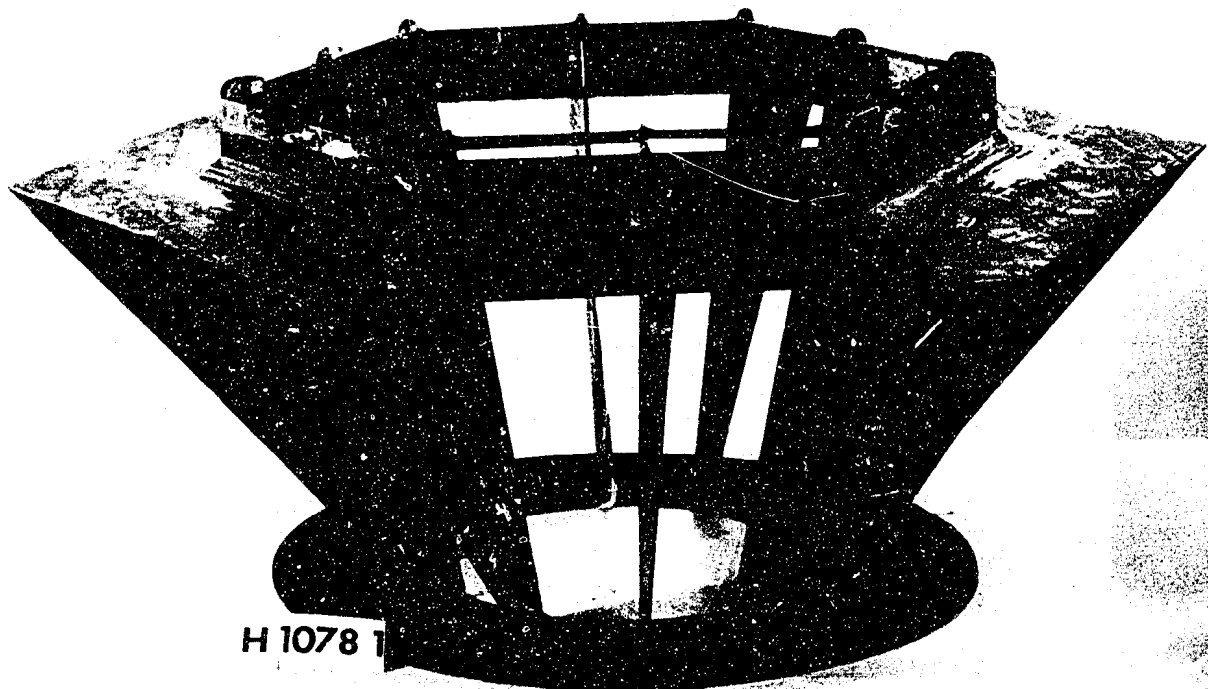
* Contractor to furnish suitable high-class commercial materials that are satisfactory to the Engineer

ITEM	DESCRIPTION	MATERIAL SPECIFICATION
35	1" Dia. gasket	20 Rubber
36	1/2" BSP (tap) socketed hd plug	18 Steel
37	1/2" BSP (tap) socketed hd plug	25 Steel
38	1" Dia. x 3/8" long dowel	96 Steel
39	1" Dia. x 3/8" long dowel	12 Steel
40	1/2" Std plain washer	57 Steel
41	1/2" BSW x 2 1/2" hex hd screw	19 Steel
42	1/2" BSW x 2 1/2" hex hd bolt	12 Steel
43	1/2" BSW x 2 1/2" hex hd bolt	340 Stainless Steel
44	1/2" BSW x 2 1/2" hex hd bolt	216 Steel
45	1/2" BSW x 2 1/2" hex hd bolt	57 Steel
46	1/2" BSW x 2 1/2" hex hd bolt	24 Steel
47	1/2" BSW x 2 1/2" hex hd bolt with hex nut	48 Steel
48	1/2" BSW x 2 1/2" hex hd bolt with hex nut	36 Steel
49	1/2" BSW x 2 1/2" hex hd bolt with hex nut	36 Steel
50	1/2" BSW x 2 1/2" hex hd bolt with hex nut	36 Steel
51	1/2" BSW x 2 1/2" hex hd bolt with hex nut	36 Steel
52	1/2" BSW x 2 1/2" hex hd bolt with hex nut	36 Steel
53	1/2" BSW x 2 1/2" hex hd bolt with hex nut	36 Steel
54	1/2" BSW x 2 1/2" hex hd bolt with hex nut	36 Steel
55	1/2" BSW x 2 1/2" hex hd bolt with hex nut	36 Steel
56	1/2" BSW x 2 1/2" hex hd bolt with hex nut	36 Steel

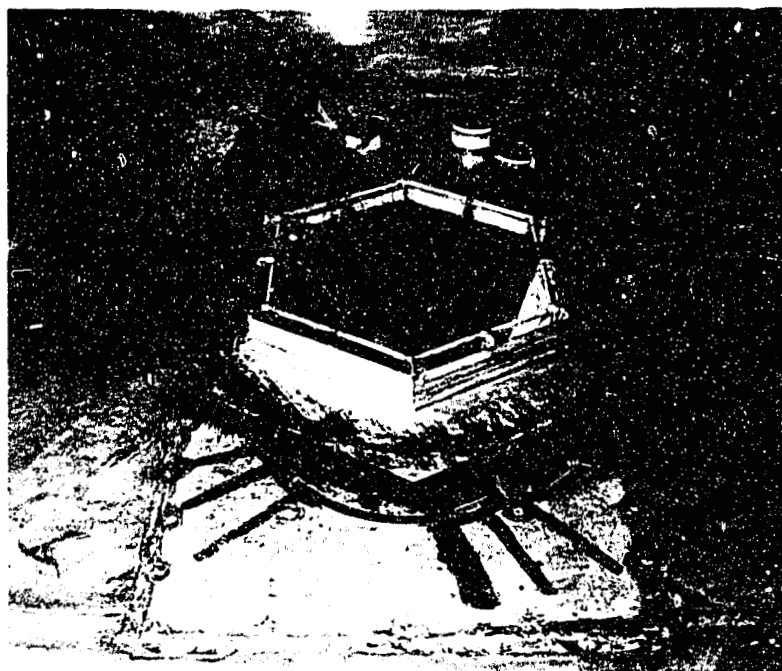
NO. 1000 SUBMITTED
 BY E.O. RECOMMENDED
 ON 10/1/51 APPROVED
 DESIGNER, CIVIL, NOV. 10, 1951
 SHEET OF 8 OA-9-279



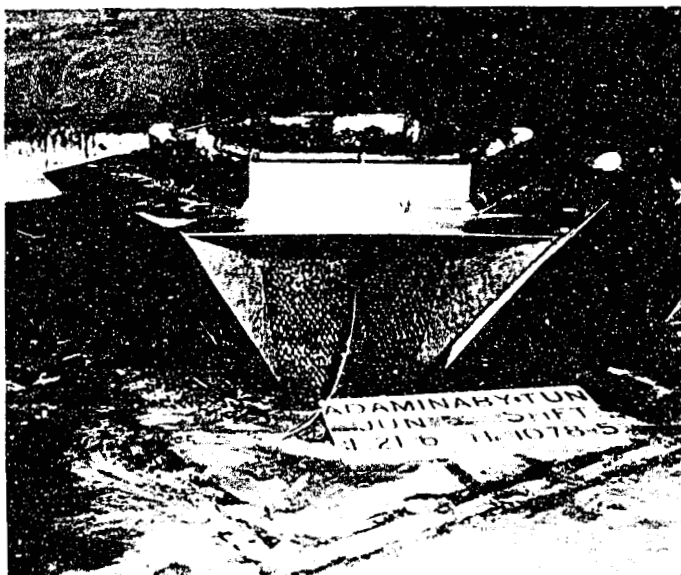
A. 1:21.6 SCALE MODEL-SHAFT INLET STRUCTURE



B INLET TEMPLATES AND FRAMEWORK
EUCUMBENE-TUMUT TUNNEL JUNCTION SHAFT
MODEL INLET AND CONSTRUCTION DETAILS



A. WIRE LATH ON INLET FRAMEWORK

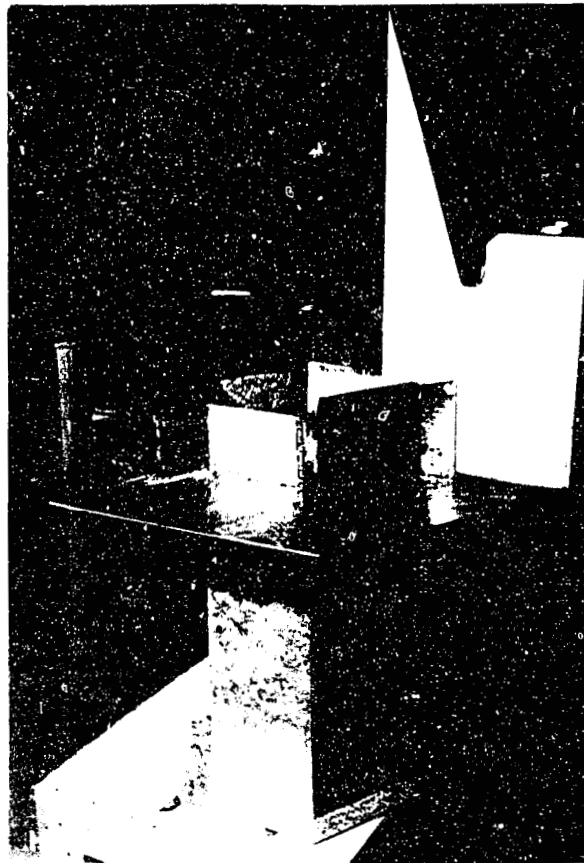


B. CEMENT-SAND MORTAR COATING

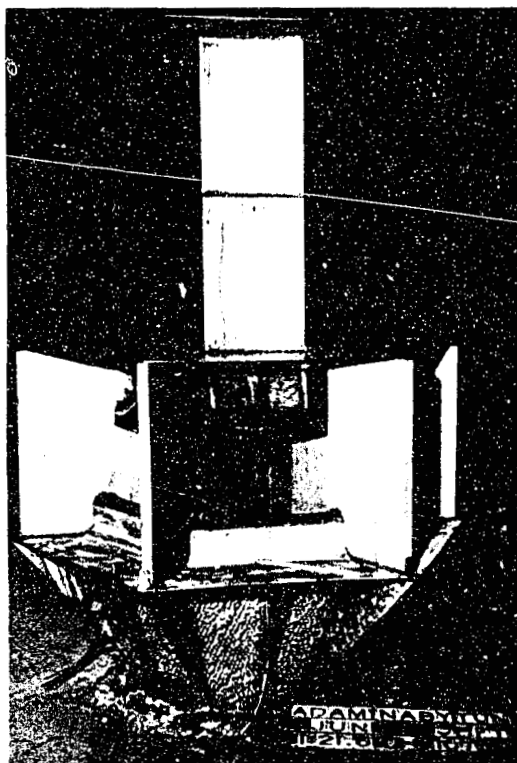


C. FINISHED INLET SURFACE

EUCUMBENE-TUMUT TUNNEL JUNCTION SHAFT
CONSTRUCTION DETAILS OF MODEL INLET OVERFLOW SECTION



A. INLET ENCLOSURE AND WOODEN PIER



B. INLET STRUCTURE



C. TOPOGRAPHY

EUCUMBENE-TUMUT TUNNEL JUNCTION SHAFT
CONSTRUCTION DETAILS OF INLET STRUCTURE AND TOPOGRAPHY



A. INLET CREST-FREE FLOW OPERATION



B. WATER SURFACE WITHIN INLET



C. FLOW OF WATER AND ENTRAINED AIR DOWN SHAFT, EXPOSURE APPROXIMATELY 1/10,000 SEC.

EUCUMBENE-TUMUT TUNNEL JUNCTION SHAFT
FREE FLOW AT INLET CREST DISCHARGE
REPRESENTING 3,000 CFS-RES. EL. 3889.6



A. INLET CREST-FREE FLOW OPERATION



B. WATER SURFACE WITHIN INLET

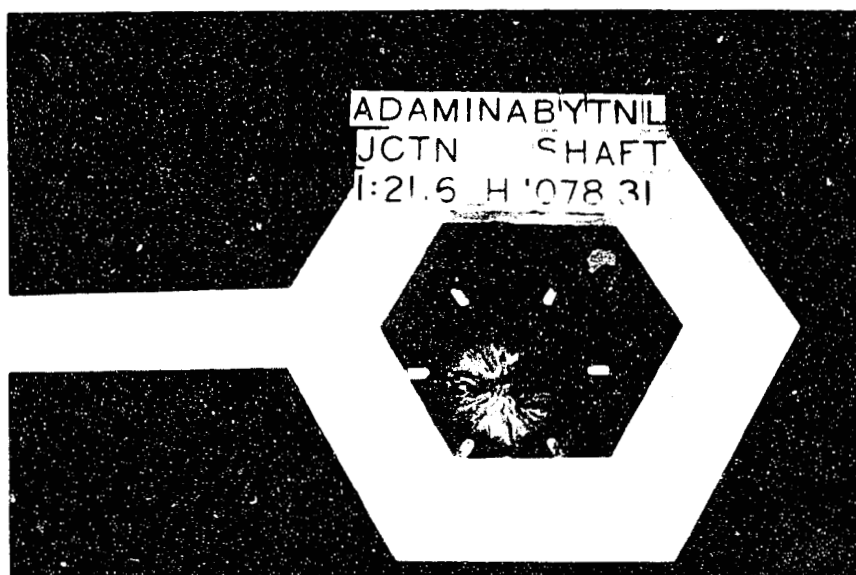


C. FLOW OF WATER AND ENTRAINED AIR DOWN SHAFT. EXPOSURE APPROXIMATELY 1/10,000 SEC.

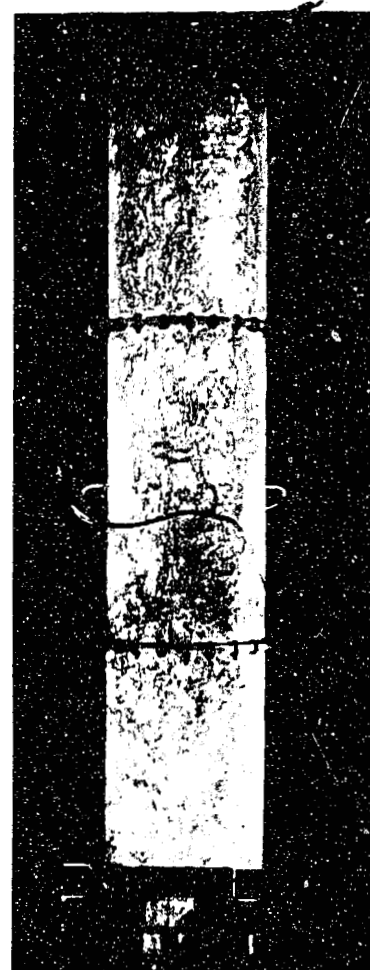
EUCUMBENE-TUMUT TUNNEL JUNCTION SHAFT
FREE FLOW AT INLET CREST DISCHARGE
REPRESENTING 5,000 CFS-RES. EL. 3891.3



A. INLET CREST-FREE FLOW OPERATION



B. WATER SURFACE WITHIN INLET-NOTE NAPPE FLOWING AGAINST SURFACE AT RIGHT.



C. FLOW OF WATER AND ENTRAINED AIR DOWN SHAFT, EXPOSURE APPROXIMATELY 1/10,000 SEC.

EUCUMBENE-TUMUT TUNNEL JUCTION SHAFT
FREE FLOW AT INLET CREST DISCHARGE
REPRESENTING 9,000 CFS-RES. EL. 3893.2

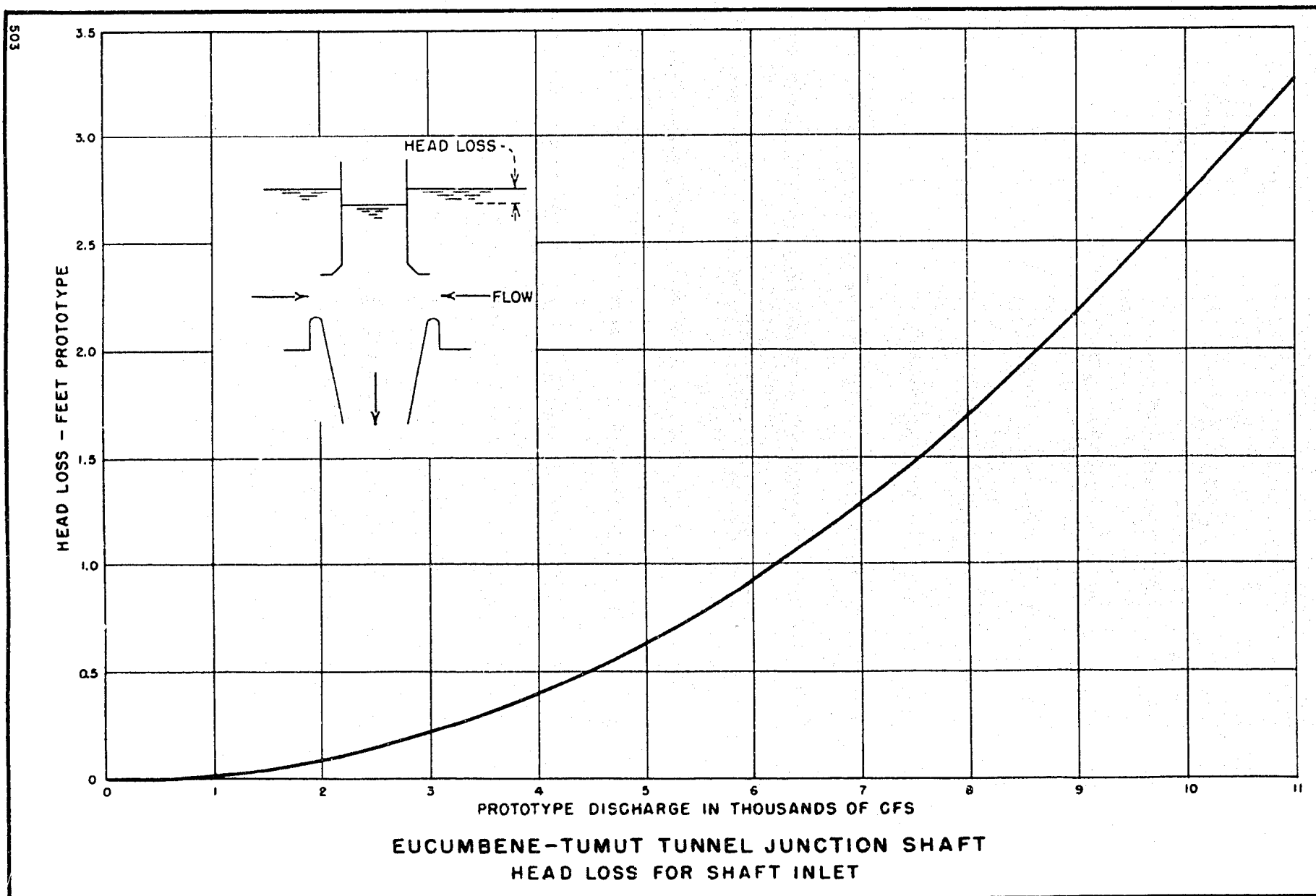
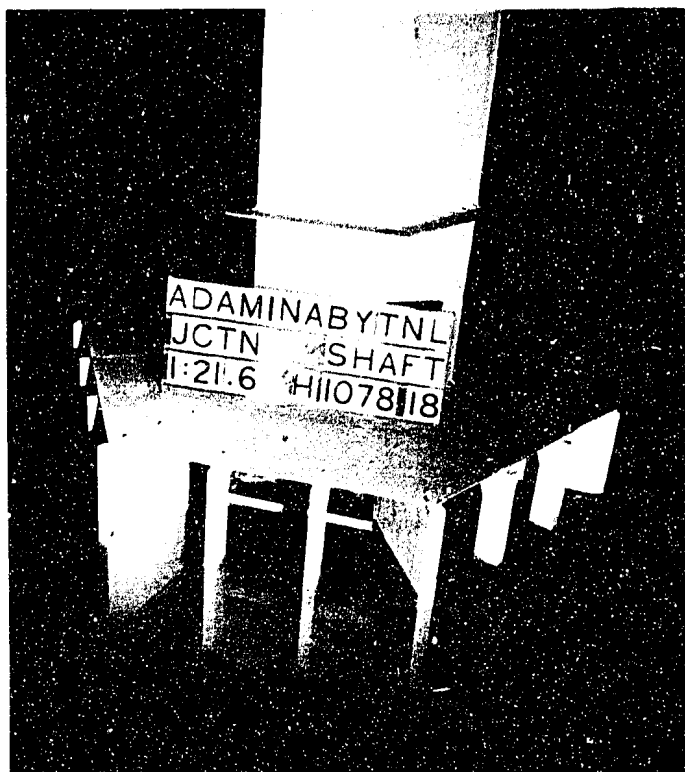


FIGURE 11
REPORT HYD.382



A. DISCHARGE 3,000 CFS
RESERVOIR ELEVATION 3895

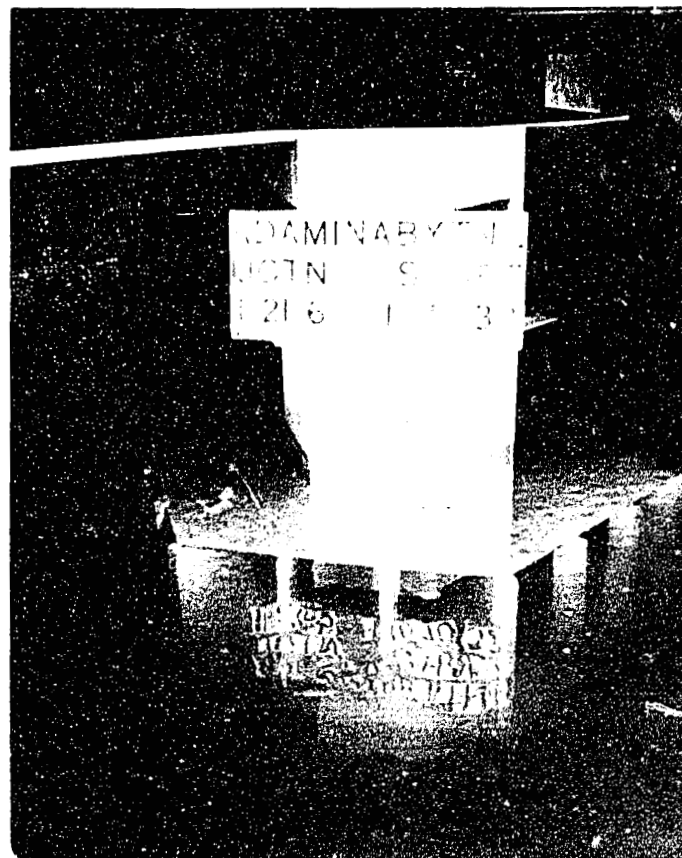


C. DISCHARGE 5,000 CFS,
RESERVOIR ELEVATION 3900

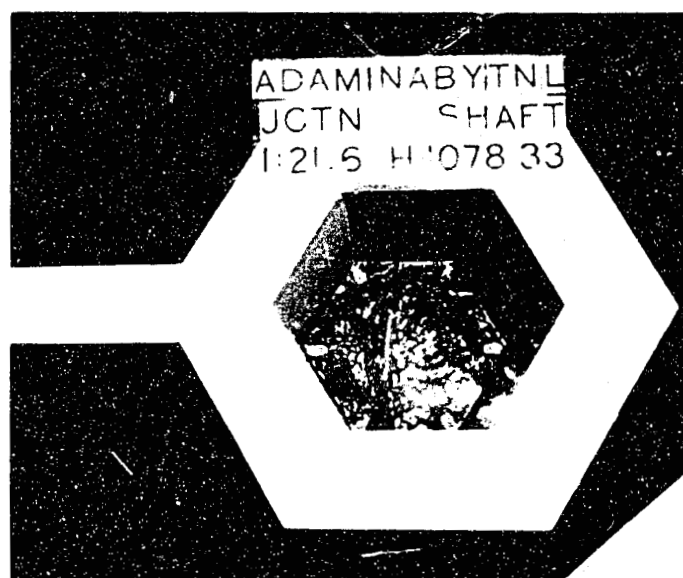


B. SHAFT WATER SURFACE-3,000 CFS

EUCUMBENE-TUMUT TUNNEL JUNCTION SHAFT
SUBMERGED FLOW AT INLET CREST DISCHARGES
REPRESENTING 3,000 AND 5,000 CFS

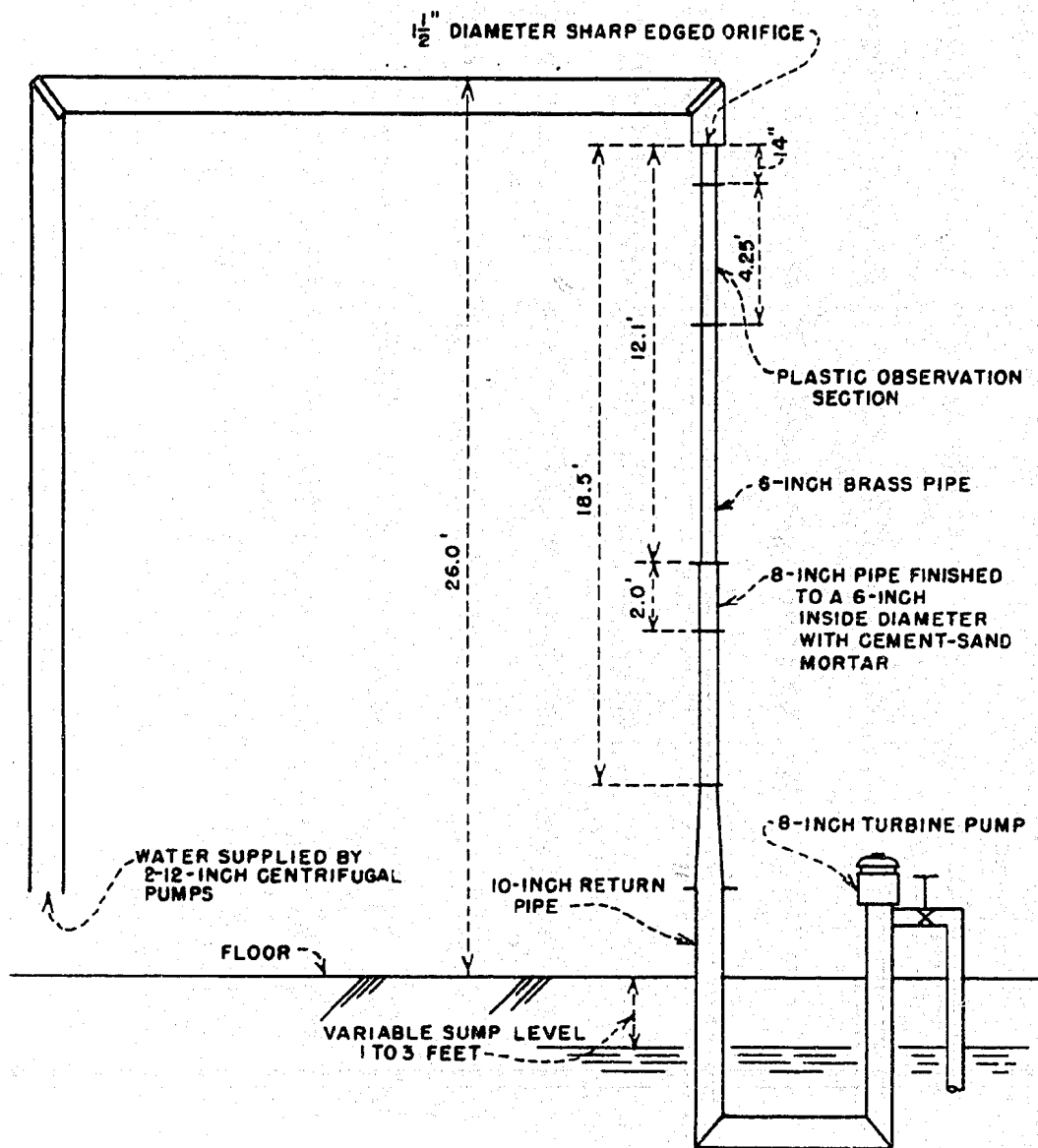


A. RESERVOIR WATER SURFACE ELEVATION
AT 3910



B. SHAFT WATER SURFACE

EUCUMBENE-TUMUT TUNNEL JUNCTION SHAFT
SUBMERGED FLOW AT INLET CREST
DISCHARGE REPRESENTING 9,000 CFS



EUCUMBENE-TUMUT TUNNEL JUNCTION SHAFT
SCHEMATIC MODEL OF SHAFT
WITH INLET CONTROL



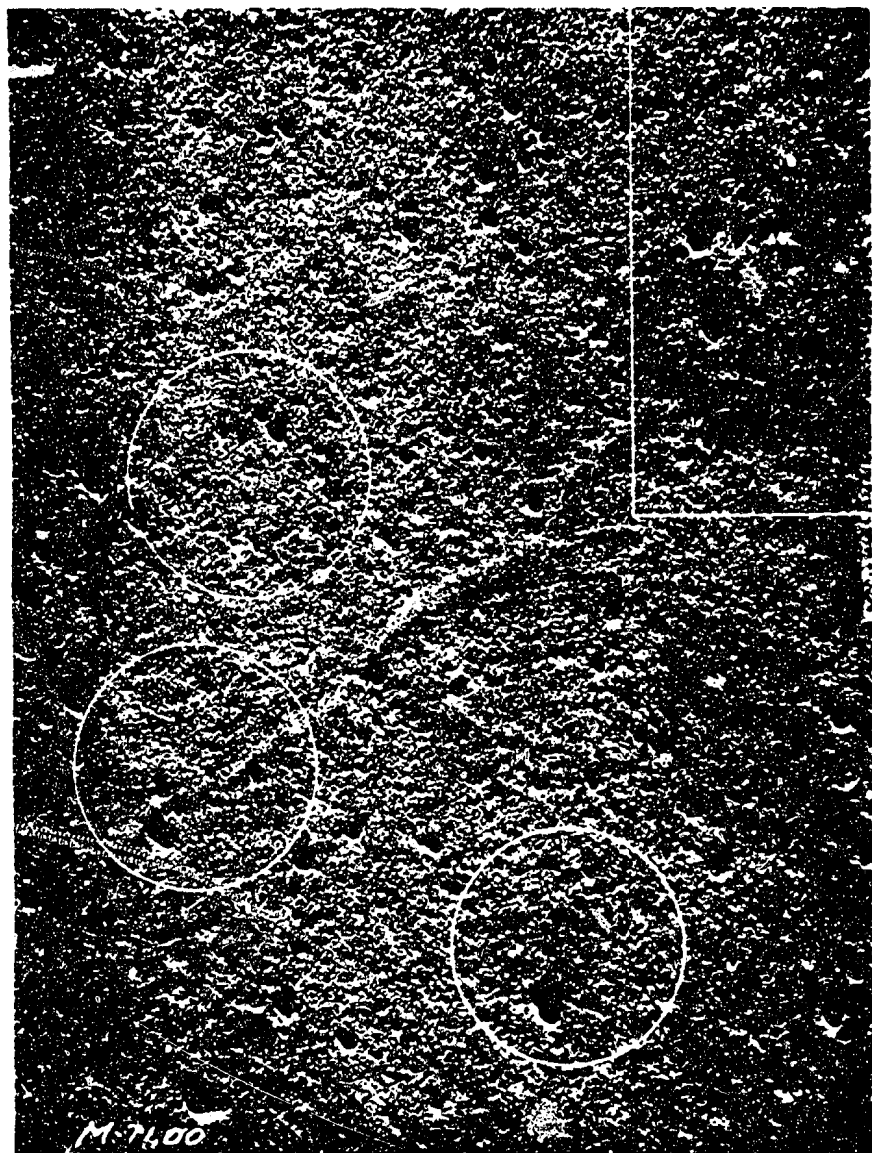
A. JET APPEARANCE 1/100
SECOND EXPOSURE



B. HIGH-SPEED PHOTOGRAPHY OF TURBULENT SURFACE
ERUPTIONS-1/10, 000 SEC.

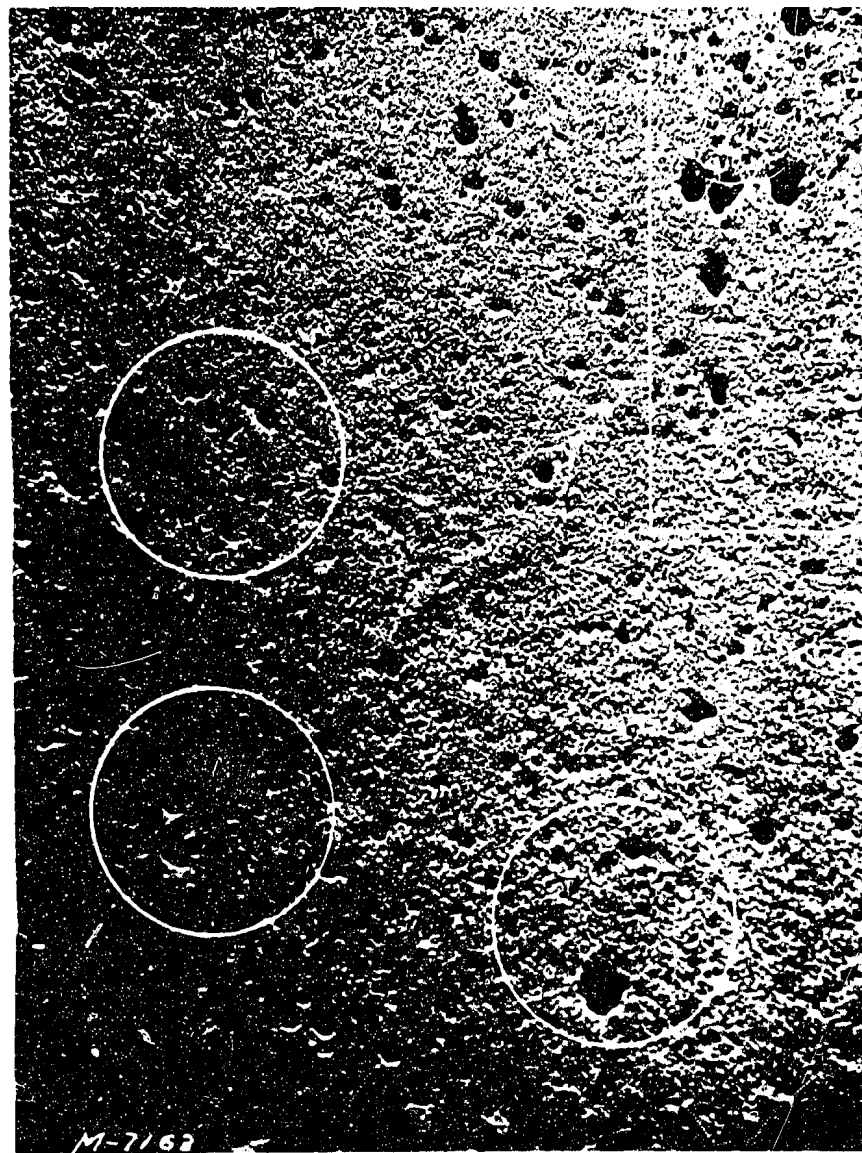


DISCHARGE CONTROL 1-1/2 INCH SHARP EDGED ORIFICE
14 INCHES ABOVE 51 INCH LENGTH OF 6 INCH I.D. PLASTIC
PIPE DISCHARGE=0.81 CFS, VELOCITY=110 FPS, PRESSURE
AROUND JET=9 INCHES OF WATER ABSOLUTE, VAPOR
PRESSURE=7 INCHES OF WATER, JET EXPANSION=1 TO 50



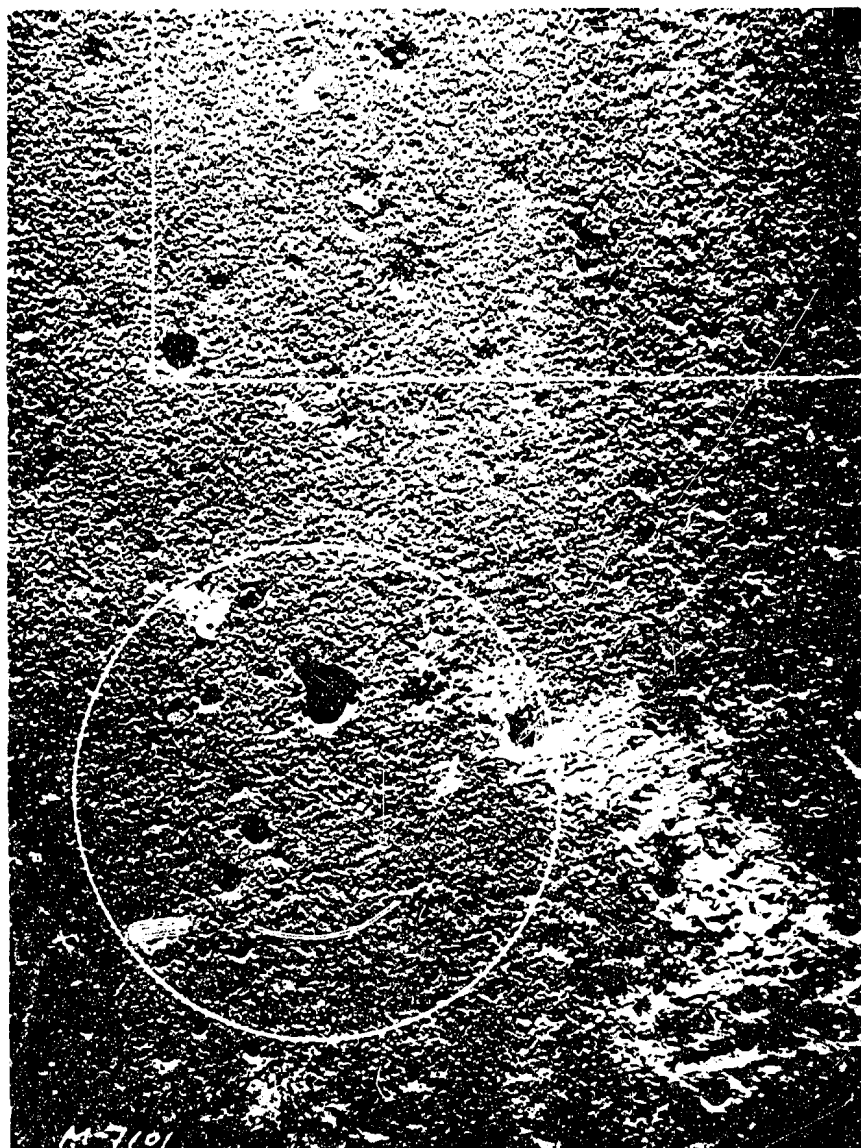
SURFACE AFTER 25 HOURS TEST

FLOW —→



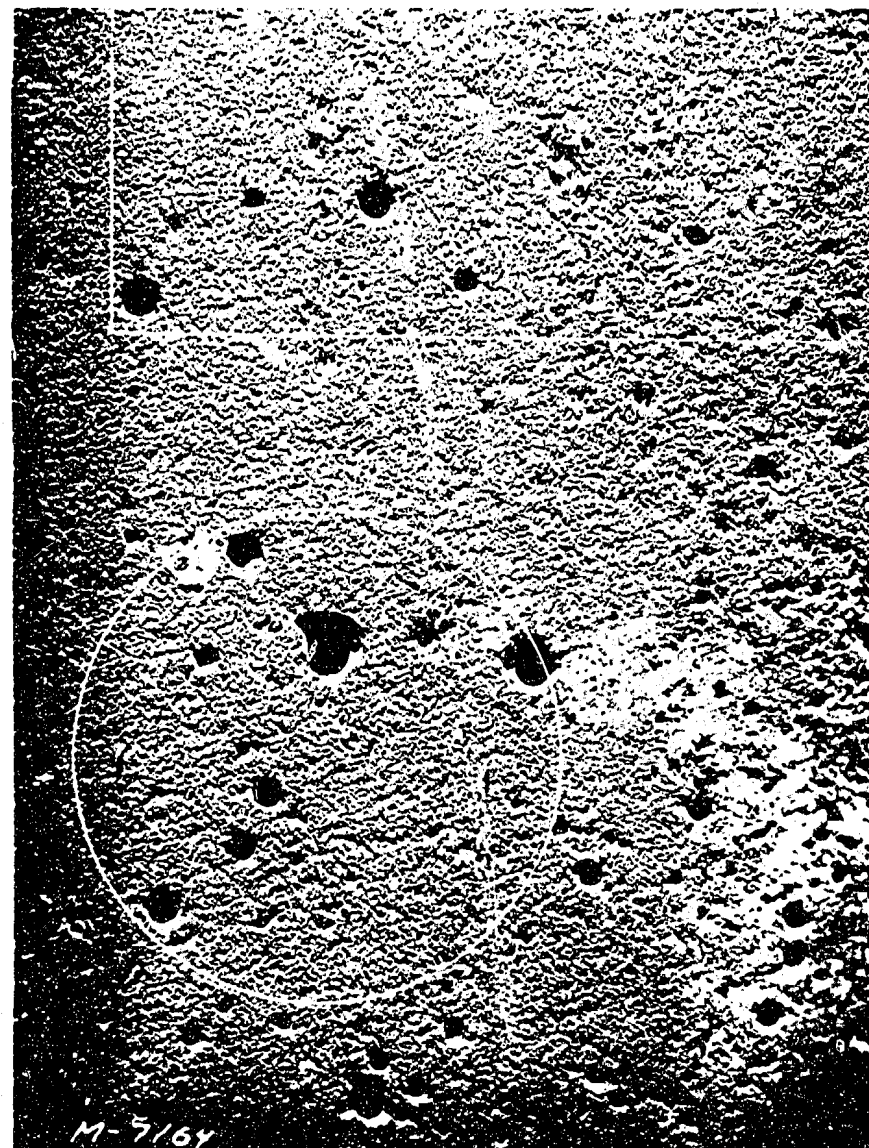
SURFACE AFTER 100 HOURS TEST

EUCUMBENE-TUMUT TUNNEL JUNCTION SHAFT
 PHOTOMICROGRAPHS OF SURFACE OF CONCRETE LINED PIPE DAMAGED BY CAVITATION -
 FIRST AREA - APPROXIMATELY 2-INCHES FROM TOP OF 2-FOOT PIPE SECTION MAGNIFIED
 12X - MODEL WITH INLET CONTROL



SURFACE AFTER 25 HOURS TEST

↑
FLOW



SURFACE AFTER 100 HOURS TEST

EUCUMBENE-TUMUT TUNNEL JUNCTION SHAFT
 PHOTOMICROGRAPHS OF WALL OF CONCRETE LINED PIPE DAMAGED BY CAVITATION -
 SECOND AREA APPROXIMATELY 2 INCHES FROM TOP OF 2-FOOT PIPE SECTION
 MAGNIFIED 12X-MODEL WITH INLET CONTROL



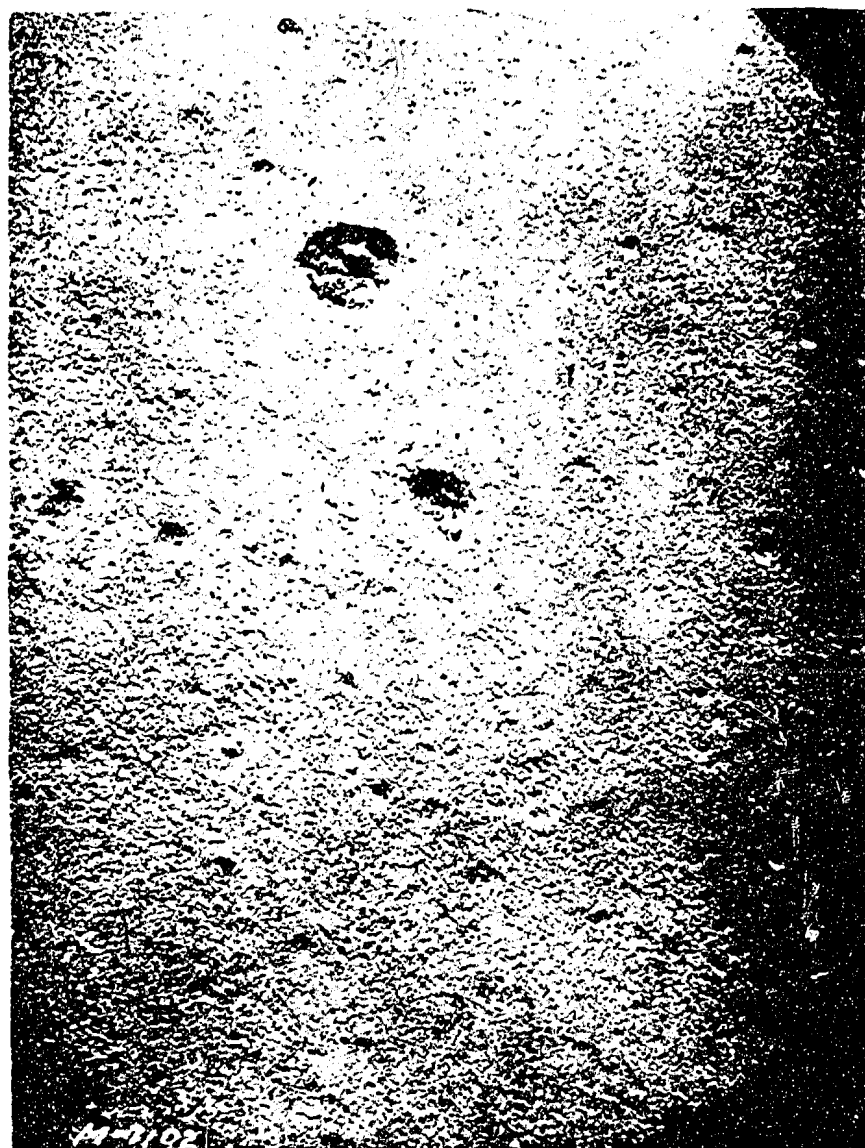
SURFACE AFTER 25 HOURS TEST



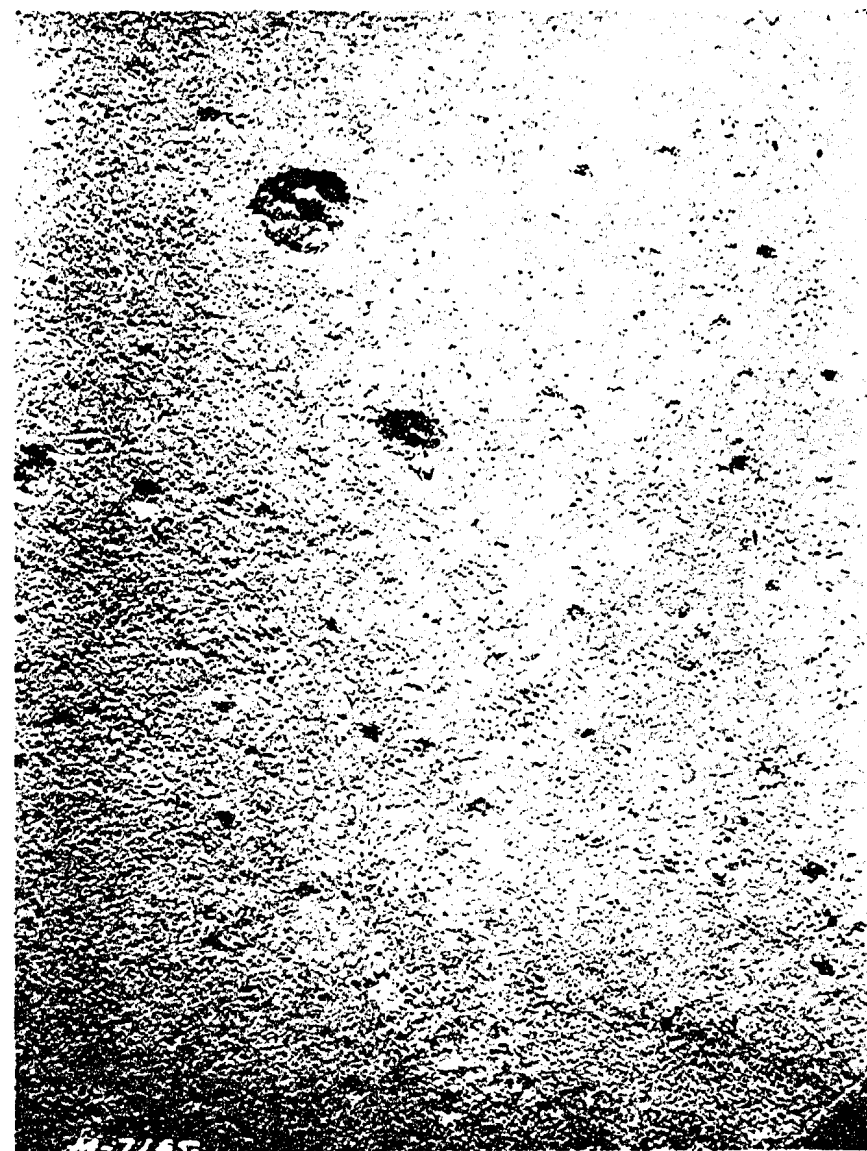
SURFACE AFTER 100 HOURS TEST

FLOW
↓

EUCUMBENE-TUMUT TUNNEL JUNCTION SHAFT
PHOTOMICROGRAPHS OF SURFACE OF CONCRETE LINED PIPE DAMAGED BY CAVITATION -
THIRD AREA APPROXIMATELY 2 INCHES FROM BOTTOM OF 2-FOOT PIPE SECTION-MODEL
WITH INLET CONTROL

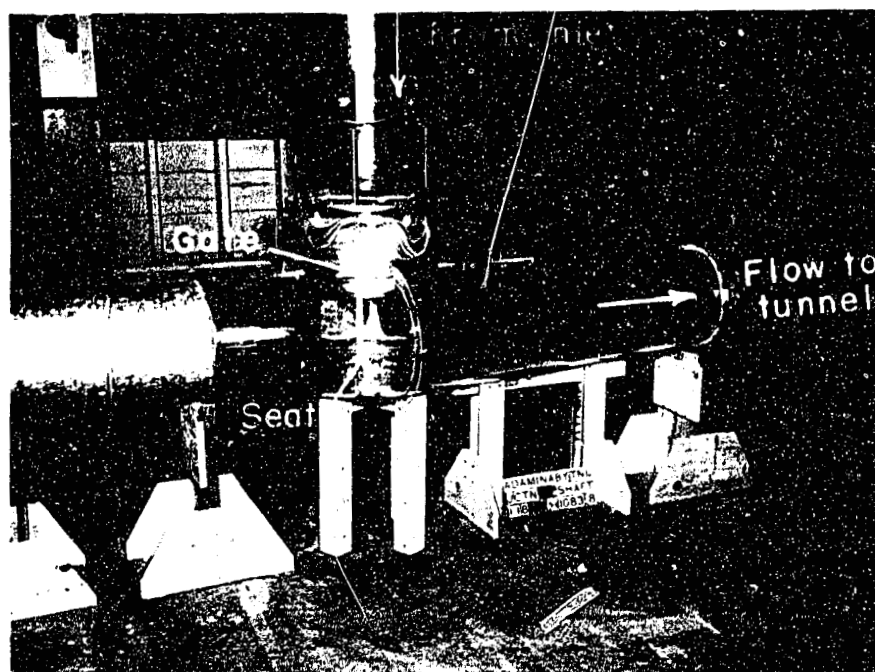


SURFACE AFTER 25 HOURS TEST

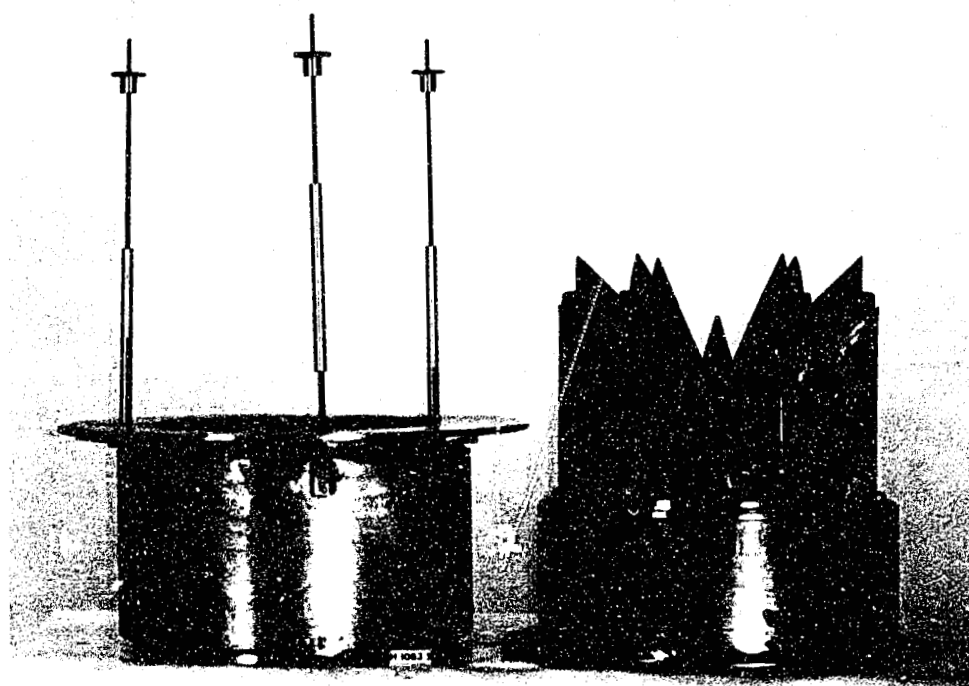


SURFACE AFTER 100 HOURS TEST

ELCUMBENE-TUMUT TUNNEL JUNCTION SHAFT
 PHOTOMICROGRAPHS OF SURFACE OF CONCRETE LINED PIPE DAMAGED BY CAVITATION -
 FOURTH AREA APPROXIMATELY 2 INCHES FROM BOTTOM OF 2-FOOT PIPE SECTION-MODEL
 WITH INLET CONTROL

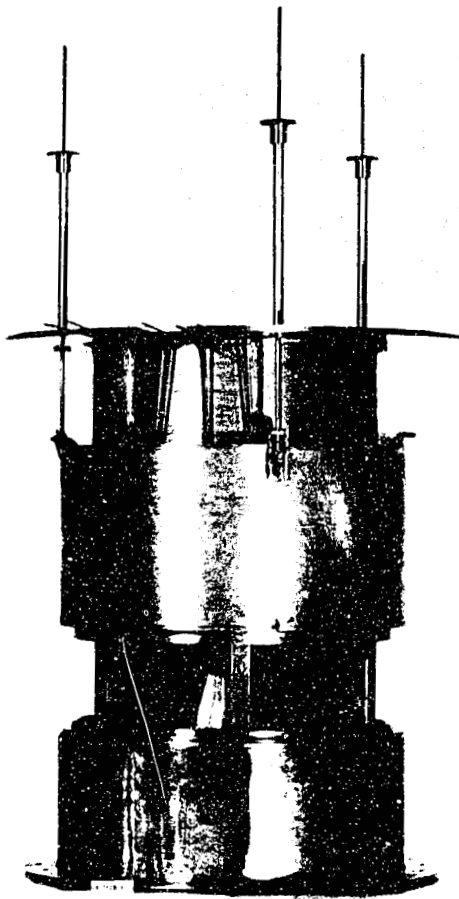


A. MODEL OF CYLINDER GATE AND TUNNEL TRANSITION

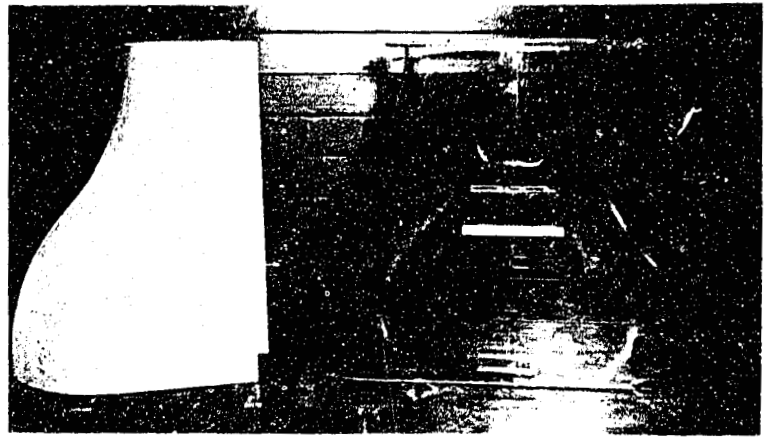


B. 1-GATE, GATE STEMS AND UPPER AND LOWER FRAME
2-SPLITTERS, CONE, GATE SEAT AND PEDESTAL

EUCUMBENE-TUMUT TUNNEL JUNCTION SHAFT
PRELIMINARY CYLINDER GATE MODEL TRANSITION AND GATE SECTIONS



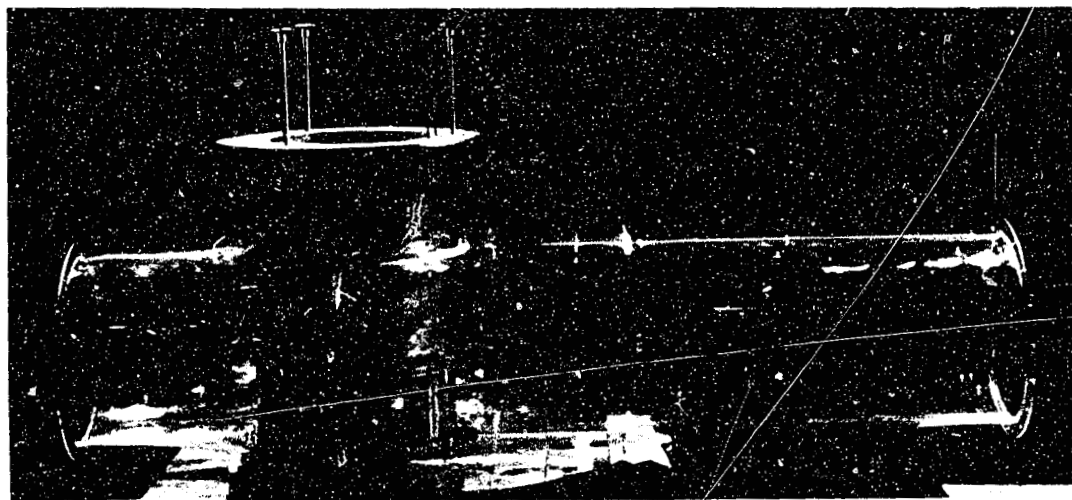
A. ASSEMBLED GATE



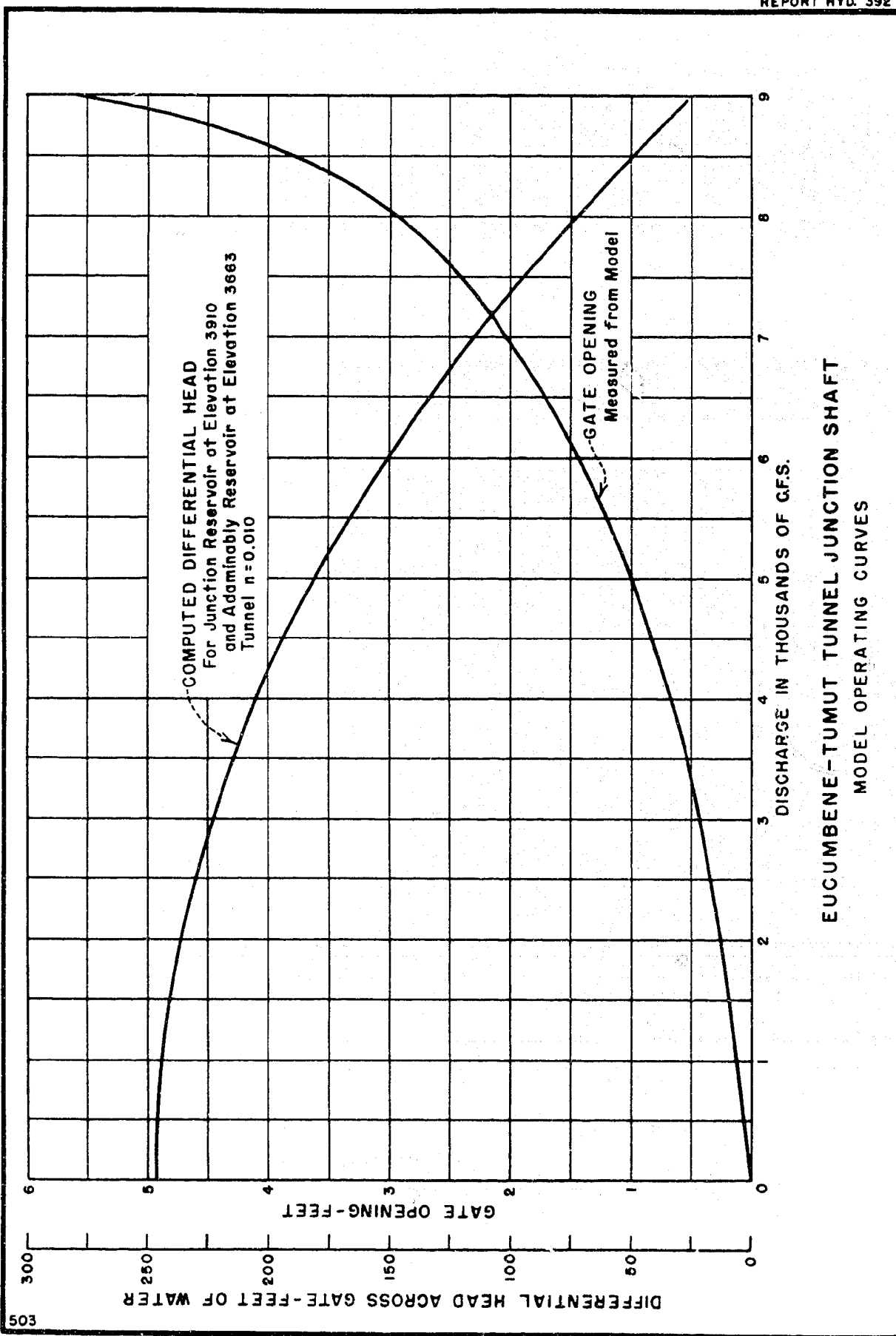
B. TUMUT SIDE OF GATE CHAMBER
WOODEN MOLD- 23 FOOT RADIUS REVERSE CURVE



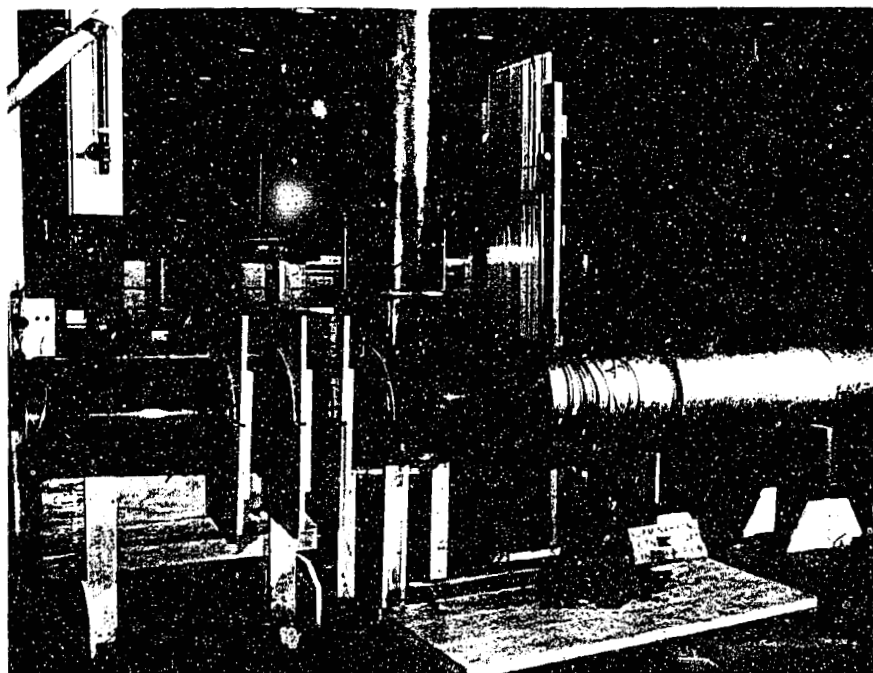
C. PRELIMINARY ADAMINABY SIDE OF GATE CHAMBER
WITH WOODEN MOLD-10 DEGREE CONVERGENCE



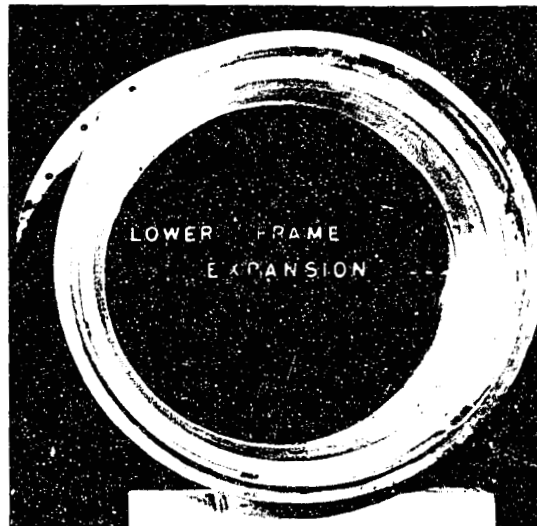
D. CYLINDER GATE AND GATE CHAMBER ASSEMBLED



EUCUMBENE-TUMUT TUNNEL JUNCTION SHAFT
MODEL OPERATING CURVES

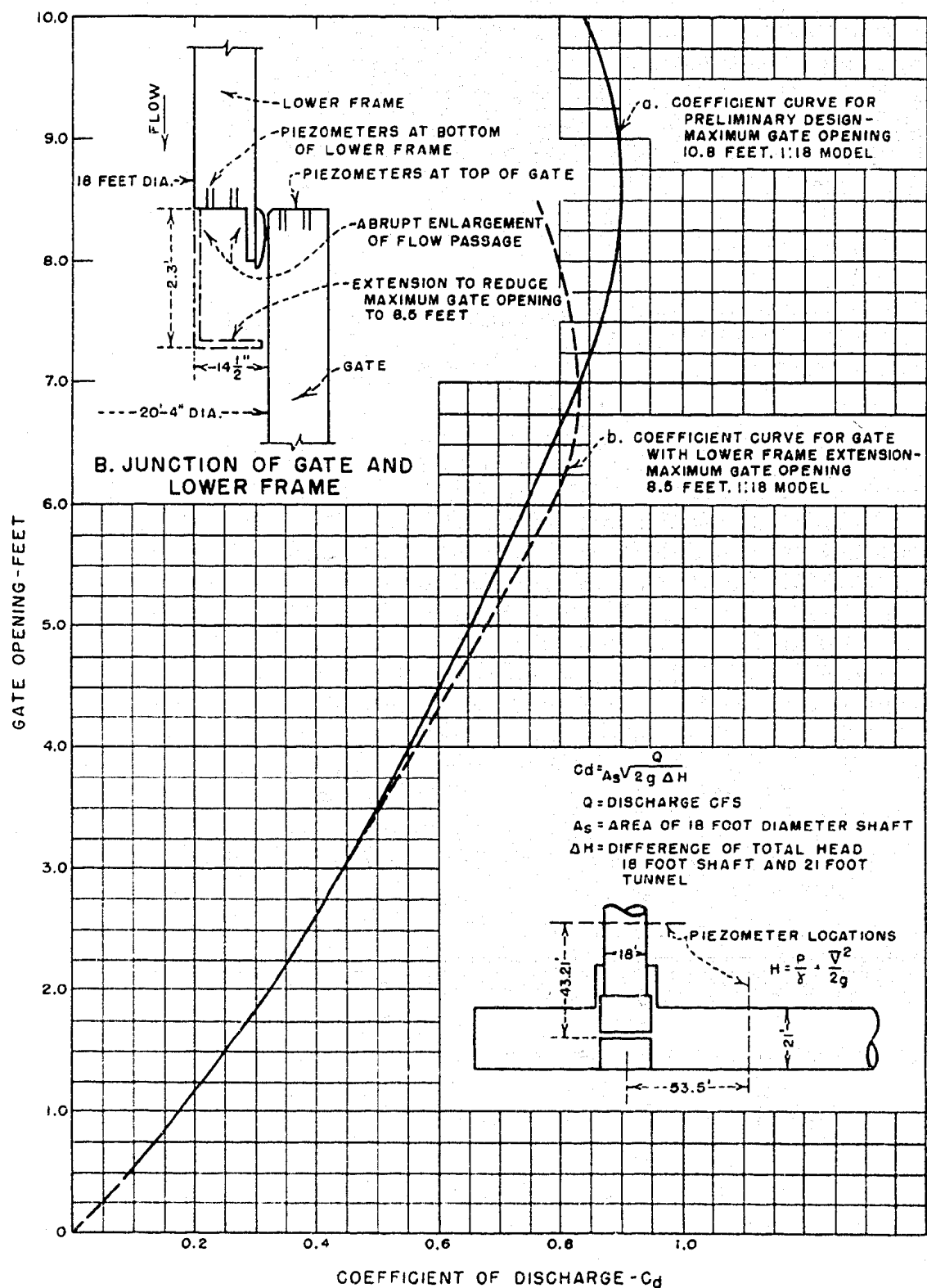


A. GATE DISCHARGING THROUGH RECOMMENDED TRANSITION TO
EUCUMBENE-TUMUT TUNNEL



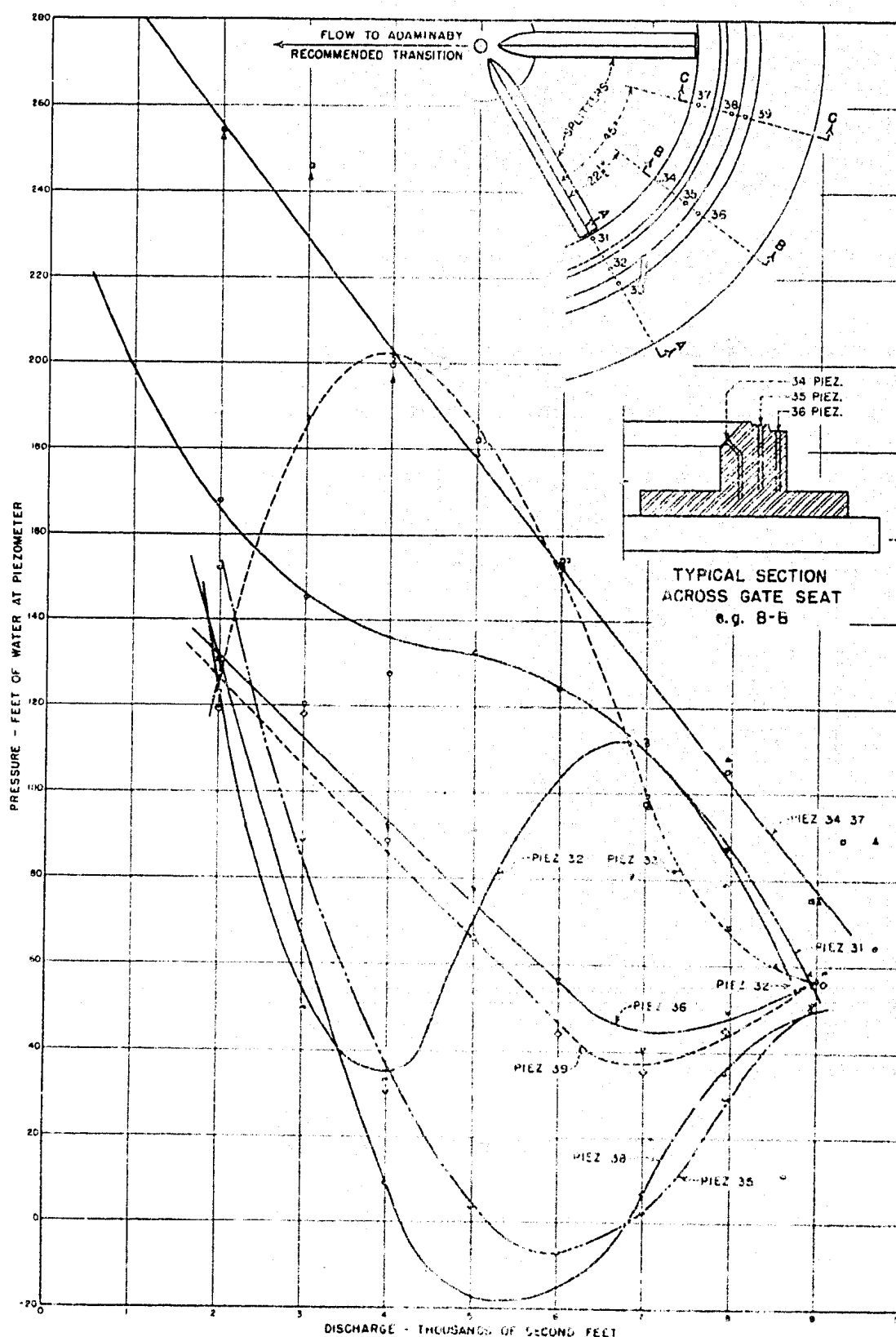
B. MODIFICATIONS TO LOWER FRAME, GATE SEAT, AND GATE PEDESTAL

EUCUMBENE-TUMUT TUNNEL JUNCTION SHAFT
MODIFICATIONS TO CYLINDER GATE MODEL

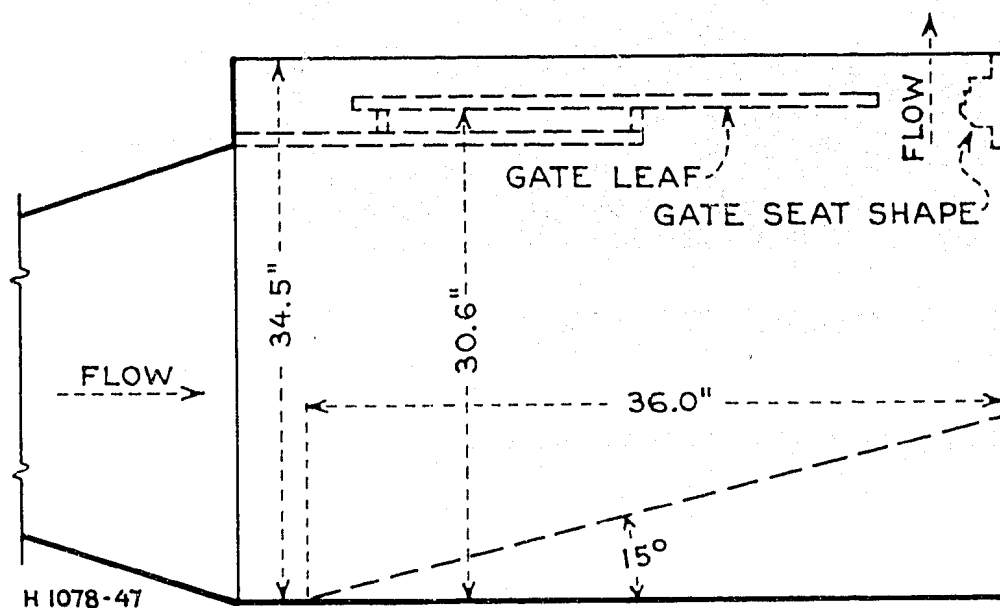


EUCUMBENE-TUMUT TUNNEL JUNCTION SHAFT
COEFFICIENT OF DISCHARGE CURVES FOR PRELIMINARY DESIGN GATES
WITH MAXIMUM OPENINGS OF 10.8 AND 8.5 FEET

FIGURE 25
REPORT HYD 392



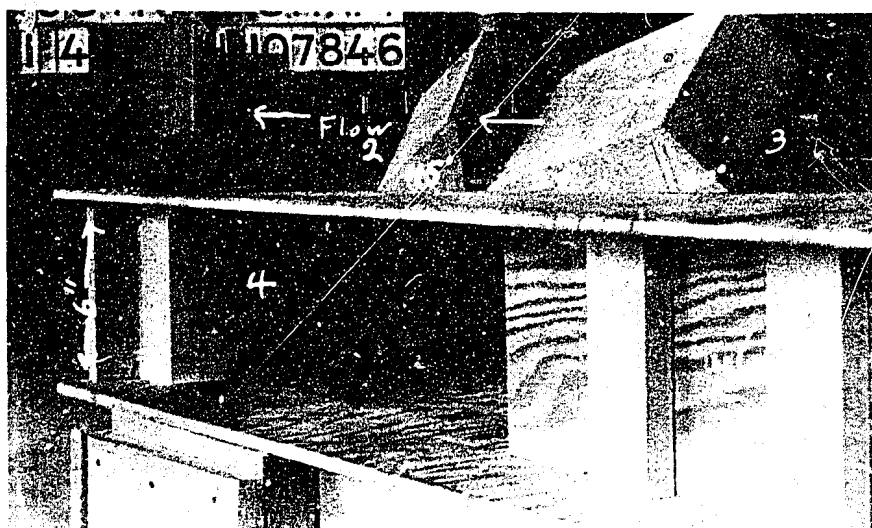
EUCUMBENE-TUMUT TUNNEL JUNCTION SHAFT
PRESSURES ON PRELIMINARY DESIGN GATE SEAT



A. PLAN OF AIR MODEL

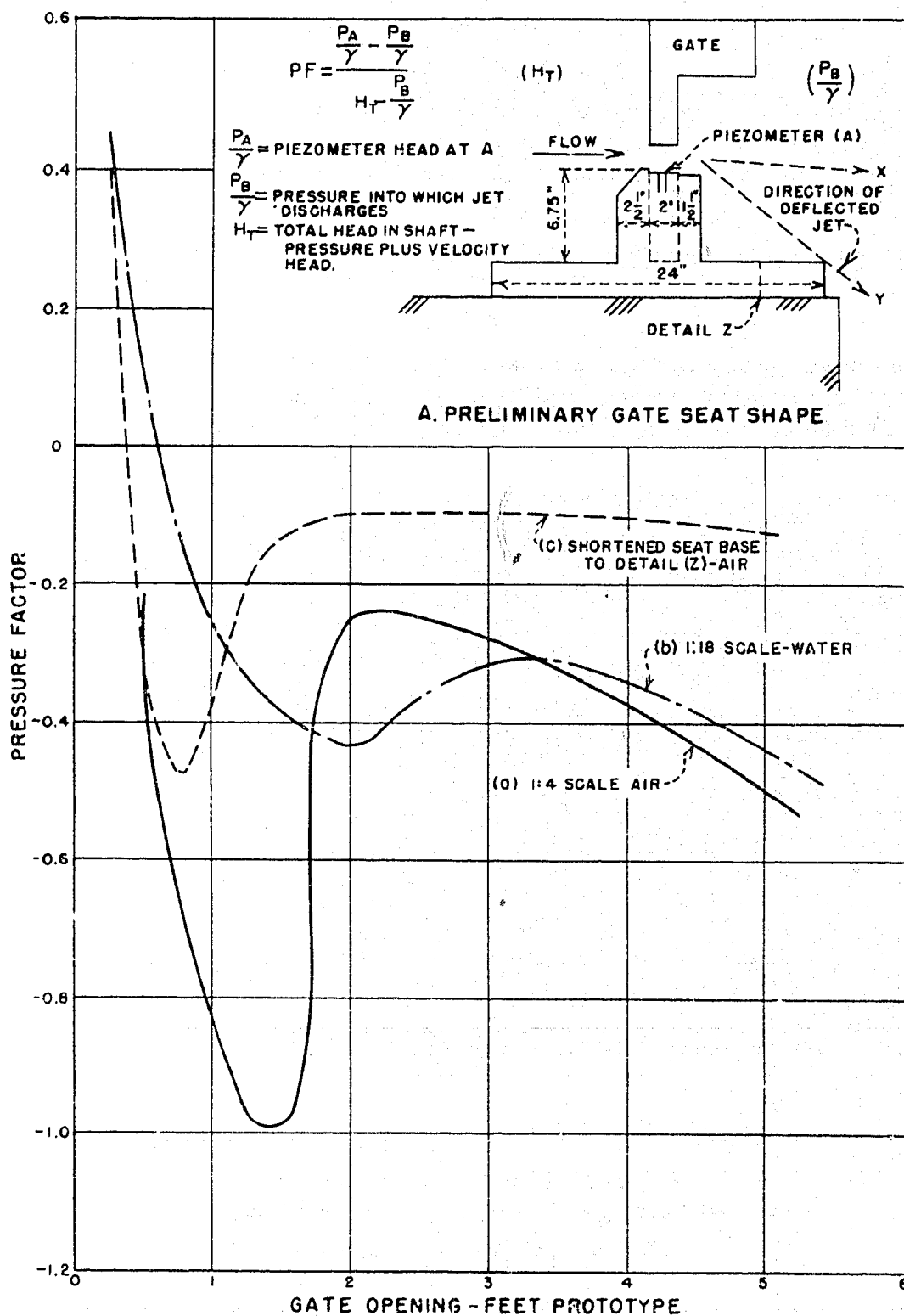


B. AIR MODEL INSTALLATION



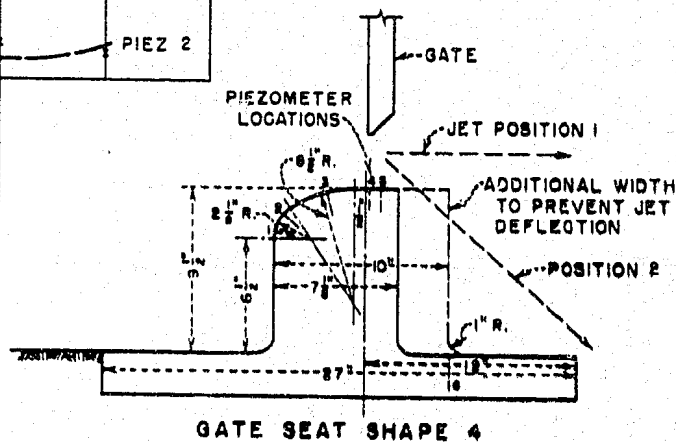
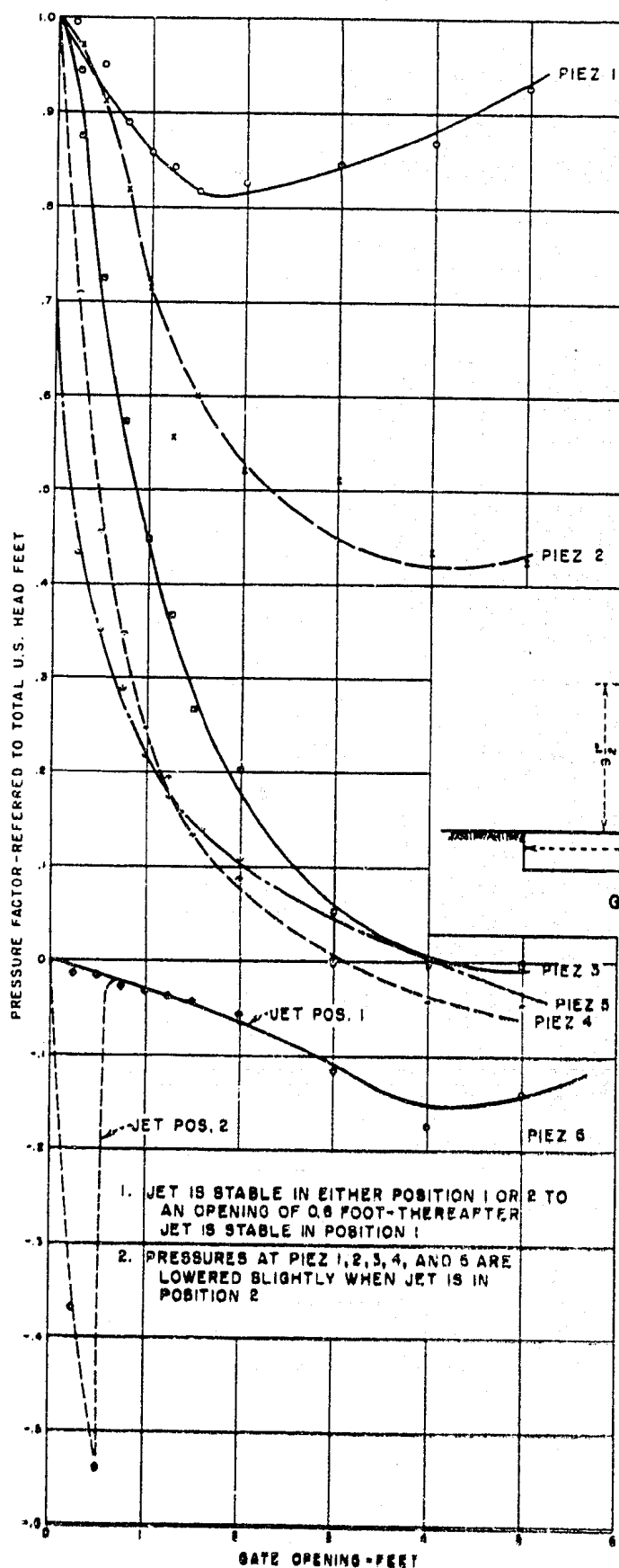
C. FLOW EXIT-4 GATE SEAT SHAPES-RECOMMENDED SHAPE INSTALLED

EUCUMBENE-TUMUT TUNNEL JUNCTION SHAFT
1:4 SCALE LOW-VELOCITY AIR MODEL

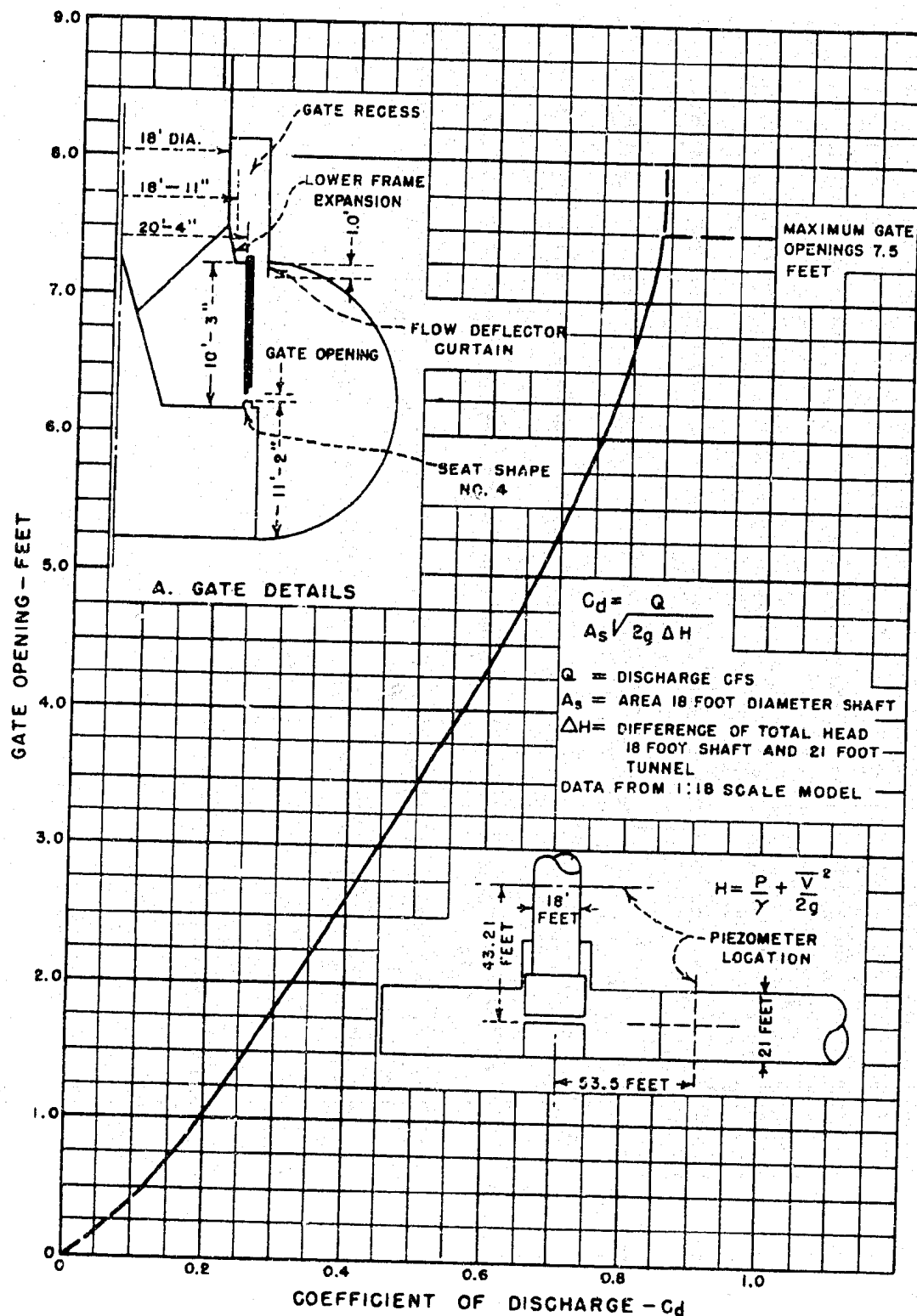


**EUCUMBENE-TUMUT TUNNEL JUNCTION SHAFT
PRESSURE FACTORS FROM WATER AND AIR MODELS
FOR PRELIMINARY DESIGN GATE SEAT**

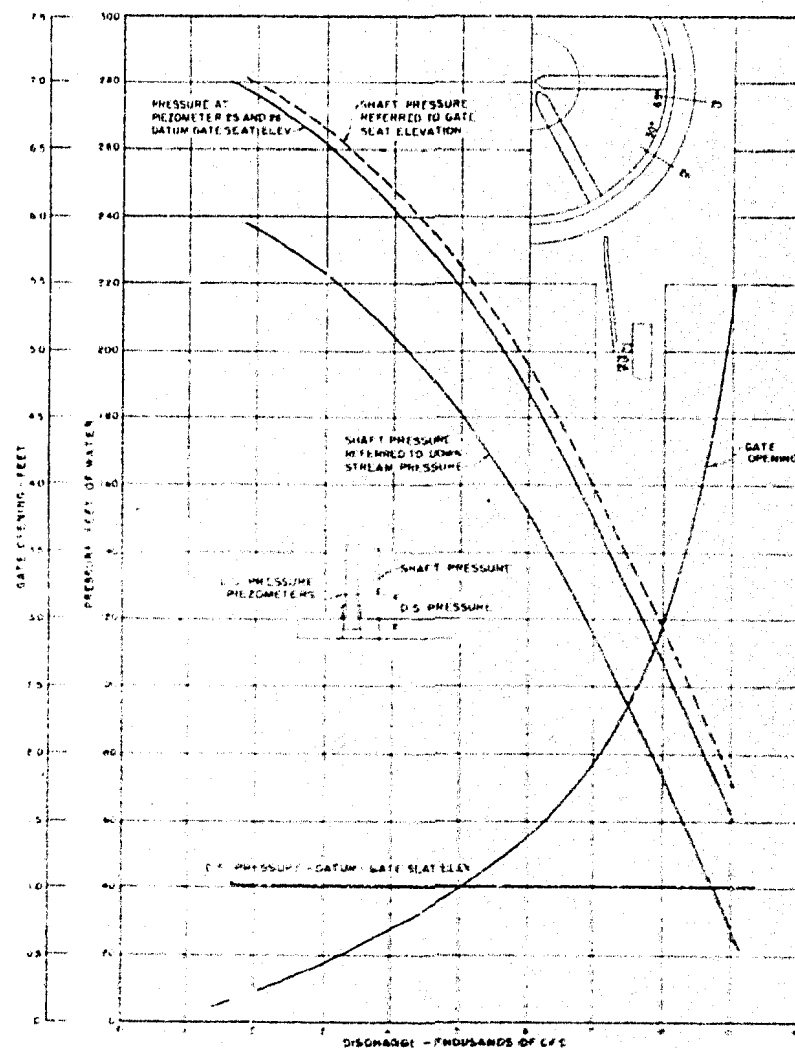
FIGURE 28
REPORT HYD. 392



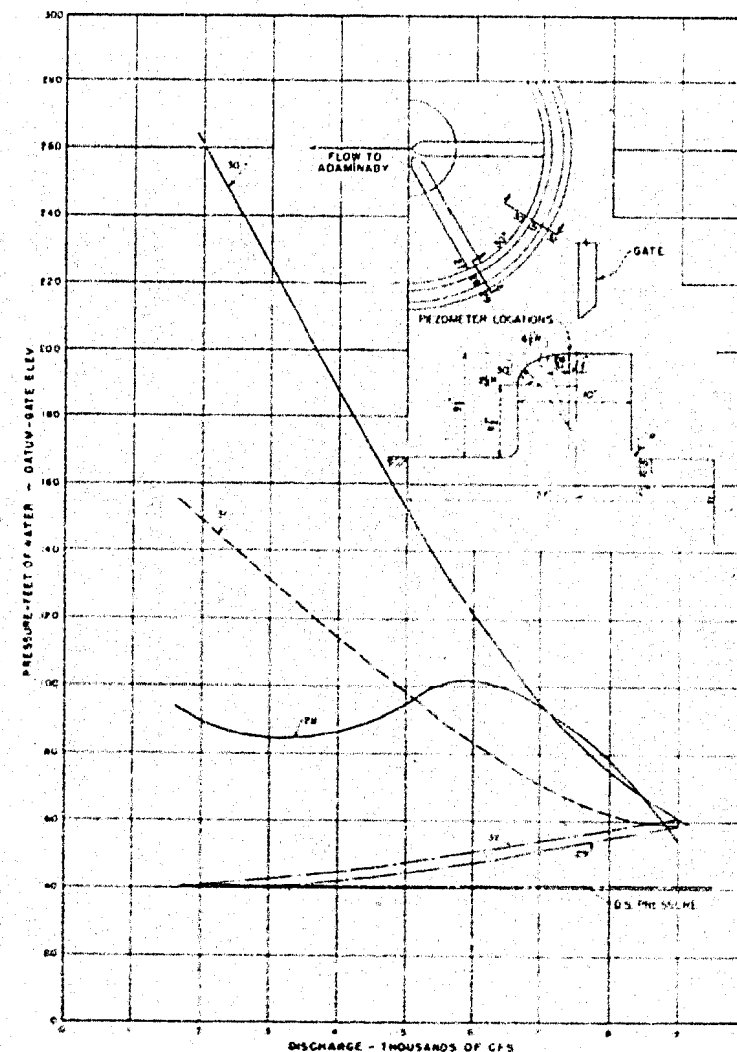
EUOUMBENE-TUMUT TUNNEL
JUNCTION SHAFT
PRESSURE FACTORS
FOR GATE WITH 2-RADIUS CURVE
1:4 SCALE MODEL



EUCUMBENE-TUMUT TUNNEL JUNCTION SHAFT
COEFFICIENT OF DISCHARGE CURVE
FOR RECOMMENDED CYLINDER GATE



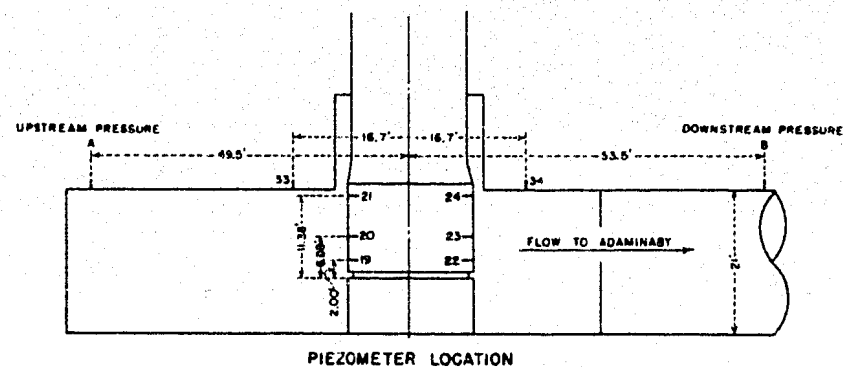
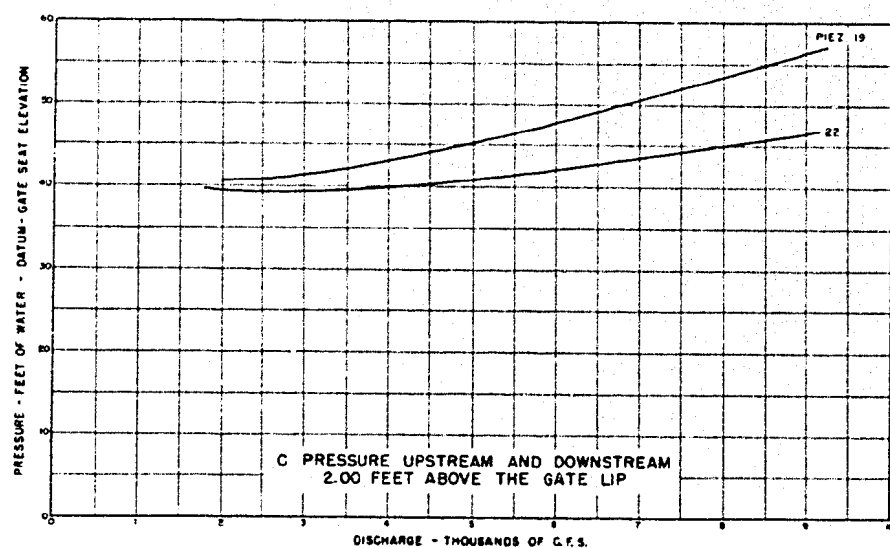
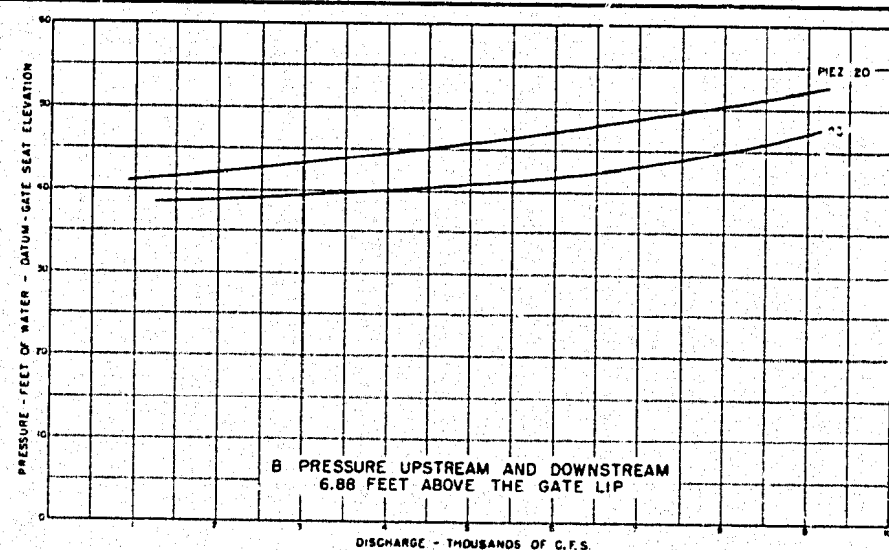
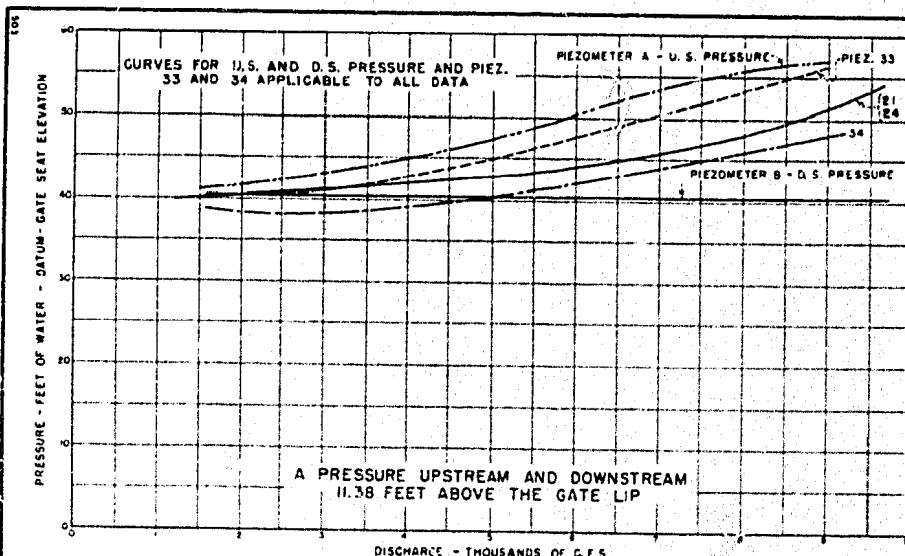
A. MODEL OPERATING CURVES AND PRESSURES AT JUNCTION OF LOWER FRAME AND GATE



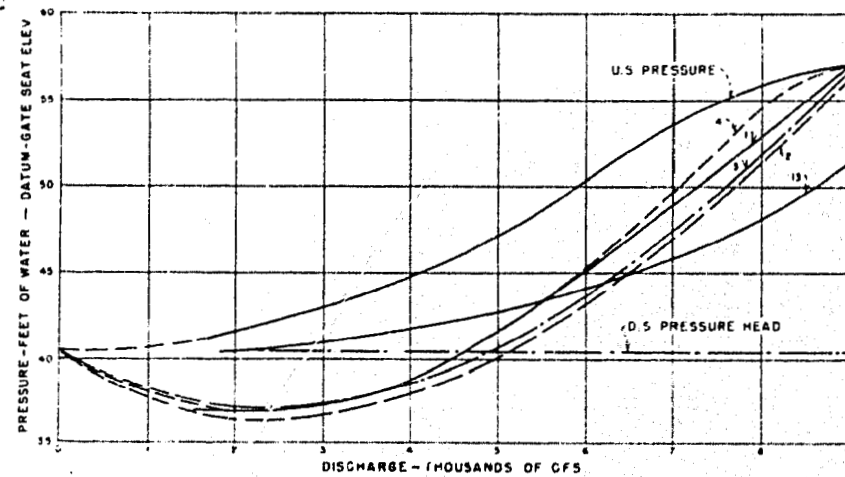
B. PRESSURES ON GATE SEAT WITH 2 RADIi CURVE - RECOMMENDED

EUCUMBENE-TUMUT TUNNEL JUNCTION SHAFT

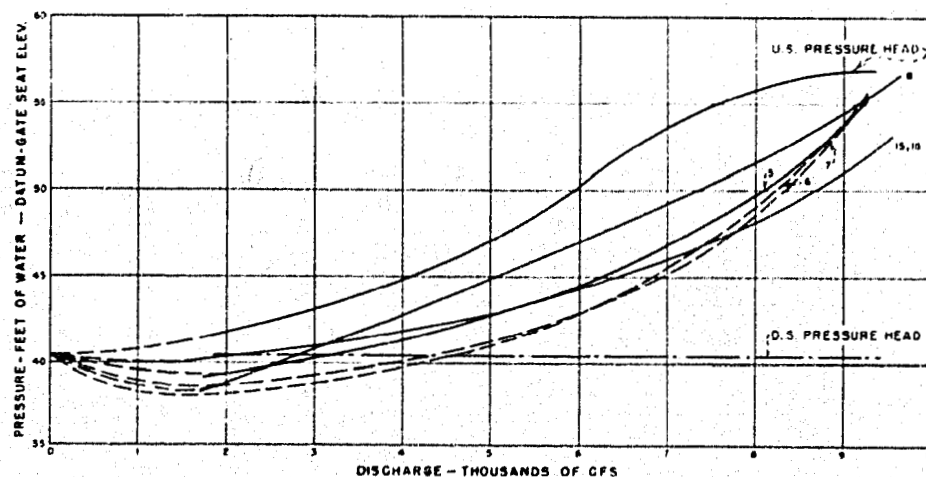
MODEL OPERATING CURVES, PRESSURES ON BOTTOM OF LOWER FRAME, AND ON GATE SEAT OF RECOMMENDED DESIGN CYLINDER GATE



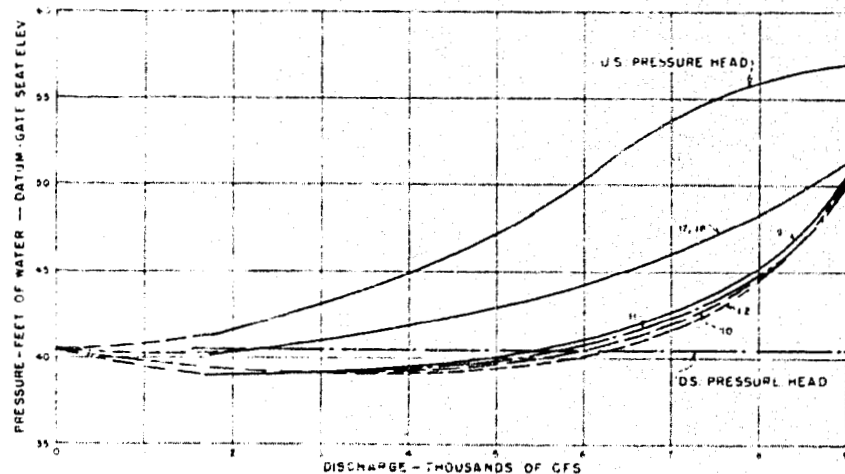
EUCUMBENE-TUMUT TUNNEL JUNCTION SHAFT
UNBALANCE OF PRESSURE ON CYLINDER GATE ALONG TUNNEL AXIS—RECOMMENDED DESIGN



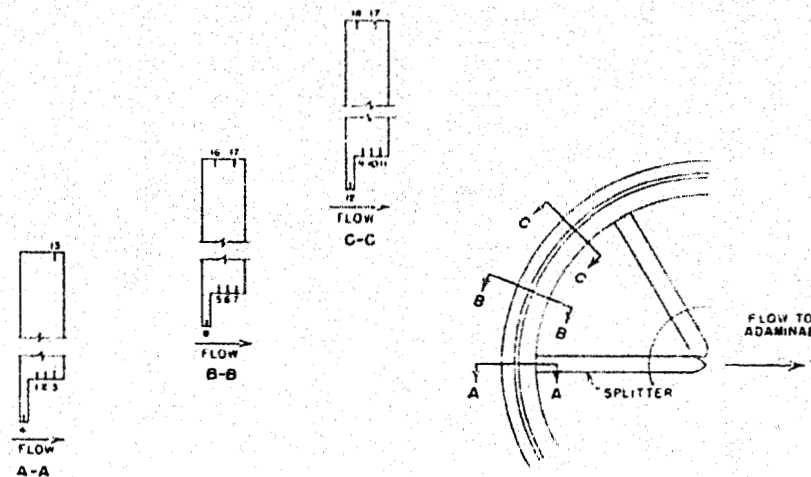
A. PRESSURES AT CENTERLINE OF UPSTREAM SPLITTER



B. PRESSURES 22 1/2 DEGREES LEFT OF SPLITTER

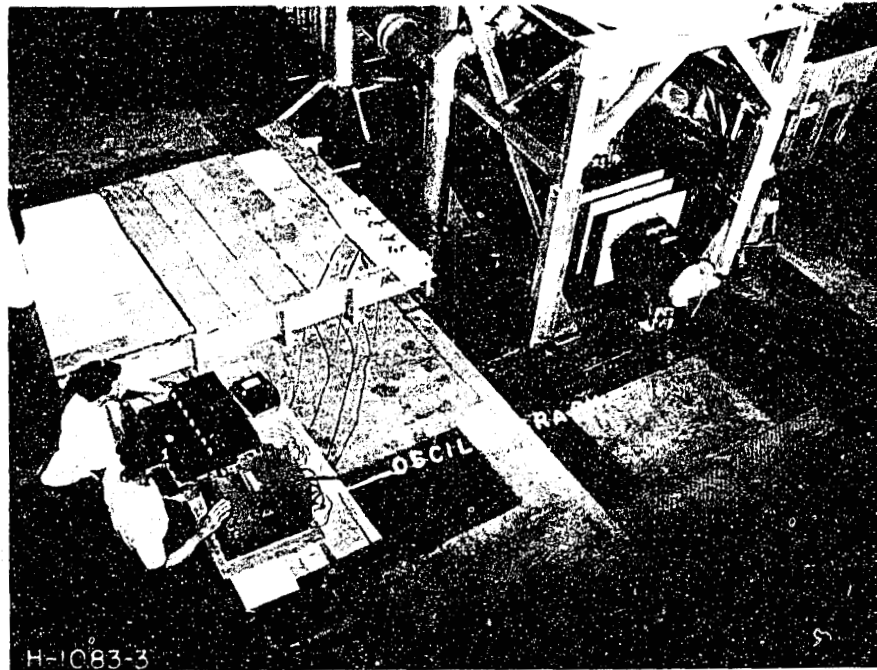


C. PRESSURES 45 DEGREES LEFT OF SPLITTER

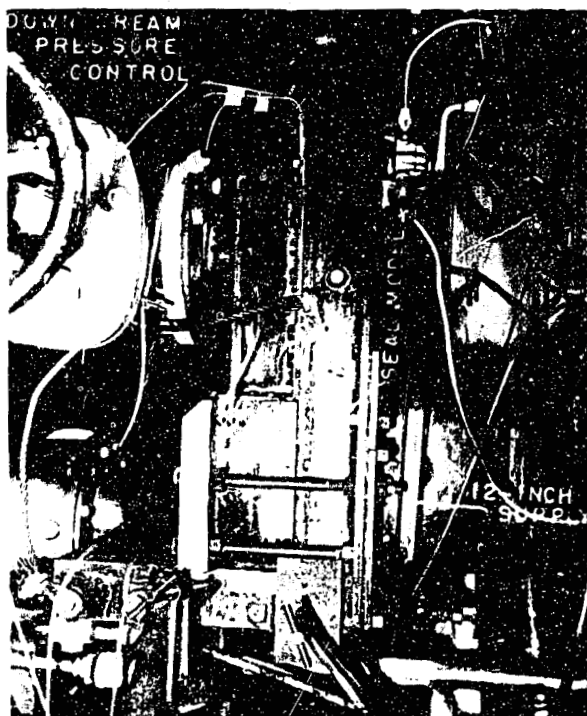


D. PIEZOMETER LOCATION

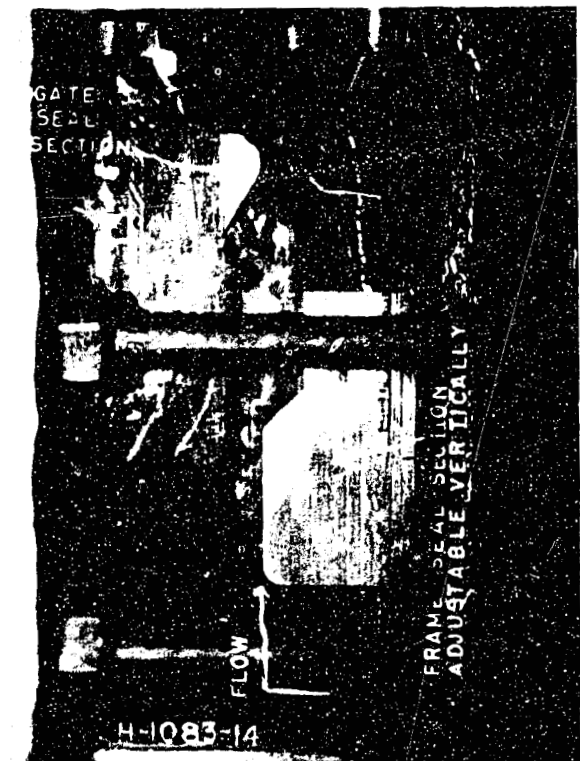
EUCUMBENE-TUMUT TUNNEL JUNCTION SHAFT
PRESSURES ON TOP AND BOTTOM OF RECOMMENDED CYLINDER GATE



A. PRESSURE CELLS AND INSTRUMENTS FOR OBTAINING PRESSURE FLUCTUATIONS ON MODEL



B. GATE SEAL MODEL

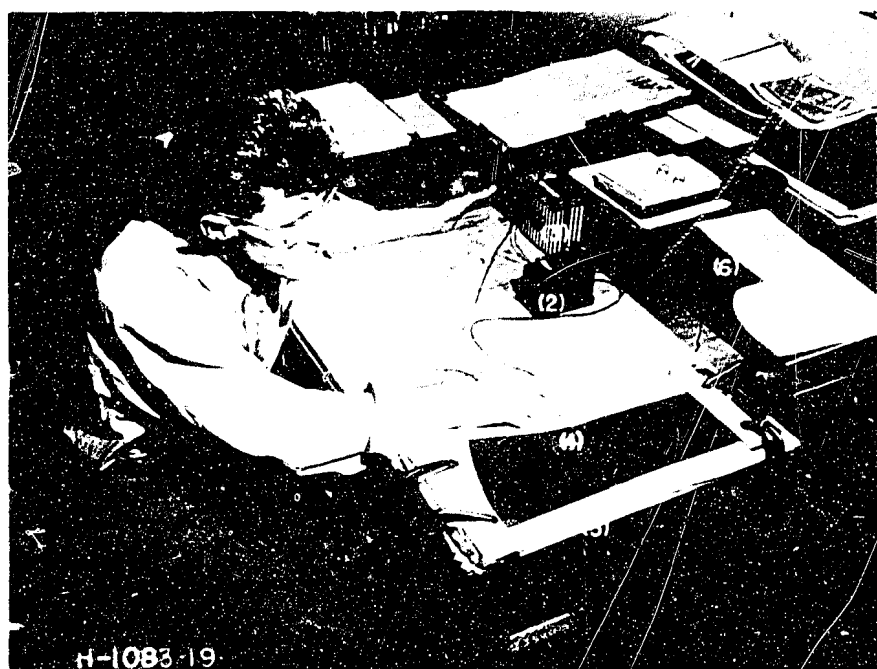


C. PRELIMINARY GATE SEAL-REPRESENTING GATE 4.5 INCHES OPEN

EUCUMBENE-TUMUT TUNNEL JUNCTION SHAFT
PRESSURE CELL INSTALLATION 1:18 SCALE CYLINDER GATE MODEL
TOP GATE SEAL MODEL



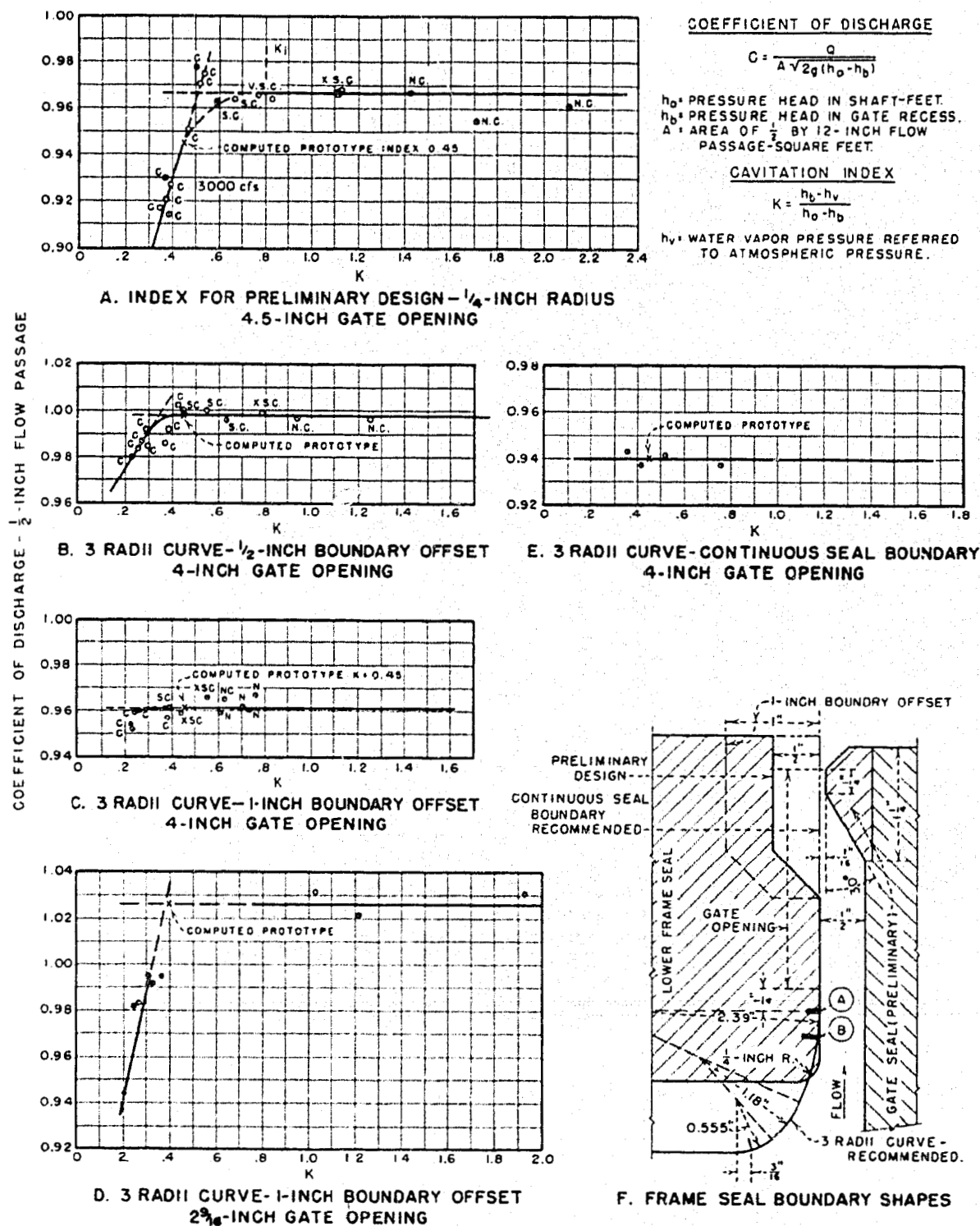
A. VAPOR POCKET - PRELIMINARY FRAME SEAL - CAVITATION INDEX 0.33



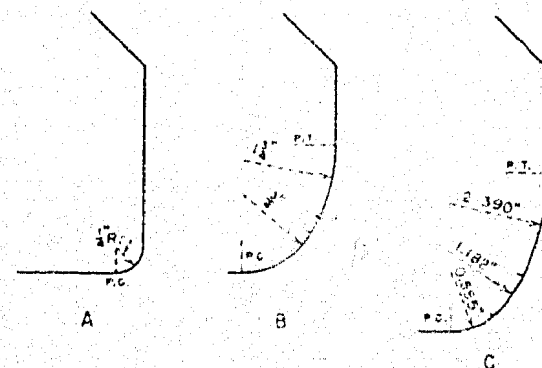
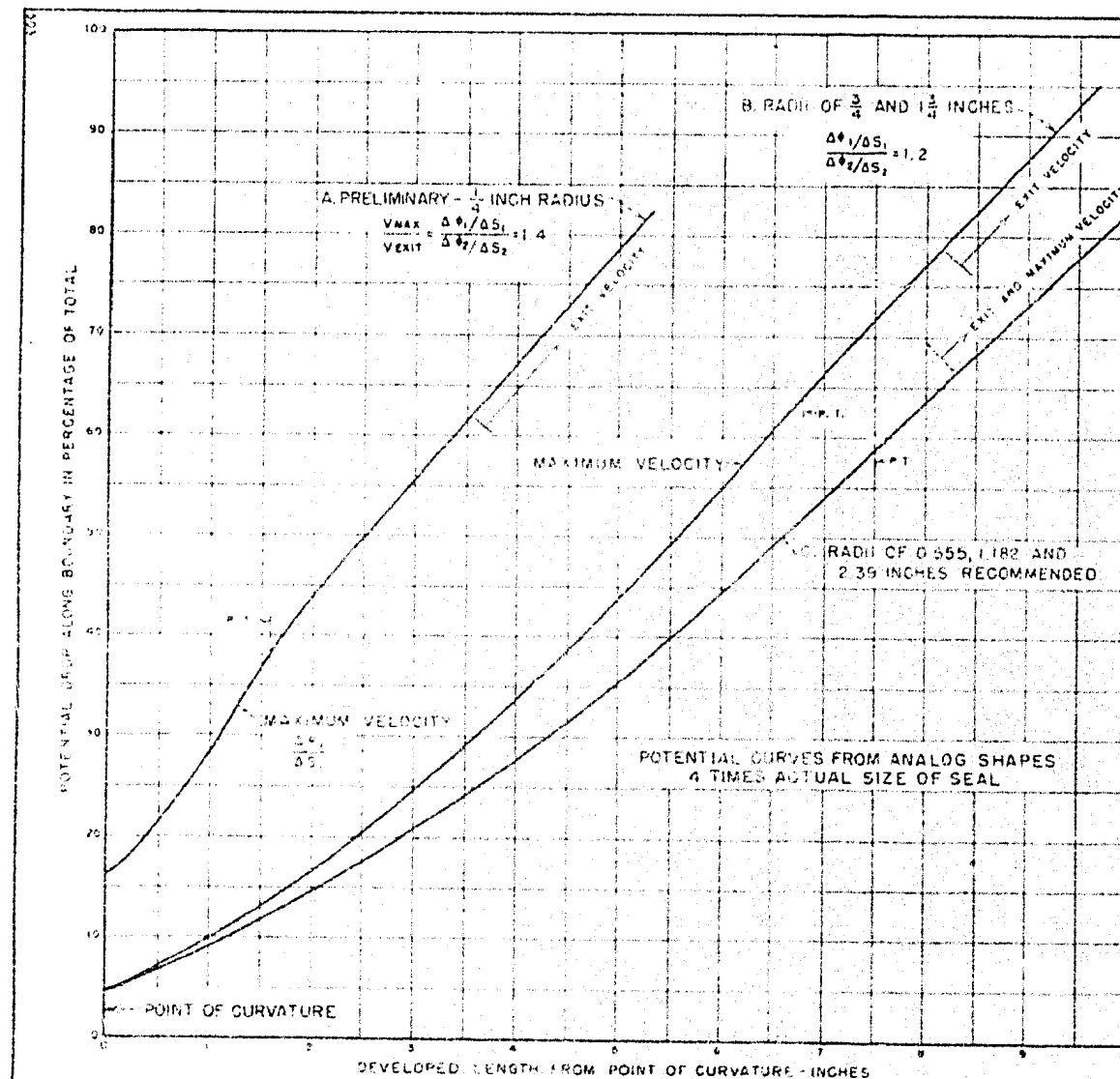
- (1) POTENTIOMETER
- (2) GALVANOMETER
- (3) BATTERY
- (4) PROBE
- (5) DETAIL MODEL 10 TIMES ACTUAL SIZE
- (6) BOUNDARY CURVE 4 TIMES ACTUAL SIZE

B. ELECTRIC ANALOG EQUIPMENT WITH GRAPHITE COATED PAPER FOR MODEL

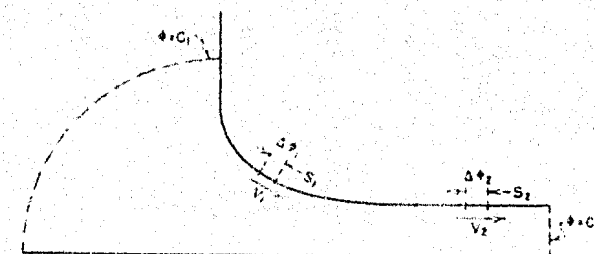
EUCUMBENE TUMUT TUNNEL JUNCTION SHAFT
CAVITATION IN PRELIMINARY SEAL FLOW PASSAGE
ELECTRIC ANALOG



EUCUMBENE-TUMUT TUNNEL JUNCTION SHAFT
CAVITATION INDEX FOR FRAME SEAL BOUNDARY SHAPES



FRAME SEAL BOUNDARY SHAPES
OF ANALOG TESTS



DEFINITION OF TERMS

EUCUMBENE-TUMUT TUNNEL JUNCTION SHAFT
POTENTIAL DROP CURVES FOR FRAME SEAL RING SHAPES



A. VAPOR POCKET IN 1/2-INCH SEAL OFFSET
4-INCH GATE OPENING CAVITATION
INDEX 0.39



B. VAPOR POCKET IN 1-INCH SEAL OFFSET
4-INCH GATE OPENING CAVITATION
INDEX 0.33

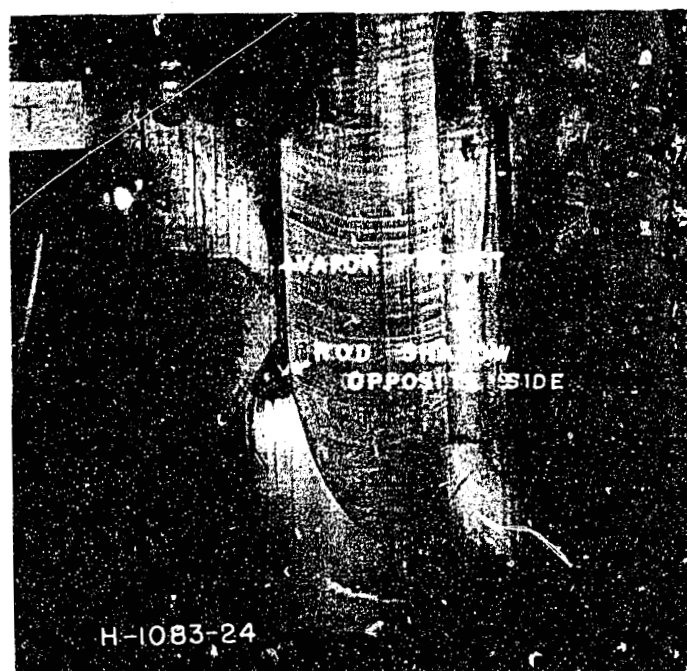


C. VAPOR POCKET IN 1-INCH SEAL OFFSET
2-9/16-INCH GATE OPENING CAVITATION
INDEX 0.35

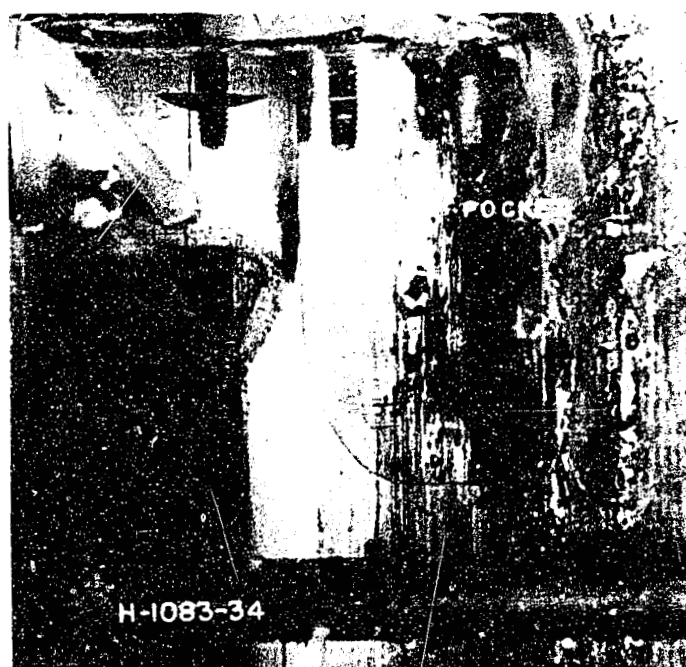


D. SEAL RING BOUNDARY
GATE OPENING 4-INCHES

EUCUMBENE-TUMUT TUNNEL JUNCTION SHAFT
VAPOR POCKETS ON FRAME SEAL BOUNDARY--OFFSET--
RECOMMENDED FRAME SEAL RING

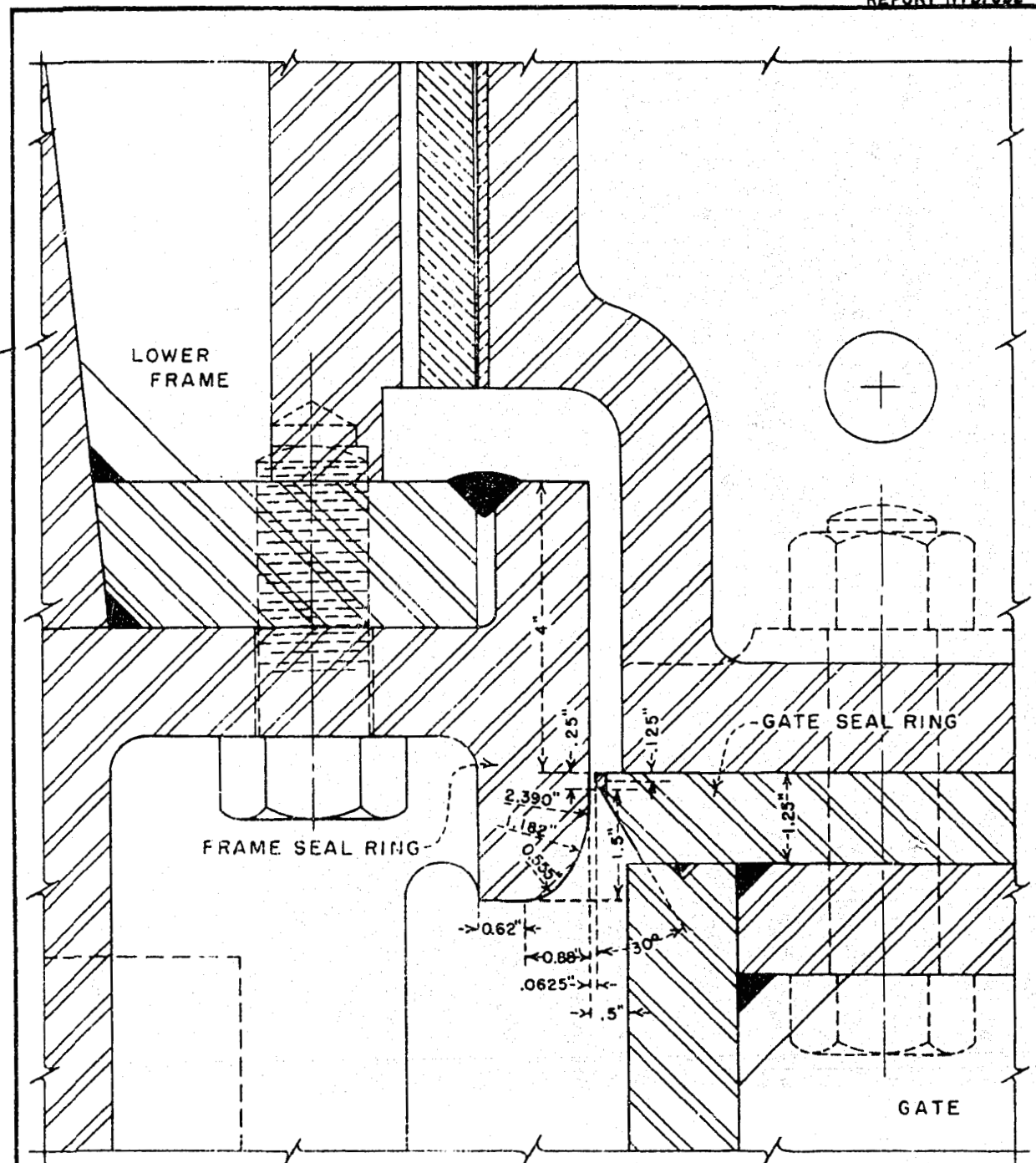


A. VAPOR POCKET IN 1/16-INCH FLOW PASSAGE
1/4-INCH LONG GATE SEAL SURFACE



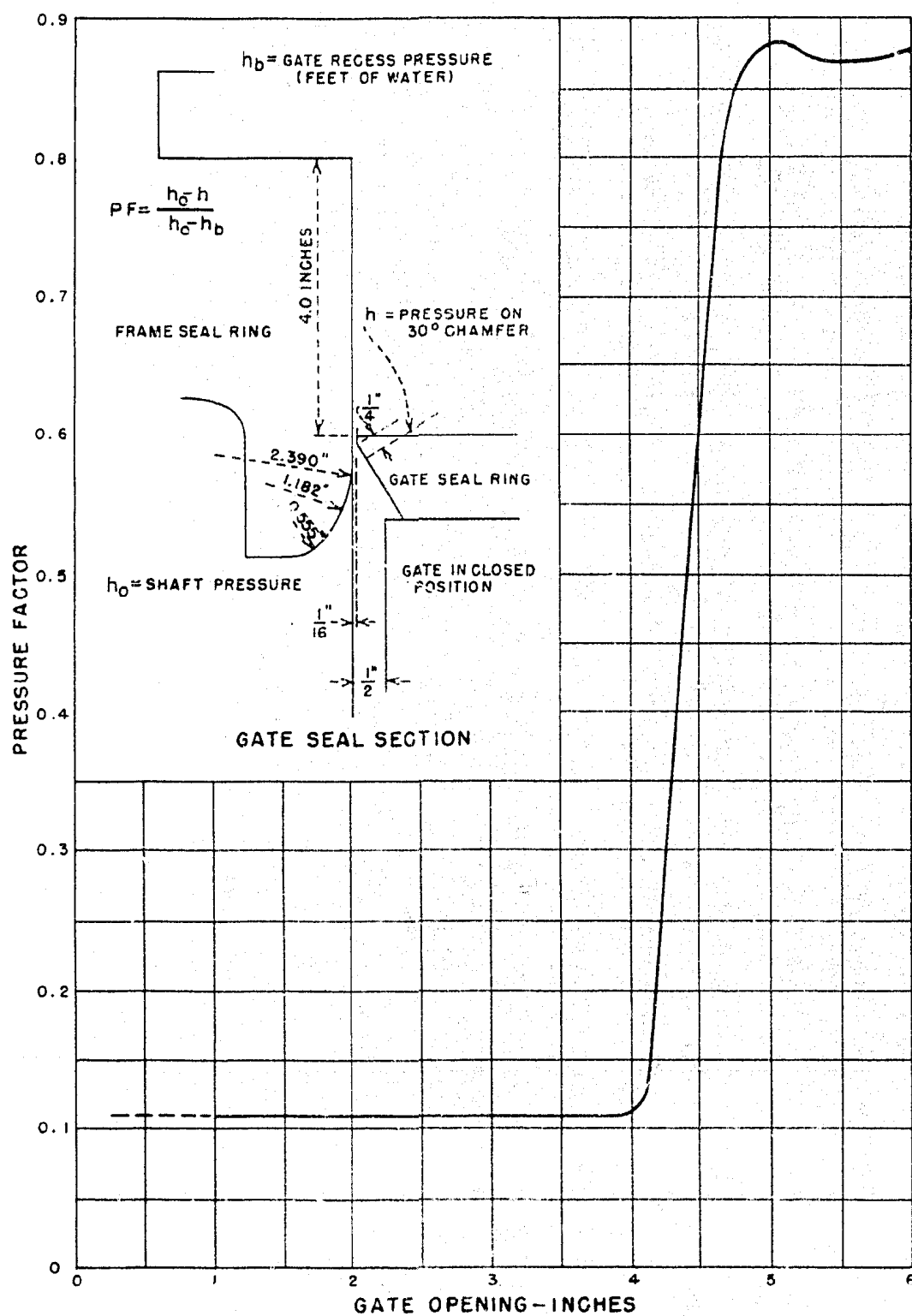
B. VAPOR POCKET IN 1/16-INCH FLOW PASSAGE
1/16-INCH LONG GATE SEAL SURFACE

EUCUMBENE-TUMUT TUNNEL JUNCTION SHAFT
CAVITATION IN GATE SEAL FLOW PASSAGE



EUCUMBENE-TUMUT TUNNEL JUNCTION SHAFT
RECOMMENDED CYLINDER GATE TOP SEAL

FIGURE 40
REPORT HYD, 392



EUCUMBENE-TUMUT TUNNEL JUNCTION SHAFT
PRESSURE CHANGE ON 30 DEGREE CHAMFER
OF GATE SEAL RING